UNIVERSITY OF
KWAZULU-NATAL

INYUVESI
YAKWAZULU-NATALI

An in-silico and in-vivo investigation on the effects of acute fumonisin b1 exposure on inflammation and epigenetics in C57BL/6 mice hearts

SELWYN KYLE GOUNDER

220074124

Master of Medical Science (MMDSC)

Discipline of Medical Biochemistry

School of Laboratory Medicine and Medical Sciences

College of Health Sciences

University of KwaZulu-Natal

2024

Plagiarism Declaration Form

I, **Selwyn Kyle Gounder**, Student Number: **220074124** declare that

i. The research reported in this dissertation, except where otherwise indicated, is my original work.

ii. This dissertation has not been submitted for any degree or examination at any other university.

iii. This dissertation does not contain other persons' data, pictures, graphs, or other information unless specifically acknowledged as being sourced from other persons.

iv. This dissertation does not contain other person's writing unless specifically acknowledged as being sourced from other researchers. Where other written sources have been quoted:

a. Their words have been rewritten, but the general information attributed to them has been referenced.

b. Where their exact words have been used, their writing has been placed inside quotation marks and referenced.

v. Where I have reproduced a publication of which I am an author, co-author, or editor, I have indicated in detail which part of the publication was actually written by myself alone and have fully referenced such publications.

vi. This dissertation does not contain text, graphics, or tables copied and pasted from the internet, unless specifically acknowledged, and the source is in the dissertation and the reference sections.

Student signed: [redacted] **Date:** 27 November 2024

Supervisor signed: _____ **Date:** November 2024

Dedication

I dedicate this work to my family, friends, and the community of Ixopo, whose unwavering support and values have inspired and shaped my journey to contribute meaningfully to the field of medical research.

Acknowledgements

God

I extend all my gratitude to the creator of this universe God foremost for the strength, patience and diligence given to me throughout my master's journey. I am everlastingly thankful for the power of the divine for guiding me throughout this project allowing me to successfully contribute to the world of science.

My Family & Friends

I would like to thank every member of my family who has supported me through this journey. Firstly, to my partners in crime, my three siblings Sha, Pooh, and Fishy: your unwavering support, advice, and listening ears were much appreciated. You all helped me maintain my sanity during tough times and uplifted my spirits during the good times, encouraging me to do my best. To my parents, Selva and Joslyn Gounder: I am thankful for your tireless efforts to provide me with opportunities you did not have. I am also grateful for the love, support, and guidance you have given me throughout this tiring journey. My gratitude extends to my granny, Anne Varden, for taking care of me and sending me off to university with well wishes and prayers every morning. I am truly thankful for all the love and support you have provided me throughout my university and master's journey. I am also grateful to my cousin Kaitlyn for her help and positivity, always cheering me up and ensuring I was my best self during this project. I deeply appreciate the time you spent to support me. My friends Abhay and Sash: you have been like family to me, encouraging me, listening to my never-ending stories, and providing support and love that kept me sane and comforted during rough times. I am overwhelmingly grateful to you both. My absolute treasure at the medical biochemistry department, future Dr. Noxolo Radebe: our endless lab shenanigans and constant joking around provided much entertainment for us and everyone around us. Hanging out with you was one of my favourite highlights of this year. Finally, I would love to express my gratitude to my four-legged companions, Lara, Lacey, and Lexi, for being the best doggies anyone could ask for.

Supervisors

I am thankful to all my supervisors.

Foremost, Dr. Terisha Ghazi: your endless and unwavering support throughout my master's journey has been impeccable. I appreciate every effort you made to ensure my work's success, allowing me to create a work of art despite setbacks and complications. To Prof. Anil

Chuturgoon: I am grateful for all the advice and attention you dedicated to my work. Your invaluable guidance has shaped this project's journey, and for that, I am truly thankful. Finally, I extend my thanks to Dr. Mhlongo, who paved a new way for me in computational chemistry. You introduced me to a world of new possibilities with your enthusiastic love for your work. For that, I am truly grateful and hope to continue expanding my knowledge in the field.

Funding

To the National Research Foundation, I am eternally thankful for granting me the master's research grant. The funding was crucial in spearheading the success of my research project. Your support allowed me to pursue my academic aspirations and make progress in a study that I believe will contribute to expanding the medical sciences research field. This opportunity has encouraged me to acquire new, innovative skills and knowledge to drive the success of future projects. I am grateful for the trust the NRF has placed in me. I would also like to thank CHS funding for covering the running expenses, which helped me purchase lab reagents essential for the success of this project. Your support was invaluable in ensuring the smooth progress of my research.

Presentations

1. S. Gounder, T. Ghazi, N. Mhlongo, and A.A. Chuturgoon. An in silico and in vivo investigation on the effects of acute fumonisin B1 exposure on inflammation and epigenetics in C57BL/6 mice hearts. School of Laboratory Medicine and Medical Sciences Research Symposium, Durban, University of KwaZulu-Natal Westville, South Africa, Oral presentation (3rd Prize).

Publications

1. Gounder, S. K., Ghazi, T., and Chuturgoon, A. A. (2024). Unveiling the Potential Cardiotoxicity of Fumonisin B1: A Focus on Inflammatory Pathways and Epigenetic Modifications. Critical Reviews in Toxicology (*In Review;* manuscript ID: 247019782).

Table of Contents

List of Figures

List of Tables

Abbreviations

3,3',5,5'-Tetramethylbenzidine	TMB
Apoptosis-associated speck-like protein	ASC
Asparagine 202	Asn202
Bicinchoninic acid	BCA assay
Bovine serum albumin	BSA
Cardiotrophin 1	CT-1
Catalase	CAT
Ceramide	cer
Ceramide-1-phosphate	C1P
Cysteine 194	Cys194
Cysteine aspartyl specific proteases	Caspases
Danger-associated molecular patterns	DAMPs
DNA methyltransferases	DNMTs
DNA methyltransferase 1	DNMT1
DNA methyltransferase 3 alpha	DNMT3A
DNA methyltransferase 3 beta	DNMT3B
Enzyme-linked immunosorbent assay	ELISA
Free radicals	FRs
Fumonisin	FB
Fumonisin B2	FB_2
Fumonisin B3	FB_3
Fumonisin B1	FB_1
Gasdermin D	GSDMD

Gasdermin E	GSDME
Glutamine 274	Gln274
Glutathione	GSH
Glutathione peroxidase	GPx
Heart failure	HF
Hepatoblastoma cell line	HepG2
Histone 3	H3
Histone 4	H4
Histone acetyltransferases	HATs
Histone deacetylases	HDACs
Histone demethylases	HDMs
Histone methyltransferases	HMTs
Horseradish peroxidase	HRP
Human breast cancer cell line	MCF-7
Human embryonic kidney cell line	HEK293
Human monocytic leukaemia cell line	THP-1
Inducible nitric oxide synthase	iNOS
Interferon gamma	IFN-γ
Interleukin 10	IL-10
Interleukin 6	IL-6
Interleukin-1-beta	IL-1β
Lysine 20 histone 4	H4K20
Methyl-CpG binding domain protein 2	MBD2
Nitric oxide	NO

Nitric oxide synthase assay	NOS assay
N-terminal GSDMD	N-GSDMD
N-(1-naphthyl) ethylenediamine	NEDD
Nucleotide-binding oligomerisation domain	NOD
Nod-like receptor protein 3	NLRP3
Nuclear factor kappa B	NF-κB
Pathogen-associated molecular patterns	PAMPs
Pattern recognition receptors	PRRs
Phosphate buffered saline	PBS
Phosphorylated NF-κB	P-NF-κB
Proline 113	Pro113
Quantitative polymerase chain reaction	qPCR
Rat kidney epithelial cells	NRK-52E
Reactive oxygen species	ROS
Relative Band Density	RBD
S-adenosyl methionine	SAM
5-methylcytosine	5mc
Serine 203	Ser203
Serine 99	Ser99
Sodium dodecyl sulfate-polyacrylamide gel electrophoresis	SDS-PAGE
South Africa	SA
Sphinganine/sphingosine ratio	Sa/So ratio
Sphingosine-1-phosphate	S1P
Superoxide dismutase	SOD

Transforming growth factor-beta 1	TGF-β1
Tumour necrosis factor-alpha	TNF-α
Tyrosine 115	Tyr115

Abstract

Fumonisin B_1 (FB_1), a mycotoxin produced by *Fusarium* species, is a significant contaminant in cereal grains, posing serious health risks. This pilot study investigated the cardiotoxic effects of acute FB_1 exposure on inflammation and epigenetic modifications in C57BL/6 mice. Given the pilot nature of this study, acute exposure was prioritised to establish initial findings. Molecular docking was employed to predict the binding interactions of FB_1 with key inflammatory proteins, including tumour necrosis factor-alpha (TNF-α), inducible nitric oxide synthase (iNOS), and nuclear factor kappa B (NF-κB) subunits. In vivo experiments involved treating mice with 5 mg/kg FB_1 for 24 hours, followed by heart tissue analysis using quantitative polymerase chain reaction (qPCR), Western blotting, nitric oxide synthase assay (NOS assay), and enzyme linked immunosorbent assay (ELISA) to assess selected gene and protein expression levels of inflammatory markers and DNA methylation.

Docking results indicated that FB_1 binds to inflammatory proteins TNF-α, iNOS, NF-κB (p65), and NF-κB (p50), potentially altering their function. Gene expression analysis revealed significant downregulation of pro-inflammatory cytokines (*TNF-α, interleukin-6 (IL-6), interleukin-1β (IL-1β)*) and the anti-inflammatory cytokine *interleukin-10* (*IL-10*), while protein analysis showed an upregulation of these cytokines, suggesting a complex regulatory mechanism. Additionally, FB_1 exposure led to increased levels of reactive nitrogen species and significant upregulation of DNA methylation, indicating epigenetic modulation.

This study elucidates the cardiotoxic effects of FB_1 on mice, emphasizing the intricate interplay between inflammatory pathways and DNA methylation. Molecular docking studies suggest that FB_1 may bind to key residues on TNF-α, iNOS, and NF-κB subunits, potentially modulating these proteins' activity and triggering inflammatory responses. In vitro analysis demonstrated significant dysregulation of inflammatory and DNA methylation-related genes, with a notable upregulation of pro-inflammatory cytokines (TNF-α, IL-6, IL-1β) and anti-inflammatory mediators (IL-10, Transforming growth factor beta 1 (TGF-β1)) at the protein level. The observed disparity between gene and protein expression could be attributed to several factors, including post-transcriptional and post-translational modifications. These modifications are crucial in biological processes and can cause differences between mRNA and protein levels. Translational regulation, which involves the recruitment of various mRNA species to the ribosome, can lead to a decreased correlation between mRNA and protein amounts. Additionally, the study found contradictory DNA methylation results: global DNA methylation levels were upregulated, indicating hypermethylation, while DNA methylation

gene (DNMT) expression was decreased. This suggests a complex interplay between DNA methylation and gene expression, potentially influenced by other regulatory mechanisms like microRNAs. These findings highlight the need for further validation using additional tests, such as Northern blots and microarray assays. Overall, the study underscores FB_1's ability to activate inflammatory pathways and cause cardiac distress through cytokine dysregulation and epigenetic changes. Further research is essential to fully understand the mechanisms of FB_1-induced cardiotoxicity and the potential therapeutic role of DNA methylation in mitigating these effects.

Chapter 1: Introduction

1.1 Background

Food is necessary for the sustenance of life for all living organisms. A major food source for countries around the world is derived from cereal crops such as wheat, sorghum, and maize (Wrigley, 2019). These grains have therefore been identified as a major source of energy and hence are prevalent in significant quantities in both human and animal diets predominantly in African countries such as South Africa (SA). One of the pioneering producers of maize worldwide is SA with an estimated 16 million metric tonnes produced in 2017 (Tebele *et al*., 2020). Whilst these grains are essential for life, they are susceptible to disease caused by toxins specifically, mycotoxins. As a leading manufacturer of cereal grains, SA is at the forefront of susceptibility to mycotoxin contamination, which leads to not only economic losses but also adverse health outcomes in humans and animals (Beukes, 2017). Fungal secondary metabolites known as mycotoxins can infiltrate and infect crops at various stages during cultivation, namely, harvest, storage, and processing (Adebo *et al*., 2019). Whilst manmade processes affect the contamination of these crops in substantial amounts they are not the sole factor responsible as environmental conditions such as humidity, elevated temperatures, drought, and unpredictable rainfall have been identified as important contributors to the total mycotoxin contamination (Tebele *et al*., 2020, Zahra *et al*., 2019, Adebo *et al*., 2019). A plethora of mycotoxins have been isolated and recognised with a specific subset of 30 mycotoxins posing as key disease-causing contaminants. Some of these mycotoxins include ochratoxin, aflatoxins, patulin, zearalenone, citrinin, and fumonisins, which pose imminent threats to human and animal health (Marcelloni *et al*., 2023). Amongst these mycotoxins, fumonisins have been shown to contribute copious amounts to disease in humans and animals as a potent toxicant. Fumonisins are produced by *Fusarium* spp., with *Fusarium verticilliodes* and *Fusarium proliferatum* being highlighted as species within the family that possess the ability to produce high amounts of fumonisin contamination (Zahra *et al*., 2019, Chen *et al*., 2021b). There have been 28 different analogues of fumonisin that have been identified with the ability to cause contamination. Present amongst these analogues is fumonisin B_1 (FB_1), which has been identified as the leading fumonisin prevalent in most global contamination cases, accounting for approximately 70% of these contamination cases (Chen *et al*., 2021a). Due to high contamination cases, research into FB_1 remained imperative thus initiating successive research into the mycotoxin. Research uncovered a high similarity between the chemical structure of

FB_1 and the structures of sphingoid bases, sphinganine, and sphingosine. Both FB_1 and sphingoid bases share a long-chain backbone with multiple hydroxyl groups and an amino group, which are essential for their biological functions. Moreover, FB_1 has been involved in the inhibition of sphingosine and ceramide synthase as it acts as a competitive inhibitor for the substrates involved. Therefore, it can interrupt sphingolipid synthesis and cause downstream negative effects (Lumsangkul *et al*., 2021, Merrill Jr *et al*., 2001). This fundamental property of FB_1 makes it a potent cardiotoxic substance as it has been shown to block sphingosine-mediated l-type calcium channels and ultimately can lead to heart failure. Other studies have shown the ability of FB_1 to cause a decrease in heart rate, myocardial contractility, and arterial blood pressure; however, the specific mechanisms remain elucidated (Wang *et al*., 2016, Chen *et al*., 2021b, Constable *et al*., 2000). Therefore, insight into the cardiotoxic effects of FB_1 remains imperative as there is limited research. Multiple cardiac abnormalities, such as atherosclerosis and heart failure, are characterised by dysregulation of the inflammatory response. Several studies have revealed the crucial role of FB_1 in exacerbating the cytokine network, leading to a heightened inflammatory response (Sharma *et al*., 2003a). This suggests the significant role that inflammatory pathways could play in these conditions.

Inflammation is a response crucial to ensure survival during infection and injury and is elicited when cells are subjected to damage by a plethora of factors such as DNA damage, oxidative stress, mitochondrial stress, autophagy, inflammasome prevalence and epigenetic alterations (Gusev and Zhuravleva, 2022). Stimuli responsible for inflammation recognition occur through the detection by the innate and adaptive immune systems via transmembrane receptors known as pattern recognition receptors (PRRs) (Chen *et al*., 2018). These PRRs are responsible for finding cellular damage, by sensing specific structures present in microbes known as pathogen-associated molecular patterns (PAMPs) and danger-associated molecular patterns (DAMP) (Gusev and Zhuravleva, 2022, Ahmed, 2011). A cascade of inflammatory responses governs these interactions between stimuli and signalling. Coordination of these inflammatory responses arises due to the transcription of genes known as pro-inflammatory cytokines such as tumour necrosis factor-alpha (TNF-α), interleukin-1 beta (IL-1β), interleukin-18 (IL-18), interleukin-6 (IL-6), and nuclear factor kappa B (NF-κB) (Shaikh, 2011). The increase in pro-inflammatory factors has therefore been characteristic of numerous disease pathogenesis such as neurodegenerative disorders, obesity, hepatosis, atherosclerosis, cardiopathy and heart failure (Gusev and Zhuravleva, 2022). Research has depicted that the increasing circulation of proinflammatory cytokines such as TNF-α, IL-6, IL-1β, and IL-18 in cardiac tissue due to stress

has been associated with structural and functional changes in cardiomyocytes. Key changes induced in cardiomyocytes due to inflammation include hypertrophy, contractile dysfunction, and cardiomyocyte apoptosis which eventually leads to the onset of chronic heart failure (HF) (Gusev and Zhuravleva, 2022, Hedayat *et al*., 2010). A pathway involved in the inception of heart failure is the pyroptotic mechanism which has been shown to have regulatory functions in cardiovascular diseases, especially HF. The canonical pathway of pyroptosis is initiated when infected cells activate PRRs, which subsequently stimulates PAMPs and DAMPs which activates downstream interactions that result in the cleavage of pro-caspase 1 into caspase 1 (Chen *et al*., 2022). The activation of caspase 1 has multiple major effects, namely, the formation of the inflammasome when it is combined with PRRs, and apoptosis-associated speck-like protein (ASC) and it can prompt the cleavage of pro-IL-1β and pro-IL-18 into IL-1β and IL-18 which heightens the inflammatory response (Franchi *et al*., 2009). However, caspase 1 is also responsible for the activation of Gasdermin D (GSDMD) which induces the execution of pyroptosis. Studies have thus shown that pyroptosis can induce cardiomyocyte death, myocardial hypertrophy, and cardiac fibroblast by inducing specific proinflammatory factors such as TNF-α, IL-6, IL-1β, and IL-18 and inflammasomes such as the NOD-like receptor protein 3 (NLRP3) (Yu *et al*., 2021, Chai *et al*., 2022). This is linked with FB_1 toxicity as a crucial defining characteristic of FB_1 toxicity is readily seen by the increase in sphingosine levels due to the structure of FB_1. A study showed that endogenous lipid metabolite sphingosine can act as a DAMP by inducing the NLRP3-inflammasome-dependent secretion of IL-1β. Moreover, other studies have shown that FB_1 can contribute to a heightened inflammatory response (Luheshi *et al*., 2012, Sharma *et al*., 2003a). This complex interplay between inflammation and pyroptosis which can be induced by FB_1 is susceptible to epigenetic alterations as FB_1 has been shown to cause genome instability by causing alterations in DNA methyltransferase (DNMT) activity which leads to epigenetic dysfunction (Sugiyama *et al*., 2021).

Epigenetics is categorised as the regulation of gene activity by external modifications on DNA by processes such as DNA methylation and histone modifications. DNA methylation is regulated by DNMTs whereas histone modifications depend on a variety of enzymes such as histone acetyltransferases (HATs) and deacetylases (HDACs), methyltransferases (HMTs) and demethylases (HDMs), ubiquitin ligases, phosphatases, and kinases (Li, 2021, Kanwal and Gupta, 2012). Investigations into the role of FB_1 and epigenetic alterations have depicted the ability of FB_1 to induce alterations such as hypermethylation, hypomethylation, di- and tri-

methylation of lysine 9 on histone 3, and reduced methylation of lysine 20 of histone 4 (H4K20) (Arumugam and Chuturgoon, 2021). Epigenetic changes can lead to disease pathogenesis. Therefore, the emerging role of epigenetics in multiple diseases, especially cardiovascular disease has been of interest. Various research studies have shown that epigenetic alterations, namely, DNA demethylation leads to cardiac hypertrophy, HDAC1 increases cardiac fibrosis in a mice model of HF, and deletion of DNMT3B in adult cardiomyocytes led to impairment of heart function and subsequent heart failure (Lei *et al*., 2021, Nural-Guvener *et al*., 2014, Vujic *et al*., 2015). It is therefore crucial to understand the role FB_1 plays in eliciting disease via inflammation, pyroptosis and epigenetic pathways in cardiac tissues.

1.2 Problem Statement / Rationale

In 2019, the BIOMIN mycotoxin survey recorded an alarming 73% of mycotoxin contamination in food and feed in a selected tested sample group. An abundant mycotoxin plaguing various cereal grains around the world is FB_1. Statistics have shown that 70% of global contamination cases caused by mycotoxins are attributed to FB_1, it is further stated that 50% of FB_1 contamination is found in spoiled maize and maize-based products, (Dey *et al*., 2023, Lumsangkul *et al*., 2021, Chen *et al*., 2021b). The high prevalence of FB_1 contamination is distressing as this mycotoxin has been shown to have adverse effects in both animals and humans. Studies have shown that FB_1 can induce pulmonary oedema in pigs, equine leukoencephalomalacia, nephrotoxicity and hepatotoxicity in rodent models (Haschek *et al*., 2001, Kellerman *et al*., 1990, Domijan, 2012). In humans, FB_1 has been linked with the increasing predisposition to cancers such as primary liver cancer and oesophageal cancer in different regions around the world with Transkei, South Africa being a hub as maize is a staple dietary component (Rheeder *et al*., 2002). Research has shown that FB_1 has serious cardiotoxic effects, including decreased heart rate, myocardial contractility, and arterial blood pressure; however, the specific mechanisms of action remain unclear (Constable *et al*., 2000). Therefore, understanding the mechanism of FB_1 in cardiac tissue is crucial. Inflammation and epigenetics are potential pathways linking FB_1 to cardiac distress. This study aimed to investigate FB_1-induced inflammation and DNA methylation changes in C57BL/6 mice hearts after 24 hours of exposure.

1.3 Significance / Implications

Research has identified several toxic effects of FB_1, including changes in sphingolipid biosynthesis, oxidative stress, mitochondrial dysfunction, apoptosis, and inflammation (Chen

et al., 2021b). Many animal studies have shown FB_1's harmful effects on various tissues and organs, particularly the kidneys, liver, and gastrointestinal tract (Chen *et al*., 2021c). However, there is limited data on its effects on heart tissue. Among the few studies on FB_1's cardiotoxicity, it has been shown to block sphingosine-mediated L-type calcium channels, leading to heart failure. Additionally, FB_1 can decrease myocardial contractility and arterial blood pressure. Other cardiotoxic effects of FB_1 are linked to changes in sphingolipid metabolism, causing systemic hypotension (Chen *et al*., 2021b; Constable *et al*., 2000; Wang *et al*., 2016). Key pathways involved in cardiac distress include inflammation and epigenetics. Recent data indicate that FB_1 can upregulate these pathways in the gastrointestinal tract and liver, leading to disease, which may also affect cardiac tissues (Li *et al*., 2020). Therefore, investigating inflammation and epigenetic pathways is crucial to understanding how FB_1 causes cardiac distress in both animals and humans.

1.4 Research Questions

Can 24-hour FB_1 exposure lead to inflammation and changes in DNA methylation in C57BL/6 mice hearts, as acute exposure is crucial for identifying early biomarkers of toxicity and understanding the initial pathways affected?

1.5 Hypothesis

The 24-hour exposure of FB_1 leads to cardiac distress via inflammation with subsequent DNA methylation changes in C57BL/6 mice hearts.

1.6 Aim

To investigate FB_1-induced inflammation and DNA methylation changes in C57BL/6 mice hearts after 24 hours of exposure.

1.7 Objectives

- The binding affinity of FB_1 on TNF-α, iNOS, NF-κB (p65) and NF-κB (p50) was determined in silico via molecular docking.
- Assess markers of inflammation and apoptosis such as phosphorylated NF-κB and caspase 3 using western blot.
- Measure the expression of inflammation-related genes, including the *NLRP3 inflammasome*, cytokines (*IL-1β, IL-18, IL-6, IL-10*), *GSMD*, and *caspase 1* and *3*.
- Evaluate inflammatory factors (TNF-α, IL-1β, IL-6, IL-10, TGF-β) using the ELISA assay.

- Determine the protein expression of DNA methylation regulators such as MBD2 and DNMT1 using western blot.
- Assess gene expression of *MBD2, DNMT1, DNMT3A* and *DNMT3B* using qPCR.
- Assess global DNA methylation levels using the ELISA assay.

Chapter 2: Literature Review

2.1 Fumonisin B_1 (FB_1)

A growing medical issue adding to the healthcare burden is the increasing prevalence of mycotoxin toxicity, which is linked to a variety of diseases. Over 500 mycotoxins have been identified in recent years (Awuchi *et al*., 2022). Among these, the sphingosine/sphinganine analogue mycotoxin, FB_1, has attracted significant research interest. The toxin, FB_1 belongs to the fumonisin family, which are water-soluble mycotoxins produced by *Fusarium verticilliodes* and *Fusarium proliferatum*. The fumonisin family includes several groups based on their structural moieties: A, B, C, D, P, Py, and La (Anumudu *et al*., 2024). The B group is particularly notable for its prevalence in food. The fumonisin B (FB) group consists of three main subtypes: FB_1, which accounts for 70% of total FBs; FB_2, which contributes approximately 15–25%; and FB_3, which makes up about 3–8% of contamination in maize and rice (Awuchi *et al*., 2022, Gao *et al*., 2023, Chen *et al*., 2021a). These metabolites are significant in toxicology due to their role in food and feed contamination, posing health risks to both humans and animals (Gao *et al*., 2023). FB_1 is the most researched due to its high prevalence. The structure of FB_1 is characterised as a diester of propane-1,2,3-tricarboxylic acid and a complex amino alcohol, esterified at the terminal carboxyl groups at C-14 and C-15 (Figure 2.1). This structure is similar to the sphingoid bases sphingosine and sphinganine. FB_1 toxicity is often measured by the sphinganine/sphingosine ratio; an increase in this ratio correlates with higher FB_1 toxicity (Ahangarkani *et al*., 2014).

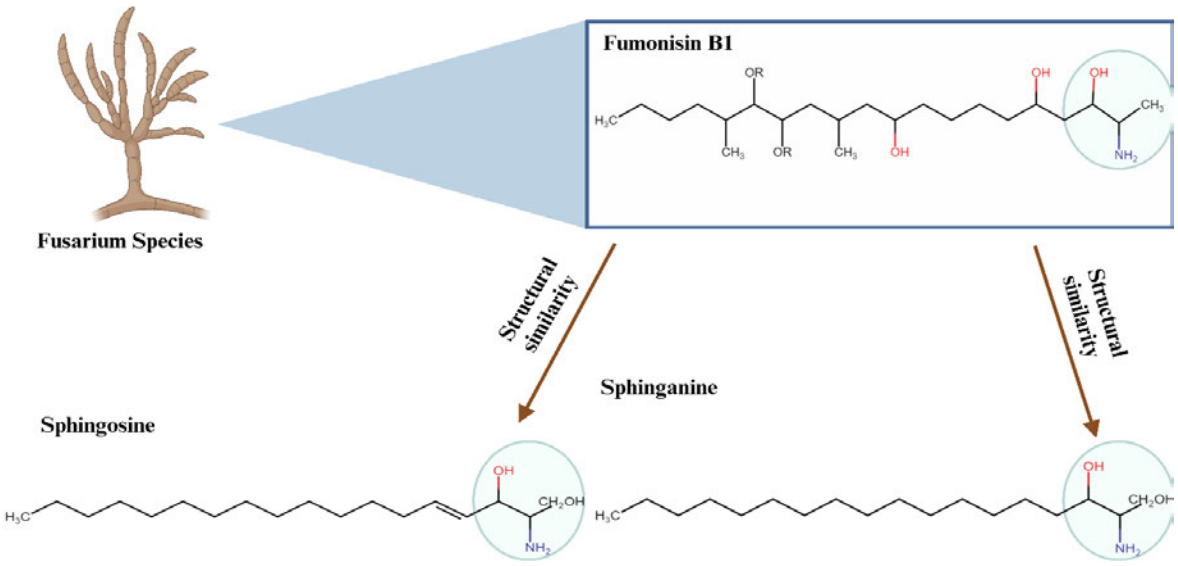

Figure 2.1: A structural comparison between FB_1 and its analogues, sphingosine and sphinganine. The sphingoid backbone is the shared chemical structure amongst these metabolites (Prepared by the Author).

2.1.1 FB_1 Contamination Rates

Countries around the world have been plagued by FB_1 contamination, and the reports of its contamination have been increasing. A study conducted in South Korea found that fumonisin contamination was found to be 93.33% and 83.33% in selected feed and feed components respectively (Kim *et al*., 2013)(Figure 2.2). Research conducted in California in 2013, revealed that FB_1 toxicity was prevalent in approximately 76% of all tested samples, which showed a relatively lower incidence of other mycotoxins thus portraying the severity of FB_1 contamination(Krout-Greenberg *et al*., 2013). African countries such as Algeria had an astonishing 96,6% FB_1 contaminated samples, this is contrasted in the same study with other mycotoxins such as zearalenone which only were detected in 7 samples when compared to fumonisins which infected 29 samples(Mahdjoubi *et al*., 2020). Other African countries including Nigeria illustrated a high presence of 97% FB_1 contamination in all tested samples and other studies conducted in South Africa revealed that maize samples obtained from subsistence farmers were 100%(Akinmusire *et al*., 2019). These statistics provide key insight into the overall severity of the contamination of FB_1. The high incidence of FB_1 around the world has sounded alarms as it can contribute to economic losses and it has been associated with a variety of toxic effects which ultimately can cause disease in both humans and animals (Kim *et al*., 2013, Krout-Greenberg *et al*., 2013, Mahdjoubi *et al*., 2020, Akinmusire *et al*., 2019, Yli-Mattila and Sundheim, 2022, Chen *et al*., 2021a).

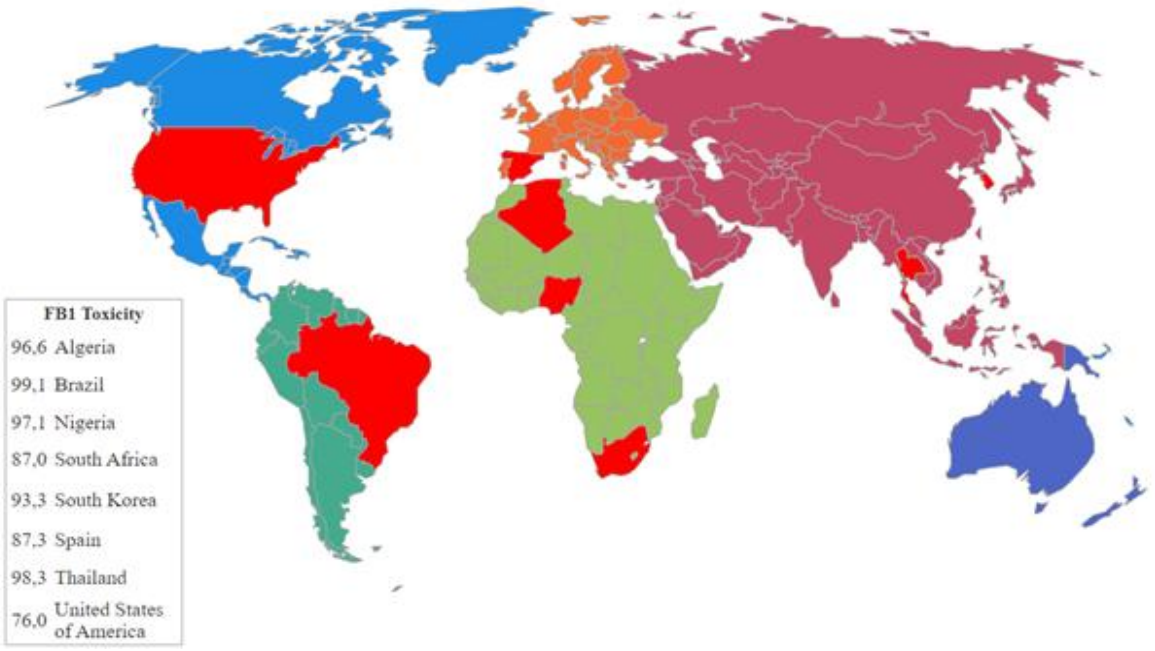

Figure 2.2: The highlighted red sections in the above map depict areas which tested a selected sample group of maize and discovered the rate of FB_1 contamination present, with Brazil denoting an alarming 99,1% rate, data obtained from a publication (Gao *et al*., 2023) (Prepared by the Author).

2.1.2 FB_1 Toxicity and Disease

Health-related risks associated with FB_1 toxicity have been identified in both animals and humans. A multitude of research has shown the ability of FB_1 to cause disease in animal models such as hepatitis in broilers, turkeys, and ducks, leukoencephalomalacia in horses, porcine pulmonary oedema, and is a potent liver and kidney carcinogen in rats and mice (Marasas *et al*., 1988, Haschek *et al*., 2001, Gelderblom *et al*., 1994). This is contrasted with research in humans, as limited data is available on the toxic effects of FB_1. Data obtained in Transkei, South Africa provided a correlation between oesophageal cancer and the consumption of FB_1 contaminated maize. This epidemiological study implicates FB_1 as a possible aetiological agent for oesophageal cancer (Marasas, 1996). Other studies revealed a potential link between FB_1 and human neural tube defects, coinciding with an outbreak of leukoencephalomalacia that devastated the Texas-Mexico border region (Hendricks, 1999). These studies provided vague associations between human health risks and FB_1. However, FB_1 has been shown to induce complex pathways such as sphingolipid biosynthesis alteration, oxidative stress, apoptosis, mitochondrial dysfunction, and inflammation which are involved in a variety of human. diseases.

2.1.3 FB_1 Mechanism of Action

The primary mechanism of action of FB_1 is its ability to alter the sphingolipid biosynthesis pathway. The structure of FB_1 is crucial, as its diester component, identified as tricarballylic acid with a polyhydric alcohol backbone, is similar to sphingosine and sphinganine (Zeng *et al*., 2020)(Figure 2.1). This similarity makes FB_1 an effective competitive inhibitor of ceramide synthase, a key enzyme in the sphingolipid biosynthesis pathway responsible for the acetylation of sphingosine. Sphingosine is part of the sphingolipid family, which includes lipids with a sphingosine and sphingoid base backbone found in the cell membranes of cardiomyocytes and neurons(Quinville *et al*., 2021). When fatty acids interact with sphingosine, they form ceramide, a core molecule in sphingolipid metabolism that can further interact with other moieties to form complex sphingolipids, such as sphingomyelin (Merrill Jr, 2011). Sphingolipids play crucial roles in various metabolic processes and function as signalling molecules. Key molecules derived from sphingolipids include sphingosine 1-phosphate (S1P), ceramide (Cer), and ceramide 1-phosphate (C1P), which are involved in cell signalling, migration, and death (Pralhada Rao *et al*., 2013a, Jamjoum *et al*., 2024). Alterations in sphingolipid metabolism due to FB_1 lead to increased intracellular levels of sphinganine and sphingosine and their 1-phosphate derivatives, while preventing the formation of dihydroceramides, complex sphingolipids, and ceramides. This alteration allows scientists to use the sphinganine/sphingosine ratio (Sa/So ratio) as a biomarker for FB_1 toxicity, with an elevated Sa/So ratio indicating FB_1-mediated toxicity (Riley and Merrill, 2019a, Soriano *et al*., 2005a, Yoo *et al*., 1996a). The effects of this mycotoxin are not limited to sphingolipid alterations. Research has identified its impact on oxidative stress and apoptotic pathways. Oxidative stress occurs when the balance between free radicals (FRs), including reactive oxygen species (ROS), and antioxidants is disrupted, leading to an accumulation of FRs (Hayes *et al*., 2020). This can cause protein, lipid, and DNA damage. Exposure to FB_1 can induce the production of ROS such as hydrogen peroxide (H_2O_2), lipid peroxide, and malondialdehyde (Kryston *et al*., 2011) (Figure 2.3). The increase in pro-oxidant activity is further amplified by a decrease in antioxidant activity, as FB_1 can inhibit superoxide dismutase (SOD), catalase (CAT), glutathione peroxidase (Gpx), and glutathione (GSH) at both molecular and gene expression levels (Gao *et al*., 2023). The resulting oxidative stress can lead to apoptosis or programmed cell death. Apoptosis can occur via extrinsic and intrinsic pathways, activated by extracellular and intracellular signals, respectively, and controlled by caspases (Carneiro and El-Deiry, 2020). Toxicity from FB_1 has been shown to activate apoptotic pathways, including

the transcription of protein kinase C, which regulates c-Jun N-terminal kinase via the mitogen-activated protein kinases pathway, leading to the induction of p53 up-regulated modulator of apoptosis and caspase 3 transcription, resulting in cell death (Figure 2.3). This mycotoxin also influences the Fas gene, mediating apoptosis through caspase 8 activation (Kim *et al*., 2018, Chen *et al*., 2021b). The harmful effects of FB_1 are not confined to these mechanisms, as evidence suggests it also activates other crucial pathways, such as inflammation and epigenetics.

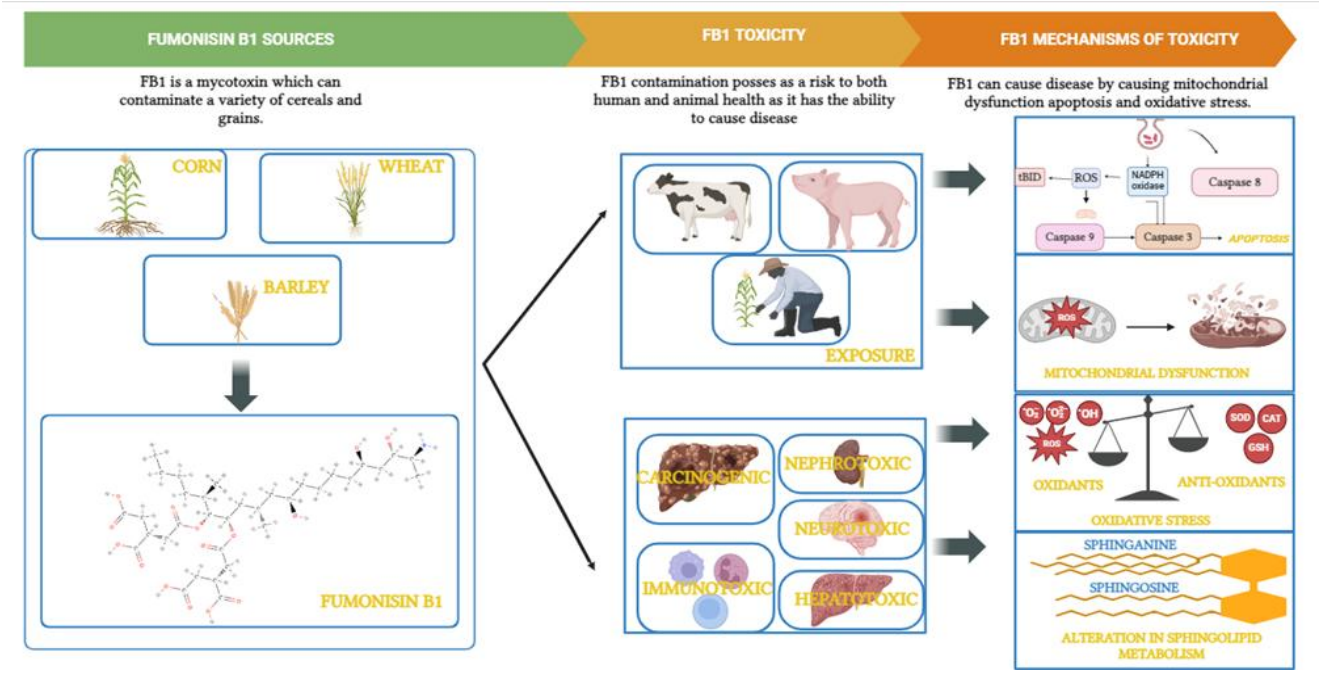

Figure 2.3: An overview of FB_1-mediated toxicity in different organs via the activation of pathways such as apoptosis, mitochondrial dysfunction, oxidative stress, and sphingolipid metabolism (Prepared by the Author).

2.2 Inflammation

Inflammation is a crucial process that helps mitigate the harmful effects of toxins, mechanical injuries, and microorganisms. It involves the recruitment of white blood cells (leukocytes) such as neutrophils, macrophages, basophils, eosinophils, and lymphocytes (Shi and Pamer, 2011). These cells release specialised proteins such as eicosanoids and proinflammatory cytokines to initiate the inflammatory response, which limits tissue damage and aids in repair and healing (Figure 2.4) (Abdulkhaleq *et al*., 2018a). Key signs of inflammation include redness, heat, pain, and swelling. The process begins with the dilation of venules and arterioles and increased blood vessel permeability, which can lead to thrombosis and stasis(Alharbi *et al*., 2023). This allows

leukocytes to infiltrate the tissue and remove plasma, followed by tissue breakdown and free radical production. These events activate cell death pathways (necrosis and apoptosis), leading to the removal of dead cells and the formation of new tissue (Schmid-Schönbein, 2006). Inflammation can be acute or chronic. Acute inflammation is a short-term response to tissue damage caused by toxins or harmful stimuli, with symptoms resolving in a few days. In contrast, chronic inflammation is long-term, lasting for months or even years (Pahwa *et al*., 2024).

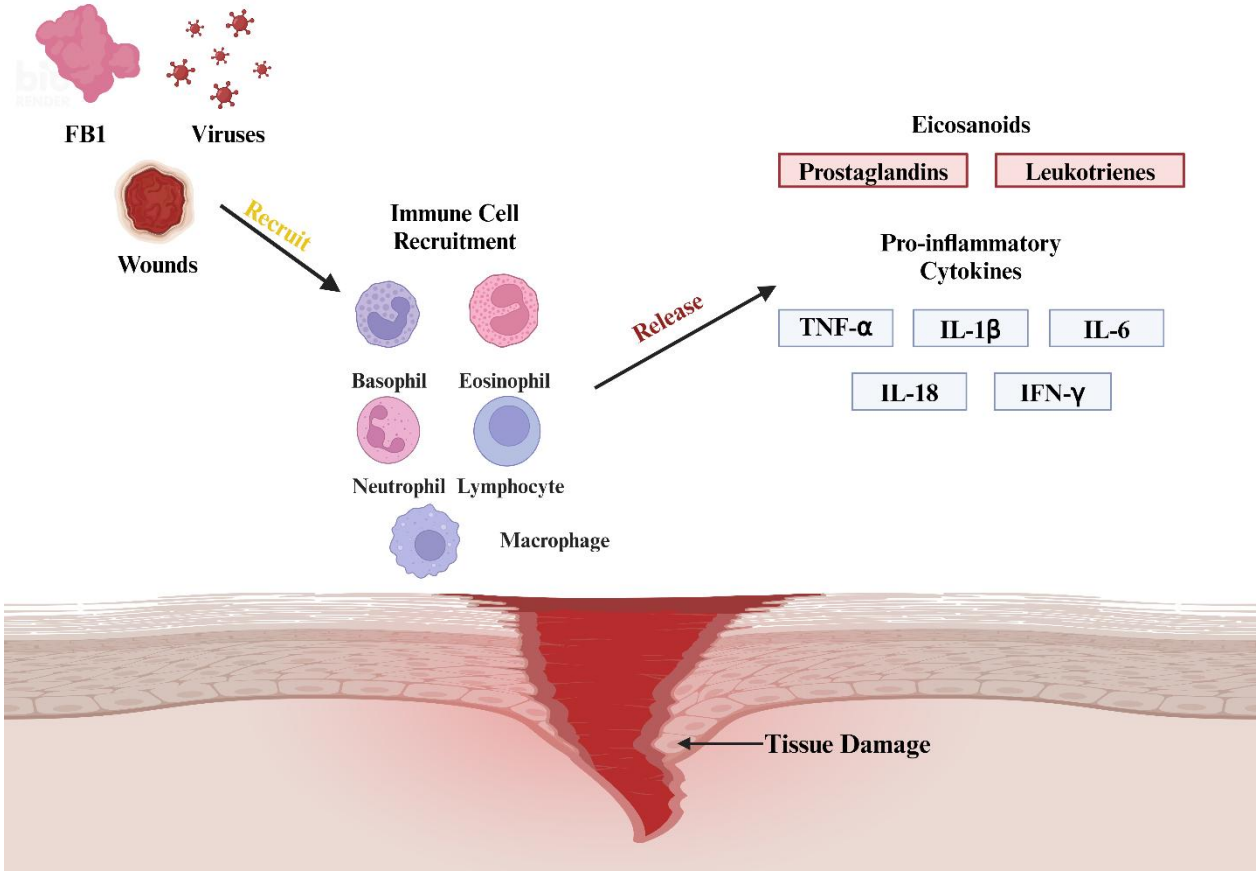

Figure 2.4: Inflammatory Response at the Site of Injury. The diagram illustrates the inflammatory response triggered at a site of injury caused by various insults such as toxins (e.g., FB_1), wounds, and viruses. These insults lead to the recruitment of immune cells, including eosinophils, basophils, neutrophils, lymphocytes, and macrophages. Upon arrival at the injury site, these immune cells release pro-inflammatory mediators. Specifically, eicosanoids such as prostaglandins and leukotrienes, along with cytokines including TNF-α, IL-1β, IL-6, IL-18, and IFN-γ, are released. These mediators play crucial roles in amplifying the inflammatory response and facilitating the healing process. FB_1: Fumonisin B_1; IFN-γ: Interferon-gamma; IL-1β: Interleukin-1 beta; IL-18: Interleukin-18; IL-6: Interleukin-6; and TNF-α: Tumour Necrosis Factor-alpha; (Prepared by author).

2.2.1 Inflammatory Pathway

The inflammatory pathway is activated when foreign entities such as toxins like FB_1, foreign cells, and tissue damage trigger a cascade of mediators that induce an inflammatory response. This process relies on essential factors: inducers (toxins and harmful stimuli), sensors (specific molecules activated by inducers), and mediators (substances that promote or inhibit inflammation and facilitate tissue repair) (Varela *et al*., 2018). The first crucial inducers identified are PRRs, which include PAMPs that recognise foreign organisms and DAMPs released by damaged host cells. These PRRs are detected by specialised receptors such as Toll-like receptors, C-type lectin receptors, and nucleotide-binding oligomerisation domain **(**NOD-like receptors). The interactions between stimuli, inducers, and receptors transmit downstream signalling, activating genes regulated both transcriptionally and post-transcriptionally (Figure 2.5) (Ahmed, 2011).

The genes responsible for coordinating the inflammatory response encode mediators, known as pro-inflammatory cytokines and chemokines, such as TNF-α, IL-1β, IL-18, and IL-6. Among these, TNF-α and IL-1β are potent inflammatory molecules, primarily functioning in acute inflammation. Stimulation of TNF-α by toxins can activate the NF-κB pathway, which regulates the expression of inflammatory genes for cytokines and molecules such as IL-1β, IL-6, IL-8, and inducible nitric oxide synthase (iNOS) (Tripathi and Aggarwal, 2006). The IL-6 cytokine family includes cardiotrophin-1 (CT-1), which can mitigate a pro-inflammatory environment by inhibiting TNF-α and degrading IκB, an inhibitory factor of NF-κB, thus playing a role in NF-κB pathway activation (Jougasaki, 2010). The enzyme iNOS, activated after NF-κB transcription, produces nitric oxide (NO) from the L-arginine pathway. At low concentrations, NO inhibits cytokines and chemokines, but at higher concentrations, it can aggravate the pro-inflammatory response and cause tissue damage (Laroux *et al*., 2001, Guzik *et al*., 2003). Increased NF-κB activity also triggers the transcriptional activation of inflammasomes, specifically the NLRP3 inflammasome. Activation of the NLRP3 inflammasome, influenced by the pro-IL-1β signal leads to caspase 1 activation, which cleaves pro-IL-1β and pro-IL-18 into their active forms, further amplifying the inflammatory response (Franchi *et al*., 2009).

Caspase 1 activation can also trigger pyroptotic cell death by cleaving GSDMD into its N-terminal form (N-GSDMD), creating pores in the cell membrane. Similarly, increased caspase 3 activity can cleave Gasdermin E (GSDME) at the N-terminal, leading to pore formation and pyroptotic cell death (Zmora *et al*., 2017, Tsuchiya *et al*., 2019, Jiang *et al*., 2020). These

mediators exacerbate inflammation by altering vascular permeability, leading to neutrophil recruitment to the injury site. The duration of inflammation depends on the injury's severity and is often associated with excessive pro-inflammatory cytokine activation (Ahmed, 2011).

To mitigate the detrimental effects of an altered inflammatory response, the anti-inflammatory cytokine IL-10 is stimulated to limit inflammation. IL-10 inhibits macrophages at the injury site, decreasing pro-inflammatory cytokines, and suppresses antigen presentation in dendritic cells, attenuating the pro-inflammatory response (Steen *et al*., 2020). Another anti-inflammatory cytokine, TGF-β1, regulates apoptosis, cell growth, and differentiation. When pro-inflammatory cytokines such as TNF-α activate the NF-κB pathway, they can induce TGF-β1 expression (R Skeen *et al*., 2012). The expression of TGF-β1 suppresses pro-inflammatory TNF-α and IL-1β, creating a more anti-inflammatory environment (Kim *et al*., 2021).

This pathway's complexity can be altered by xenobiotics such as FB_1. Over the years, crucial links have been established between FB_1 toxicity and its ability to alter inflammatory responses. A study by Wan *et al.* showed that FB_1 treatment upregulated pro-inflammatory genes such as IL-1α, IL-1β, IL-6, IL-8, and TNF-α in a porcine jejunal epithelial cell line, although protein expression levels were not measured (Wan *et al*., 2013). High-dose FB_1 exposure in mice intestines significantly upregulated both pro-inflammatory mediators (TNF-α, IL-1β) and anti-inflammatory mediators (IL-4, IL-10), indicating FB_1's complex role in altering the inflammatory response (Li *et al*., 2020). Studies on mice livers revealed increased levels of IL-1β, IL-2, IL-6, TNF-α, and NF-κB (p-p65), contributing to a heightened inflammatory response, along with elevated TGF-β1 and caspase 3, indicating apoptosis activation (Cao *et al*., 2022). In porcine kidney cells, FB_1 treatment significantly increased the gene and protein expression of TNF-α, NF-κB, and caspase 3, reinforcing FB_1's role as a potent pro-inflammatory and apoptotic stimulator (Chen *et al*., 2020). Numerous studies by Sharma *et al*. in 2003 and 2001 highlighted the critical roles of TNF-α and interferon gamma (IFNγ) in FB_1-induced hepatotoxicity. Further research by Sharma *et al*. showed that cytokines TNF-α, IL-1β, IL-6, IL-10, IL-12, and IFNγ were all upregulated after FB_1 exposure, exacerbating the cytokine network (Sharma *et al*., 2003a, Bhandari *et al*., 2001b). Given the evidence of FB_1's ability to provoke inflammatory and apoptotic pathways across different tissues and species, investigating its effects on the heart is imperative. The inflammatory pathway is influenced by key post-translational modifications, including epigenetic changes, indicating a more complex role in regulating inflammation.

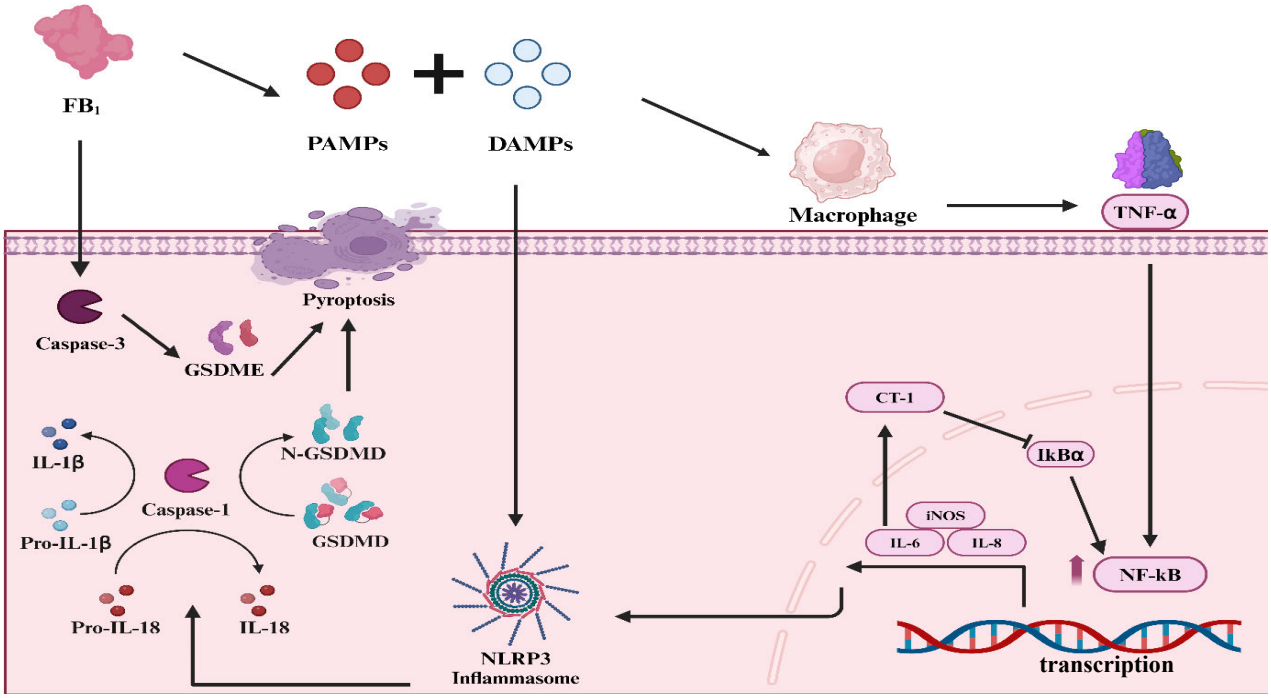

Figure 2.5: Activation of Inflammatory Pathways in Response to Cellular Damage. The inflammatory pathways activated in response to cellular and tissue damage can be caused by toxins such as FB_1. This damage stimulates the activation of PRRs, specifically PAMPs and DAMPs. These receptors trigger the transcriptional activation of cytokines and chemokines from immune cells, such as macrophages, at the site of injury. The activation sequence typically begins with TNF-α, which activates NF-κB by phosphorylating its inhibitory complex IκBα. This activation can be inhibited by CT-1. NF-κB then binds to DNA sites to regulate the expression of other inflammatory mediators, including iNOS, IL-6, and IL-8. The activation of these cytokines can subsequently prompt the activation of the NLRP3 inflammasome, which signals caspase-1 to cleave inactive IL-18 and IL-1β into their active forms. Additionally, caspase-1 can cleave GSDMD, leading to the activation of pyroptosis. Pyroptotic pathways can also be induced by the activation of caspase-3, which activates GGSDME. CT-1: Cardiotrophin-1; DAMPs: Damage-Associated Molecular Patterns; FB_1: Fumonisin B1; GSDMD: Gasdermin D; GSDME: Gasdermin E; iNOS: Inducible Nitric Oxide Synthase; IκBα: Inhibitor of Nuclear Factor Kappa-B Alpha; IL-1β: Interleukin-1 Beta; IL-18: Interleukin-18; IL-6: Interleukin-6; IL-8: Interleukin-8; NF-κB: Nuclear Factor Kappa-B; NLRP3: NOD-like Receptor Protein 3; PAMPs: Pathogen-Associated Molecular Patterns; PRRs: Pattern Recognition Receptors; and TNF-α: Tumour Necrosis Factor-Alpha; Prepared by the Author.

2.3 Epigenetics, FB_1 and Inflammation

Epigenetics is an emerging field characterised by heritable changes in gene expression that do not involve mutations or alterations in the gene sequences. Instead, these changes rely on modifications to the external structure of DNA. One of the most studied epigenetic mechanisms

is DNA methylation, where a methyl group is added to the 5' position of cytosine residues, forming 5-methylcytosine (5mc) (Singal and Ginder, 1999). This process is governed by enzymes called DNA methyltransferases (DNMTs), including DNA Methyltransferase 1 (DNMT1), DNA Methyltransferase 3 Alpha (DNMT3A), and DNA Methyltransferase 3 Beta (DNMT3B). DNMT1 maintains DNA methylation during replication, ensuring the methylation pattern from the parent strand is copied to the new strand. In contrast, DNMT3A and DNMT3B establish new methylation patterns on unmethylated strands. Adding these methyl groups prevents proteins from recognizing specific gene sequences, thereby repressing gene expression (Hamilton, 2011, Gibney and Nolan, 2010, Bird, 2002).

Histone modifications, another form of epigenetic alteration, primarily occur through methylation and acetylation, though phosphorylation also plays a role. Methylation typically happens at lysine (K) residues on histone 3 (H3) and histone 4 (H4), facilitated by the methyl donor S-adenosyl methionine (SAM) via histone methyltransferases (HMTs) (Peterson and Laniel, 2004). Methylation can either repress or activate gene expression. For example, methylation at H3K4, H3K36, and H3K79 is associated with active gene expression, while methylation at H3K9, H3K27, and H4K20 is linked to repression. Histone acetylation, regulated by histone acetyltransferases (HATs) and histone deacetylases (HDACs), reduces the positive charge of lysine residues, inhibiting the binding between the histone tail and the negatively charged DNA strand, thus exposing the DNA for potential transcriptional activation. Deacetylation prevents this and causes gene repression (Zhang *et al*., 2021, Chrun *et al*., 2017a).

Several studies have shown the epigenetic effects of FB_1. For instance, treatment of human embryonic kidney (HEK293) cells with FB_1 significantly upregulated global DNA methylation due to increased DNMT activity, indicating the toxin's ability to affect methylation patterns (Sugiyama *et al*., 2021). Conversely, a 2014 study on hepatoblastoma (HepG2) cells revealed a significant decrease in DNMT activity and an increase in the demethylase methyl-CpG binding domain protein 2 (MBD2), indicating that FB_1 treatment led to DNA hypomethylation and structural changes in the DNA (Chuturgoon *et al*., 2014a). Similar findings were observed in C6 glioma cells, where FB_1 treatment induced DNA hypomethylation (Mobio *et al*., 2000). In rat kidney epithelial cells (NRK-52E), FB_1 increased levels of H3K9me2/me3 and decreased levels of H4K20me3 and H3K9ac, further indicating FB_1's ability to alter the epigenetic landscape. These studies highlight FB_1's role in altering epigenetic status, particularly DNA methylation.

The inflammatory response is also subject to epigenetic modification, leading to changes in inflammatory pathways (Figure 2.6). For example, in human breast cancer cell (MCF-7) cells, a correlation was found between IL-6 gene hypomethylation and decreased DNA methylation (Armenante *et al*., 1999). In female Wistar rats, DNA demethylation upregulated the expression of cytokines IL-11, IL-6, and TNF-α when treated with T-2 toxin (Liu *et al*., 2019). In a human monocytic leukemia cell line (THP-1), DNA methylation and H3K9 methylation silenced the TNF-α gene, altering the inflammatory response (Gazzar *et al*., 2008). Another study showed that hypermethylation at the promoter region silenced the NLRP3 gene, while DNA demethylation at the promoter region during *Mycobacterium tuberculosis* infection activated this gene, highlighting the critical role of epigenetics in regulating inflammatory responses (Wei *et al*., 2016). Given the complexities and overlap between these pathways, this study focuses on the crucial role of FB_1 in targeting DNA methylation as a primary mechanism for altering gene expression related to inflammation in mice hearts.

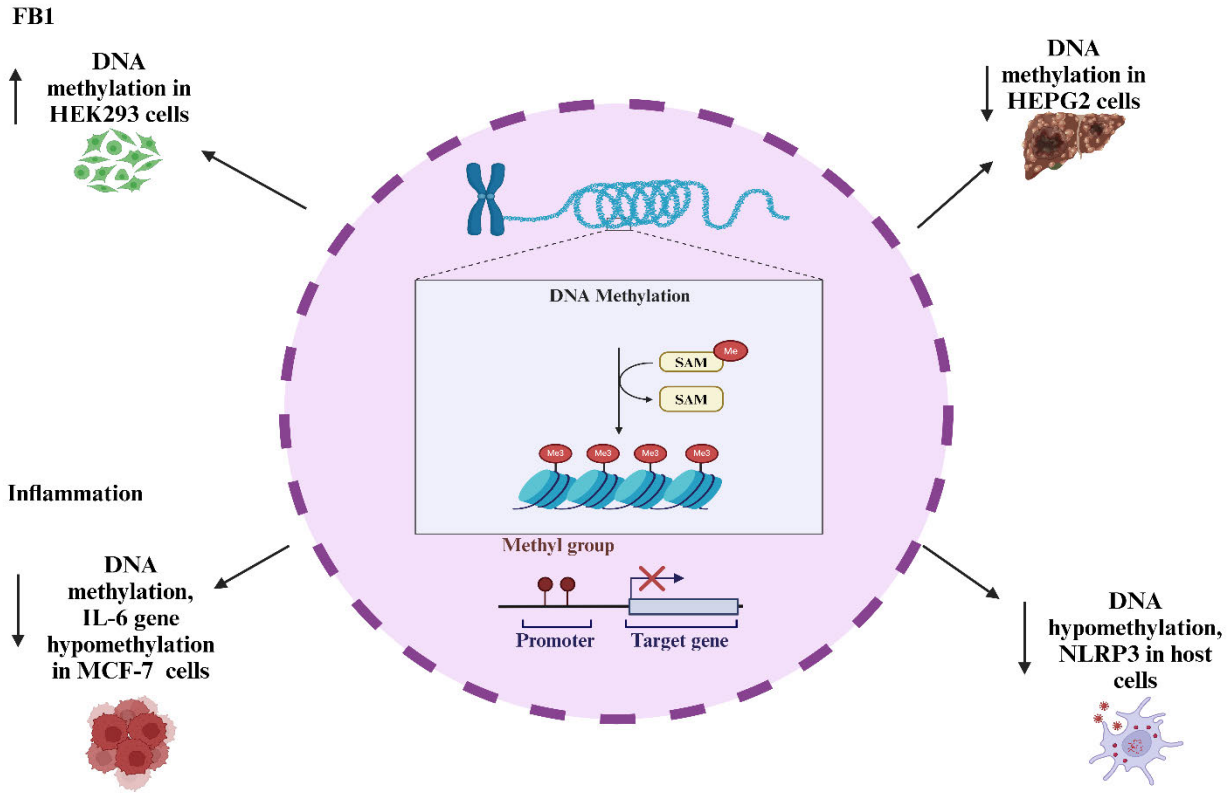

Figure 2.6: Effects of DNA Methylation on Gene Expression in Various Cell Types. The above figure illustrates DNA methylation occurring at both genomic and mitochondrial DNA. A methyl group, donated by SAM, is added to cytosine bases, leading to repressed gene transcription. The arrows in the diagram point to four different studies where DNA methylation was either increased or decreased due to FB_1 and inflammation, resulting in altered gene functions. These studies included HEK293 Cells:

Treatment with FB_1 upregulated DNA methylation, HEPG2 Cells: Treatment with FB_1 led to decreased DNA methylation. MCF-7 Cells: A correlation was found between IL-6 gene hypomethylation and decreased DNA methylation. Mycobacterium tuberculosis Infection: DNA demethylation at the promoter region activated the NLRP3 gene, whereas promoter region silencing occurred in other contexts. FB_1: Fumonisin B_1; HEK293: Human Embryonic Kidney 293 Cells; HEPG2: Human Hepatocellular Carcinoma Cells; IL-6: Interleukin-6; MCF-7: Human Breast Cancer Cells; NLRP3: NOD-like Receptor Protein 3; and SAM: S-adenosylmethionine; Prepared by the Author.

2.4 The Heart

The heart is a muscular organ located behind the sternum, consisting of two ventricles and two atria, which are separated by valves that regulate blood flow. The upper chambers, known as the atria, receive venous blood, while the lower chambers, the ventricles, pump blood from the heart to the arteries and lungs (Shaffer *et al.*, 2014). Blood flow through the heart begins when deoxygenated blood enters the right atrium, then passes through the tricuspid valve into the right ventricle. From there, it is pumped through the pulmonary arteries to the lungs, where it receives oxygen. The now oxygen-rich blood returns to the heart, entering the left atrium via the pulmonary veins. It then flows into the left ventricle, which contracts to send the oxygenated blood through the aorta and into the body's arterial system (Figure 2.7) (Shaffer *et al.*, 2014).

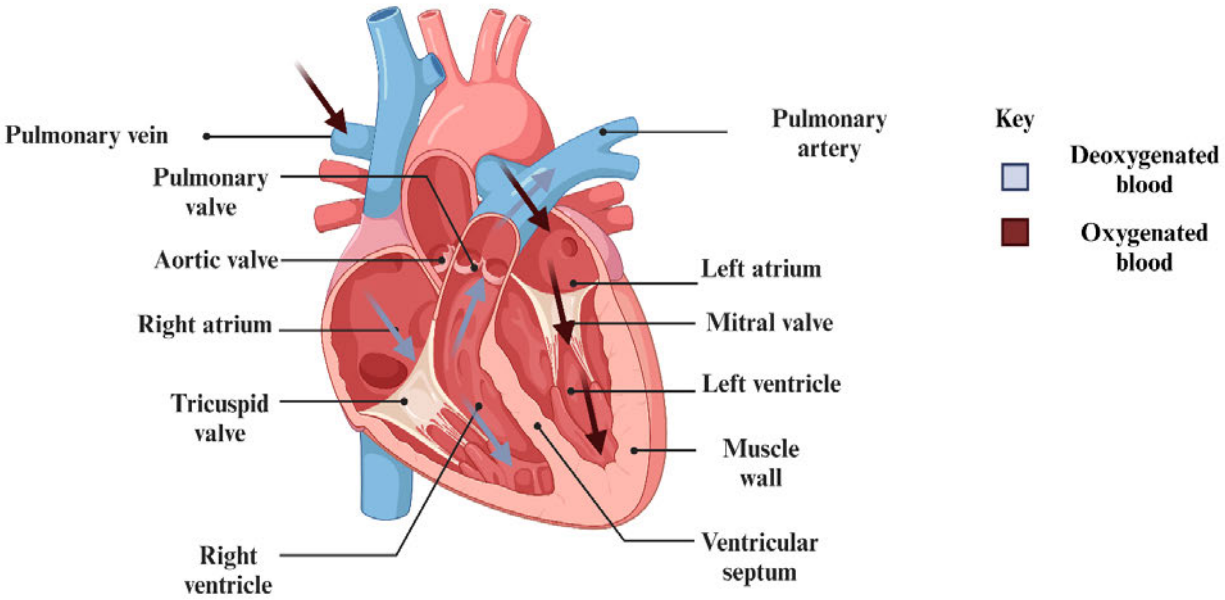

Figure 2.7: An overview of the heart's anatomy highlighting the four chambers that play a crucial role in effectively pumping blood throughout the body. It facilitates the flow of deoxygenated blood from

the atria to the ventricles and then to the lungs, where it is oxygenated before being returned to the heart and circulated throughout the body (Prepared by the Author).

The heart's complexity requires a diverse system of cell populations to manage processes such as electrical impulses and blood flow. Cardiomyocytes are the most abundant cell type in the heart, found in both the atrial and ventricular structures. They are responsible for the uniform contraction of the heart, enabling efficient pumping. This function is regulated by the control of calcium ion release, which governs the contraction and relaxation cycles of these myocytes (Woodcock and Matkovich, 2005). Pacemaker cells are another essential cell type, controlling the contraction of the heart chambers through electrical impulses regulated by a sophisticated pathway (Christoffels *et al*., 2010). Cardiac endothelial cells are highly organized and play a regulatory role in controlling immune cell recruitment and fibroblast activity, thereby influencing cardiac inflammation and the onset of cardiovascular disease (Lother *et al*., 2018).

2.5 Heart Disease Associated with Inflammation

The increase in inflammation and its relevant proinflammatory-inducing factors have been shown to lead to a variety of heart disease (Figure 2.8). Data published has revealed that inflammation plays a significant role in hypertension as it could increase reactive oxygen species (ROS) production, specifically superoxide in addition to proinflammatory factors IL-6 due to angiotensin II (Wassmann *et al*., 2004). Cardiovascular distresses such as atherosclerosis have also been affected by inflammatory pathways as angiotensin II was shown to increase the expression of NF-κB, which in turn increases atherosclerotic plaque formation (Krishnamoorthy and Honn, 2006, Ahmed, 2011). Other research has shown that foam cells can release cytokines which leads to the migration of vascular smooth muscle cells into the intima (Mahdinia *et al*., 2023). This, in addition to IL-1β secretion, can cause degradation of the fibrous cap increasing the chances of rupture and ultimately causing plaque release that leads to myocardial ischemia (Hansson *et al*., 2015). Animal studies have shown that heart failure is associated with increased proinflammatory cytokines TNF-α, IL-1, and IL-6, further showing the relevance of cytokines in cardiac distress (Dick and Epelman, 2016). Cardiac inflammation, also known as myocarditis, is a form of cardiac distress that occurs when the heart is injured, often due to pathogens such as viral infections. This injury triggers the release of DAMPs and activates an inflammatory response, leading to an increase in pro-inflammatory cytokines such as IL-1, TNF-α, IFN-α, and interferon beta (Lafuse *et al*., 2020). Chronic conditions namely, diabetes and hypertension predispose individuals to a cardiovascular phenotype characterized by low-grade chronic inflammation. The onset of this persistent

inflammation can result in cardiac injury, which activates cardiac remodelling processes aimed at repairing the damage. However, prolonged toxic responses can damage the myocardium, leading to the upregulation of extracellular matrix proteins and subsequent wall thickening. This process is driven by TGF-β1, which binds to fibroblasts, promoting their differentiation and deposition into cardiac tissue. This leads to cardiac fibrosis, a condition associated with diseases such as myocarditis. Furthermore, studies have shown that fibroblasts can exacerbate the inflammatory response by increasing cytokine production, particularly IL-1β, and activating the inflammasome (Lafuse *et al.*, 2020, Thomas and Grisanti, 2020). Given the above role of inflammation as a key player in the onset of various diseases, particularly those associated with cardiac conditions. It is thus crucial to investigate the effects that FB_1 may elicit by altering the inflammatory pathway, which could lead to cardiac distress.

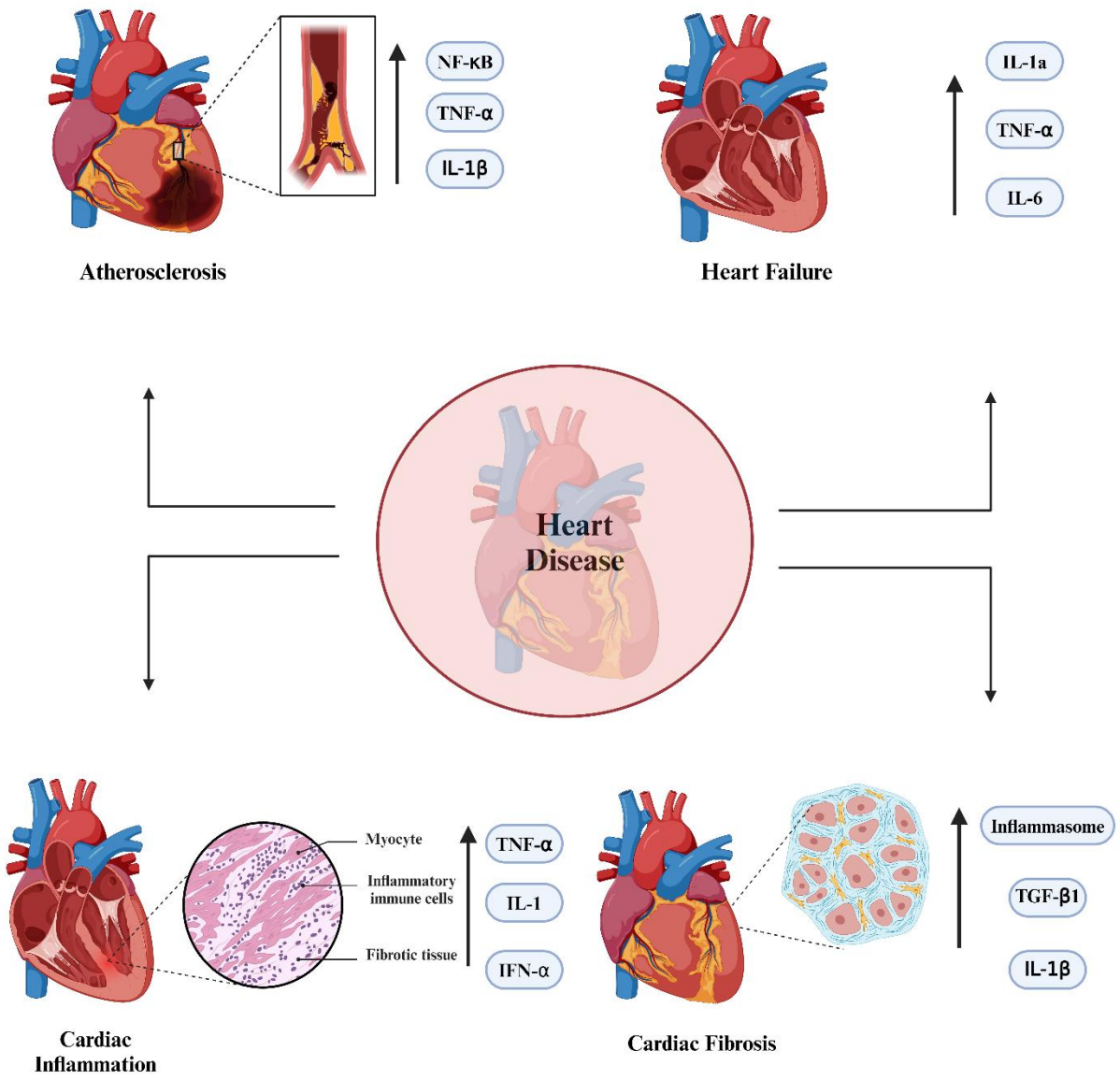

Figure 2.8: Impact of Inflammation on the Progression of Heart Diseases. The diagram illustrates various heart diseases and the role of inflammation in their progression. In atherosclerosis, arrows indicate that increased levels of NF-κB, TNF-α, and IL-1β are involved in catalysing the onset of this disease. Heart failure is characterised by elevated circulating levels of IL-1α, IL-6, and TNF-α. Cardiac inflammation at the myocyte level shows increased levels of TNF-α, IL-1, and IFN-γ. Lastly, the progression of cardiac fibrosis is exacerbated by elevated levels of inflammatory mediators such as inflammasomes, TGF-β1, and IL-1β. IFN-γ: Interferon-gamma; IL-1: Interleukin-1; IL-1α: Interleukin-1 alpha; IL-1β: Interleukin-1 beta; IL-6: Interleukin-6; NF-κB: Nuclear Factor Kappa-B; TGF-β1: Transforming Growth Factor-beta 1; and TNF-α: Tumour Necrosis Factor-alpha; Prepared by the Author.

Chapter 3: Methodology

3.1 Molecular Docking

Molecular docking is a computational technique used to predict the binding interactions between molecules, specifically in protein-ligand or protein-protein binding (Figure 3.1). These interactions provide insight into both the orientation of the molecules and the strength and stability of the resulting complex. The molecular docking process takes key electrostatic interactions into account when modelling these interactions computationally. These forces include van der Waals interactions, Coulombic interactions, and hydrogen bonds. The combination of these forces produces a docking score, which represents the binding affinity between the molecules involved (Pagadala *et al*., 2017, Agarwal and Mehrotra, 2016).

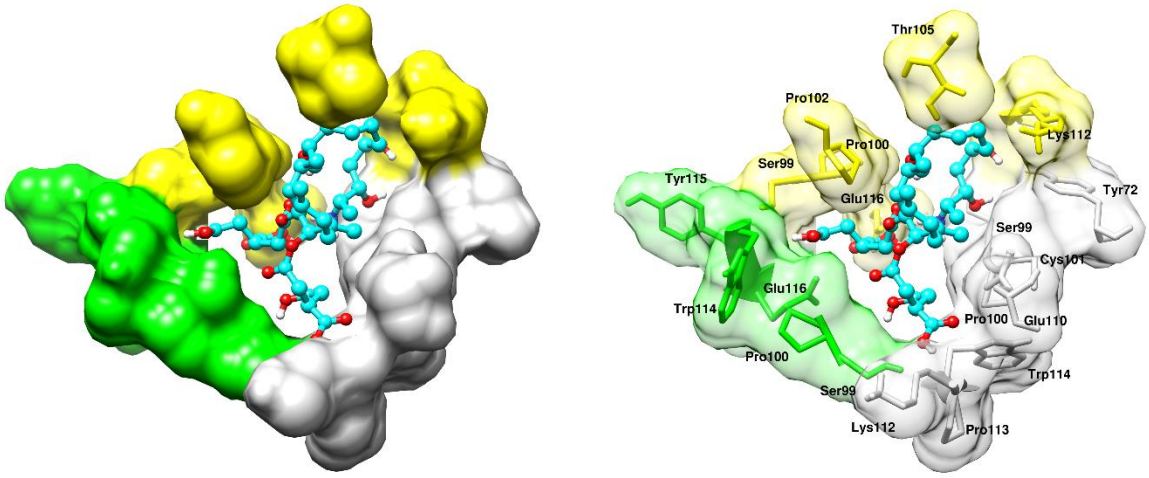

Figure 3.1: This diagram shows the surface structure of the TNF-α protein, with its three subunits A, B, and C represented by the colours white, green, and yellow, respectively. FB_1, acting as the ligand complex, is depicted as a stick figure in cyan blue. A closer look at the binding of a ligand to a protein complex reveals the interactions between the ligand and the protein. It highlights key residues involved in the interaction, providing vital information on how the ligand may influence the protein's activity. The complex was visualised using UCSF Chimera. (FB_1: Fumonisin B1), (TNF-α: Tumour Necrosis Factor-alpha), and (UCSF: University of California, San Francisco) (Pettersen *et al*., 2004),(Prepared by the Author).

The 2D structure of FB_1 was obtained from the PubChem (CID: 2733487). The geometry of the FB_1 structure was energy minimized using the General Amber Force Field (GAFF) with Steepest Descent algorithm implemented in Avogadro version 1.2.0 (Hanwell *et al*., 2012). The structure was then saved in a 3D Mol2 format. The structures of the proinflammatory factors—TNF-α, iNOS, NF-κB (p65), and NF-κB (p50) were retrieved from the RCSB Protein Data

Bank [PDB IDs: 2TNF, 2ORR, 1MY5, and 8TKM, respectively] (Baeyens *et al*., 1999, Davey *et al*., 2007, Huxford *et al*., 2002, Zhu *et al*., 2023). Molecular docking calculations were conducted using Autodock Vina version 4.2.6 (Trott and Olson, 2010). Throughout the docking procedure, Gasteiger partial charges were assigned to the bonds, and the electronegative differences between atoms and bonds were considered. A grid box was then created to cover the entire molecule to identify potential binding sites of FB_1 with TNF-α, iNOS, NF-kB (p65), and NF-kB (p50). The grid box parameters were set as follows: [(TNF-α, centre x = -7.668 Å, y = 48.272 Å, and z = -47.205 Å and the dimensions were x = 68 Å, y = 66 Å, and z = 68 Å with an exhaustiveness of 10), (iNOS, centre x = 69.648 Å, y = -15.993 Å, and z = 50.142 Å and the dimensions were x = 50 Å, y = 68 Å, and z = 66 Å with an exhaustiveness of 10), (NF-κB (p65), centre x = 23.596 Å, y = 20.946 Å, and z = 38.586 Å and the dimensions were x = 72 Å, y = 80 Å, and z = 60 Å with an exhaustiveness of 10) and (NF-κB (p50), centre x = -52.442 Å, y = 16.741 Å, and z = -9.013 Å and the dimensions were x = 102 Å, y = 104 Å, and z = 116 Å with an exhaustiveness of 10)]. Docked conformations of the respective protein-ligand complexes were generated using the Lamarckian genetic algorithm and ranked in descending order according to their docking scores. These protein-ligand complexes were then visualized using UCSF Chimera to analyse key interactions between FB_1 and the inflammatory proteins (Pettersen *et al*., 2004). The various binding conformations, along with their respective docking scores and root mean square deviations (RMSD), were calculated using Autodock Vina. The highest docking energy conformations for each interaction were analysed in this study and are highlighted in Appendix B.

3.2 Animal Treatment

The in vivo study commenced by obtaining C57BL/6 male mice, aged 6–8 weeks, from the Africa Health Research Institute at the University of KwaZulu-Natal, Durban, South Africa. The mice were housed according to the ARRIVE guidelines and rules and regulations of the University of KwaZulu-Natal Animal Research Ethics Committee (Ethics approval number: AREC/079/016). The mice weighed an average of 20 ± 2.99g and were divided randomly into two groups containing 5 mice each of non-treated (control) and treated (FB_1) mice. The mice were adapted under normal operating laboratory conditions (temperature = 25°C, humidity = 40–60%, 12 h light/dark cycle). These mice were fed a mice pellet diet and normal drinking water for the duration of the experiment. The mice were orally administered either with 0.1 M phosphate-buffered saline (PBS) (control group) or 5 mg/kg FB_1 (FB_1 group) at a rate of 0.25 ml/23 g once for a period of 24 h (Sibiya, 2018, Ghazi *et al*., 2020). Thereafter, the mice were

euthanised using halothane anaesthesia and the heart was harvested by a qualified veterinary surgeon (Figure 3.2). The hearts were washed three times in 0.1 M PBS and stored in Cytobuster reagent (500 µl; Novagen, CA, USA), Qiazol reagent (500 µl; Qiagen, 79306) and 0.1 M PBS for protein, RNA and serum extraction, respectively.

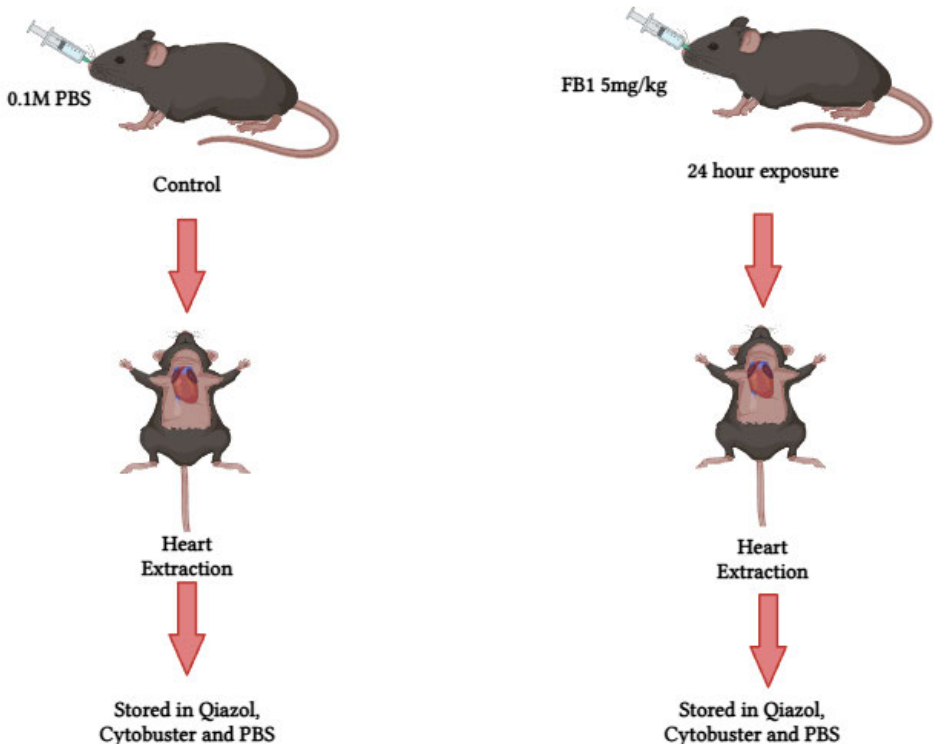

Figure 3.2: The experimental design was characterised by the treatment and non-treatment of C57BL/6 mice, followed by heart extraction and storage in Qiazol, Cytobuster and PBS (Prepared by the Author).

3.3 Tissue Preparation

Harvested whole mice hearts stored in PBS, Cytobuster, and Qiazol were thawed on ice and homogenized. The resulting tissue homogenates were transferred to microcentrifuge tubes, followed by centrifugation (10,000 xg, 4°C, 10 min). The relevant supernatants for RNA isolation, serum, and protein were retained for further testing using quantitative polymerase chain reaction (qPCR), nitric oxide synthase (NOS) assay, enzyme-linked immunosorbent assay (ELISA), and Western blotting.

3.4 Quantitative Polymerase Chain Reaction (qPCR)

An important laboratory technique that is used to amplify DNA sequences via step-by-step enzymatic reactions is known as qPCR. It is widely used as a diagnostic tool for genetic quality, infections, DNA forensics, and genotyping. As the name suggests it is a chain reaction in which

a DNA molecule is replicated multiple times. Hence, it can be summarised as alternative repetitions of heating and cooling processes which utilise a reaction combination that contains a DNA template, DNA polymerase, primers, and nucleotides. These key components are crucial as the target sequence is derived from the DNA template whereas the primers are needed to bind to specific DNA targets during cooling via complimentary base pairing. Subsequently, DNA polymerase is present to form the newer complementary strands in relation to the target sequence. These reagents are present during PCR which occurs using a 3-step process which comprises of denaturation, annealing, and extension (Figure 3.3). Denaturation is the first step and occurs to unwind the double helix structure of DNA by breaking the hydrogen bonds by applying heat at a temperature of 90°C. Thereafter, annealing takes place to allow for complimentary base pairing at approximately 45–65°C. The final step is an extension that is categorised by the formation of a new complementary strand due to DNA polymerase enzyme activity, which is optimum at 72°C. These three steps make up 1 cycle in the process and run for approximately 30-40 cycles (Jalali *et al*., 2017, Joshi and Deshpande, 2010). In qPCR, the quantification of data happens in a single step that combines both amplification and detection. This process uses various fluorescent dyes, which emit fluorescence intensities that correspond to the concentration of the PCR product. A commonly used fluorescent dye in this method is SYBR Green which intercalates itself in between the DNA molecule tagging it with fluorescence, furthermore it is valued for its cost-effectiveness and reliable chemistry (Zhang *et al*., 2015).

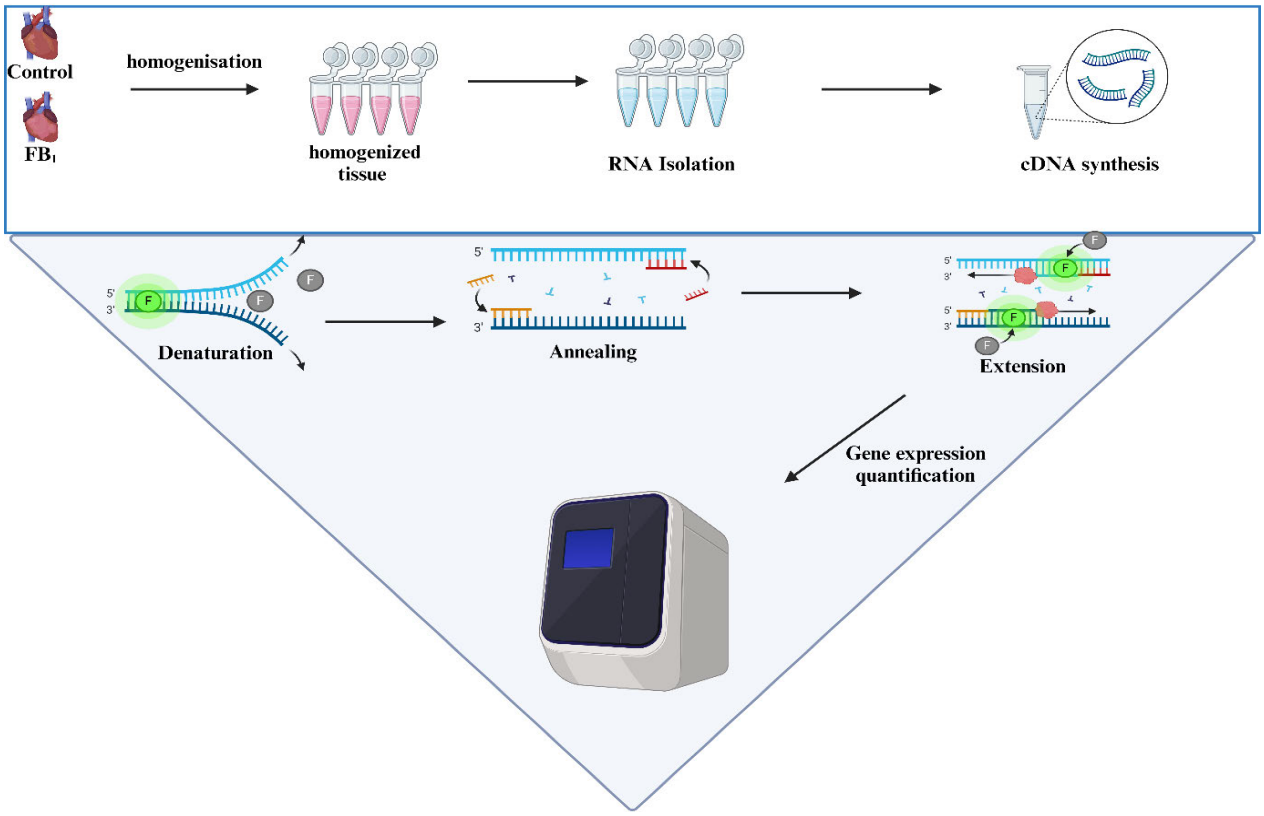

Figure 3.3: Schematic Overview of the qPCR Principle and Workflow. This diagram provides a schematic overview of the qPCR principle, detailing the steps from sample preparation to quantification. Initially, stored samples were homogenized, and RNA was extracted. The extracted RNA was then used to prepare cDNA for the qPCR experiment. The blue triangle highlights the qPCR principle for detecting gene expression. The process begins with the denaturation of the DNA strand, where F represents the forward strand. This forward strand is used for complementary base pairing depicted in red during the annealing step, followed by extension to form the new complementary strand which is blue. The green F indicates fluorescence, where a fluorescent dye emits a measurable glow using QuantStudio™ 3 Real-Time PCR Software. (cDNA: Complementary DNA), (qPCR: Quantitative Polymerase Chain Reaction), and (RNA: Ribonucleic Acid). (Prepared by the Author).

3.4.1 RNA Isolation

The mice tissue stored in Qiazol reagent underwent the specified tissue preparation procedure for total RNA extraction. After removal from the freezer, the samples were thawed and supplemented with 100 µl of chloroform. They were then vortexed for 15 seconds and incubated at room temperature for 2–3 minutes. Following this, the samples were centrifuged at 12,000 xg for 15 minutes at 4°C. The resulting aqueous phase was carefully transferred into clean microcentrifuge tubes. To the supernatant, 250 µl of isopropanol was added and gently mixed before freezing at -80°C. After an overnight freeze, the samples were thawed on ice and centrifuged at 12,000 xg at 4°C for 20 minutes. The supernatant was discarded, and the pellet was washed with 500 µl of 75% ethanol. While in ethanol, the samples were centrifuged at 7,400 xg at 4°C for 15 minutes. After centrifugation, the ethanol was removed, and the pellets

were air-dried for 45 minutes. The dried pellets were then resuspended in 15 µl of nuclease-free water and allowed to equilibrate at room temperature for about 3 minutes. The extracted RNA was measured, and its quality was assessed using the A260/A280 ratio with a Nanodrop 2000 spectrophotometer (Thermo-Fisher Scientific, Waltham, MA, USA). Finally, all RNA samples were standardised to a concentration of 500 ng/µl.

3.4.2 Determination of Gene Expression

The standardised RNA samples were used to synthesise cDNA. The cDNA synthesis followed the instructions of the cDNA Synthesis Kit (K1652, Thermo-Fisher Scientific, Waltham, MA, USA), prepared according to the manufacturer's guidelines Thereafter, the expression of relevant inflammatory and DNA methylation genes (Table 3.1) was examined using SYBR® Green Supermix (A25742, Thermo-Fisher Scientific, Waltham, MA, USA) and the QuantStudio™ 3 Real-Time PCR Software, Version 1 (Waltham, MA 02451, USA). The thermocycling instructions for each gene included the following steps: the initial denaturation was conducted for 8 minutes at 95°C, followed by 15 seconds at 95°C for 40 consecutive cycles. This was followed by the annealing stage, performed at the temperatures indicated in Table 3.1 for 40 seconds. The final extension stage was carried out at 72°C for 30 seconds. Gene expression was normalised using GAPDH, which is evenly distributed in all cells and tissues. The data obtained was analysed using the comparative threshold cycle (Ct) method and expressed as a relative fold change compared to the control.

Table 3.1: The forward and reverse primer sequences with their correlating annealing temperatures used for qPCR.

Gene	**Sequence (5′-3′)**	**Annealing Temperature (°C)**
TNF-α	Forward CATCTTCTCAAAATTCGAGTGACAA Reverse ACTTGGGCAGATTGACCTCAG	58
NF-κB	Forward ATGGCAGACGATGATCCCTAC Reverse CGGAATCGAAATCCCCTCTGTT	60
IL-6	Forward TCTATACCACTTCACAAGTCGGA Reverse GAATTGCCATTGCACAACTCTTT	58
NLRP3 Inflammasome	Forward ATCAACAGGCGAGACCTCTG Reverse GTCCTCCTGGCATACCATAGA	56
IL-18	Forward GTGAACCCCAGACCAGACTG	58

	Reverse CCTGGAACACGTTTCTGAAAGA	
Caspase 1	Forward AATACAACCACTCGTACACGTC	56
	Reverse AGCTCCAACCCTCGGAGAAA	
IL-1β	Forward TTCAGGCAGGCAGTATCACTC	58
	Reverse GAAGGTCCACGGGAAAGACAC	
GSDMD	Forward CCATCGGCCTTTGAGAAAGTG	60
	Reverse ACACATGAATAACGGGGTTTCC	
Caspase 3	Forward GGAGGCTGACTTCCTGTATGCTT	60
	Reverse CCTGTTAACGCGAGTGAGAATG	
CT-1	Forward CTCCTCAATCTCATTCCTACCCC	60
	Reverse GCTGCACGTATTCCTCCAGAA	
IL-10	Forward GCTCTTACTGACTGGCATGAG	58
	Reverse CGCAGCTCTAGGAGCATGTG	
MBD2	Forward AGAACAAGGGTAAACCAGACCT	58
	Reverse ACTTCACCTTATTGCTCGGGT	
DNMT1	Forward AGAGACCAGGATAAGAAACGCA	60
	Reverse CTCCTTTGATTTCCGCCTCAAT	
DNMT3A	Forward GGCCGAATTGTGTCTTGGTG	60
	Reverse CCATCTCCGAACCACATGAC	
DNMT3B	Forward AGCGGGTATGAGGAGTGCAT	60
	Reverse GGGAGCATCCTTCGTGTCTG	
GAPDH	Forward AGGTCGGTGTGAACGGATTTG	
	Reverse TGTAGACCATGTAGTTGAGGTCA	

3.5 Western Blotting

Western blotting, also known as immunoblotting, is used for detecting protein expression. The principle of western blotting is based on the separation of a protein mixture using sodium dodecyl sulfate–polyacrylamide gel electrophoresis (SDS-PAGE) according to molecular weight, followed by the electrophoretic transfer of the proteins onto a nitrocellulose membrane. The methodology of this technique is characterized by three key steps: separation by size, transfer to an adsorbent membrane, and identification of the target protein using the appropriate primary antibody, followed by secondary antibody incubation (Figure 3.4) (Begum *et al*., 2022). The first step in the western blotting assay is the preparation of the sample. For sample preparation, the heart tissue is mechanically homogenised, and proteins are extracted. The lysis

solution used to isolate protein is Cytobuster. The composition of this lysis buffer contains buffering compounds such as Tris-HCl and protease/phosphatase inhibitors to prevent protein degradation. Once the cells are lysed, phosphatases and proteases are released. The isolated proteins are subjected to the bicinchoninic acid (BCA) assay to determine protein concentration, ensuring that an equal amount of protein is loaded into the gel. To these samples, Laemmli buffer is added to ensure the unfolding of proteins. Thereafter, the proteins are separated according to molecular size by gel electrophoresis. The separated proteins are then electrotransferred from the gel to a membrane, typically a nitrocellulose membrane, as it is the most efficient. The membranes are further blocked using bovine serum albumin (BSA) and subsequently probed with antibodies that detect specific proteins of interest via conjugation with horseradish peroxidase (HRP). After antibody detection, the membrane is visualised using an appropriate imaging system, such as the iBright Imaging Systems (Gwozdz and Dorey, 2017). Relative band density is calculated after imaging by analysing the intensity of the protein bands. This involves capturing a high-quality image of the western blot, subtracting the background intensity, and measuring the signal within each band using image analysis software. Small blocks are placed around the bands to determine their intensity. This intensity is then normalized using the intensity of the β-actin bands, ensuring accurate and reliable quantification of protein expression levels.

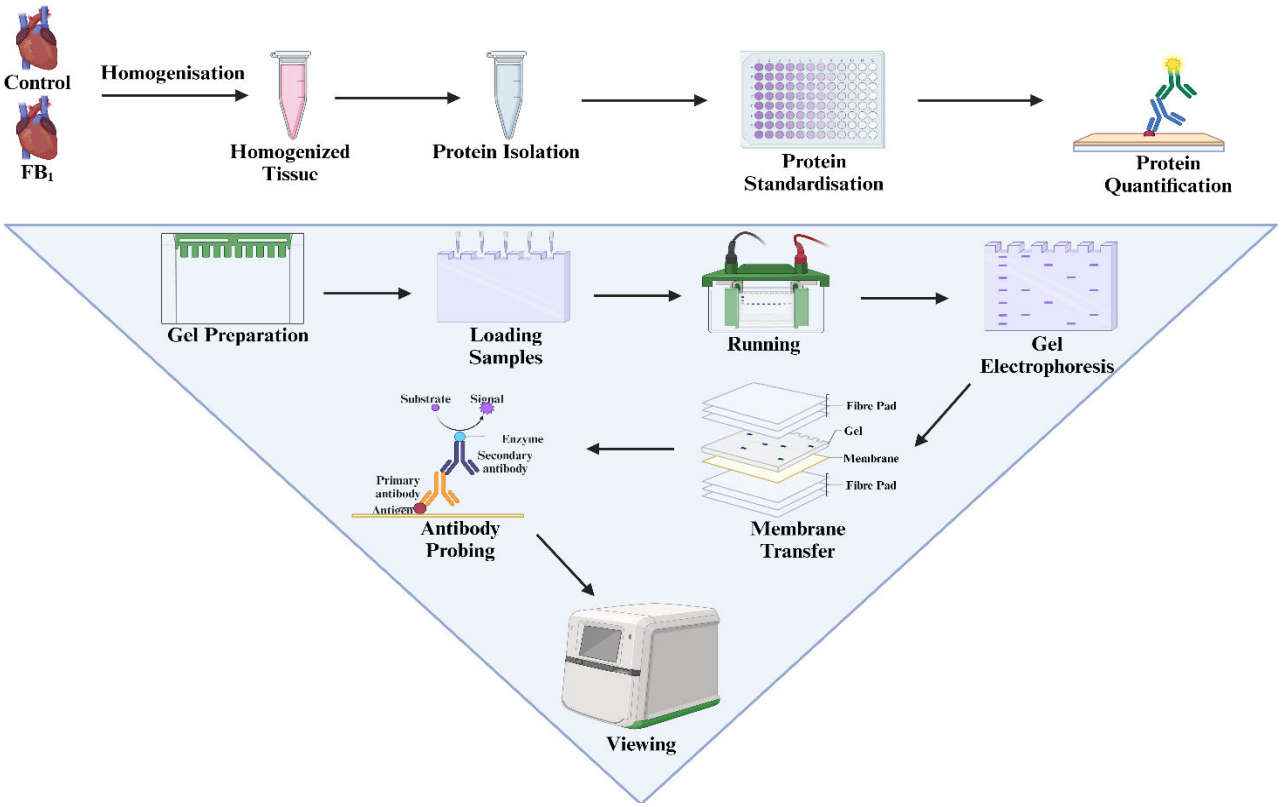

Figure 3.4: Standardisation and Quantification of Protein Extracted from Mice Tissue. This diagram illustrates the process of standardising and quantifying protein extracted from mice tissue. The protein was standardised using the BCA assay, followed by quantification through Western blotting. The first step involves preparing a polyacrylamide gel, loading the samples, and running gel electrophoresis. After electrophoresis, the proteins were transferred onto a nitrocellulose membrane using the Bio-Rad Trans-Blot® Turbo Transfer System. Following the transfer, the membrane was probed with primary antibodies and then with secondary antibodies conjugated to a horseradish peroxidase substrate. This substrate produces a detectable signal, allowing proteins to be visualized as black bands using the iBright Imaging System. BCA: Bicinchoninic Acid and HRP: Horseradish Peroxidase; Prepared by the Author.

3.5.1 Protein Isolation and Protein Quantification

To quantify the protein expression of key inflammatory factors and mediators—phosphorylated-NF-κB (P-NF-κB) and caspase 3—as well as DNA methylation-associated factors MBD2 and DNMT1, Western blotting was utilised. Proteins were extracted from untreated (control) and FB_1-treated mice using Cytobuster (200 µl; Novagen, 71009), with added protease and phosphatase inhibitors (Roche; 05892791001 and 04906837001, respectively). The protein concentration was determined using the BCA assay and standardised to 1 mg/ml. These standardised protein samples were then mixed with 1X Laemmli buffer

[dH2O, 0.5 M Tris-HCl (pH 6.8), glycerol, 10% SDS, 5% β-mercaptoethanol, 1% bromophenol blue] in a 1:1 ratio and boiled at 100°C for 5 minutes to denature the proteins. For Western blotting, the proteins were separated by size using sodium dodecyl sulphate polyacrylamide gel electrophoresis, with a 10% resolving gel and a 4% stacking gel, at 150 V for 1 hour. After electrophoresis, the proteins were transferred to a nitrocellulose membrane at 20 V for 30 minutes using the Bio-Rad Trans-Blot® Turbo Transfer System. The membrane was then blocked with 5% BSA in Tris-buffered saline containing 0.05% Tween 20 [TTBS; 150 mM NaCl, 3 mM KCl, 25 mM Tris, 0.05% Tween 20, dH2O, pH 7.5] for 1 hour at room temperature. The blocked membranes were incubated overnight at 4°C with primary antibodies (Table 3.2). The next day, the membranes were washed five times and incubated with HRP-conjugated secondary antibodies (Table 3.2, anti-rabbit and anti-mouse) for 1 hour at room temperature. After incubation, the membranes were washed and developed using the Clarity™ Western ECL Substrate Kit (Bio-Rad, #170-5060). Images of the protein bands were captured using the Invitrogen iBright CL1500 Imaging System (Thermo-Fisher Scientific, Waltham, MA, USA). Finally, the membranes were stripped for probing with the housekeeping protein β-actin by incubating them with hydrogen peroxide for 30 minutes at 37°C, followed by a TTBS wash for 10 minutes. The membranes were then probed with anti-β-actin (Table 3.2) for 30 minutes at room temperature. Protein bands were analysed using the iBright Imaging System software V1 and expressed as relative band density (RBD). Relative band density (RBD) is calculated by measuring the intensity of the bands using iBright Imaging System software. Small blocks are placed around the bands to determine their intensity. This intensity is then normalized using the intensity of the β-actin bands, ensuring accurate and reliable quantification of protein expression levels.

Table 3.2: Primary and secondary antibodies with their correlating catalogue numbers and dilutions used for western blot.

Protein	Catalogue Number	Dilution
P-NF-κB	Cell Signalling Technology, 3033S	1:1000
Caspase 3	Cell Signalling Technology, 9665	1:1000
DNMT1	Cell Signalling Technology, 5032S	1:1000

MBD2	Abcam, ab188474	1:1000
goat anti-rabbit	Cell Signalling Technology, #7076P2	1:5000
goat anti-mouse	Cell Signalling Technology, #7076P2	1:5000
β-actin	Sigma-Aldrich, A3854	1:5000

3.6 Nitric Oxide Synthase (NOS) Assay

Essential molecules involved in vasodilation, immune response, and cellular signalling are reactive nitrogen species such as NO. When the levels of NO are present in increased concentrations, it can result in the alterations of biochemical pathways such as inflammation and can exacerbate the pro-inflammatory environment which can lead to the subsequent pathogenesis of cardiovascular diseases such as atherosclerosis, myocarditis and hypertension. Therefore, nitric oxide is a crucial molecule involved in signalling, it is formed through interactions by two key pathways, L-arginine-nitric oxide pathway and the nitrate-nitrite-nitric oxide pathway, respectively (Kapil *et al*., 2020, Khazan and Hdayati, 2015). The NOS assay is identified as a colorimetric assay as it depends on the measuring of a formed end-coloured product. This assay, however, does not directly measure the effects of NO, as NO has a short half-life and hence cannot be accurately measured directly as it dissipates soon after formation. The initial reaction that occurs during this assay occurs when nitrate is reacted with vanadium III chloride to form nitrite. This is subsequently proceeded by the formed nitrite interacting with sulphanilamide to form a diazonium ion. This nitrite with the addition of N-(1-naphthyl) ethylenediamine (NEDD) creates a pink coloured, azo-dyed product which can be quantified at absorbance 540nm (Figure 3.5) (He *et al*., 2019).

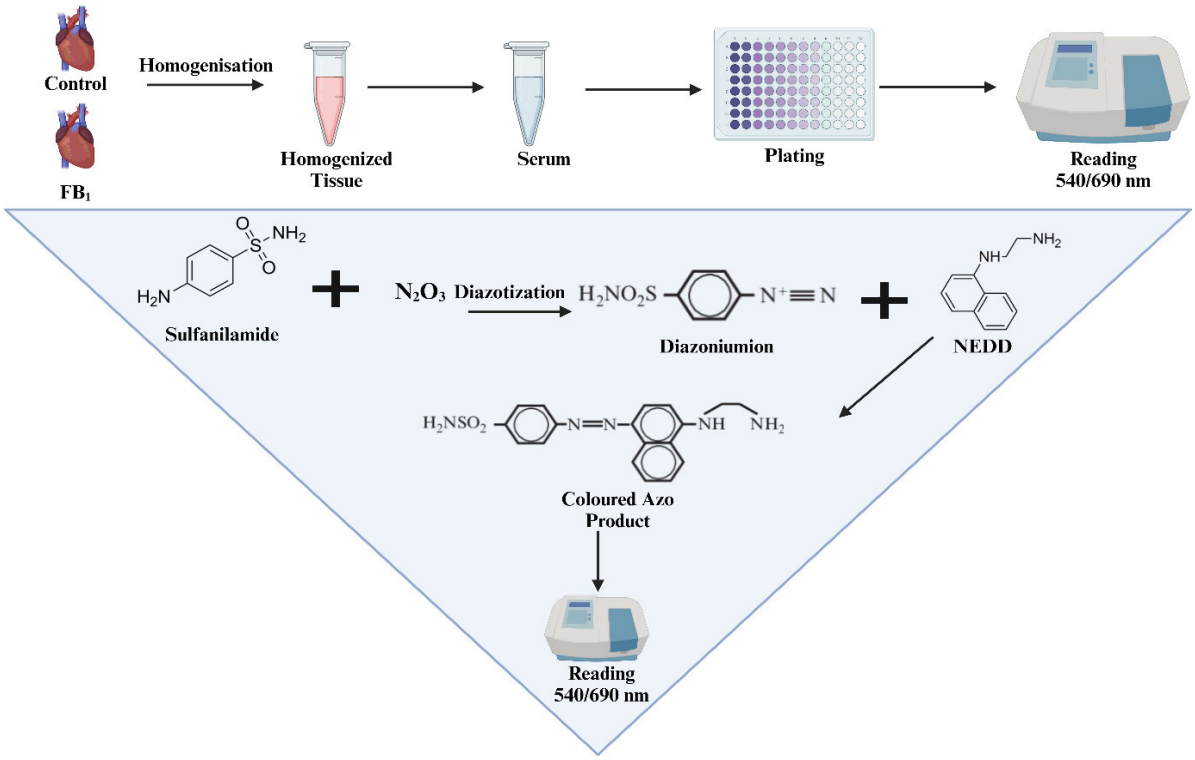

Figure 3.5: Schematic Overview of the NOS Assay. This diagram provides a schematic overview of the NOS assay. Heart tissue was homogenised in PBS to obtain serum. The serum was plated in a 96-well plate. The principle and methodology of the NOS assay are highlighted in the blue triangle. The process begins with the addition of vanadium (III) chloride, followed by sulphanilamide, which interacts with the sample to form a diazonium ion. Subsequently, NEDD is added to form a dyed azo product, which can be measured spectrophotometrically at 540/690nm. NEDD: N-(1-Naphthyl) ethylenediamine dihydrochloride; NOS: Nitric Oxide Synthase and PBS: Phosphate-Buffered Saline; Prepared by Author.

The NOS assay was employed to determine NO concentrations present in untreated and treated (FB_1) mice. The sodium nitrate standards (0, 25, 50, 75, 100, 125, 150, 175, 200 µM) and mice hearts serum were prepared by homogenising heart tissue in 500 µl of PBS and dispensed at a volume of 50 µl in triplicate in a 96-well plate. Afterwards, 50 µl VCl_3, 25 µl sulphanilamide, and 50 µl of NEDD were consecutively rapidly aliquoted into the wells with samples. Once all the reagents were added the plate was incubated (37ºC, 5% CO_2) for 45 minutes in the dark as this was a light sensitive assay. After the incubation period, the absorbance was measured using the SPECTROstar® nano microplate reader at the following wavelength, 540nm/690nm. The absorbances obtained were averaged and used to prepare a standard curve. The extrapolation of the standard curve was used to acquire the equation of the line and was subsequently used

to calculate the concentration of nitrate/nitrite that was present in the control and FB_1 mice heart serum.

3.7 Enzyme-Linked Immunosorbent Assay (ELISA)

It is used to quantify molecules such as proteins and hormones, which are typically low in molecular weight, with a high degree of specificity for antigens and antibodies. This specificity is crucial, as it allows the detection and quantification of proteins present in low concentrations without interference from external factors (Aydin, 2015). The first step in the ELISA assay involves coating the wells of polystyrene microtiter plates with the relevant antigen. The polystyrene nature of the plates plays a specialised role by increasing the affinity of proteins to bind to the wells. This is followed by a saturation or blocking step, where a blocking buffer is added to prevent non-specific binding by saturating free binding sites in the wells. The biological samples are prepared in PBS. After sample preparation, the conjugation reaction occurs, often using the enzyme HRP. The HRP enzyme is crucial because it produces the coloured end products by interacting with 3,3',5,5'-Tetramethylbenzidine (TMB). This reaction signals an endpoint which is subsequently stopped by adding phosphoric acid. The final step is signal detection, which depends on the type of ELISA kit used. Most ELISAs are colorimetric, thus entailing the colour change is read using spectrophotometry (Figure 3.6). The resulting data is used to generate a standard curve, allowing the concentration of the relevant proteins to be determined (Minic and Zivkovic, 2020).

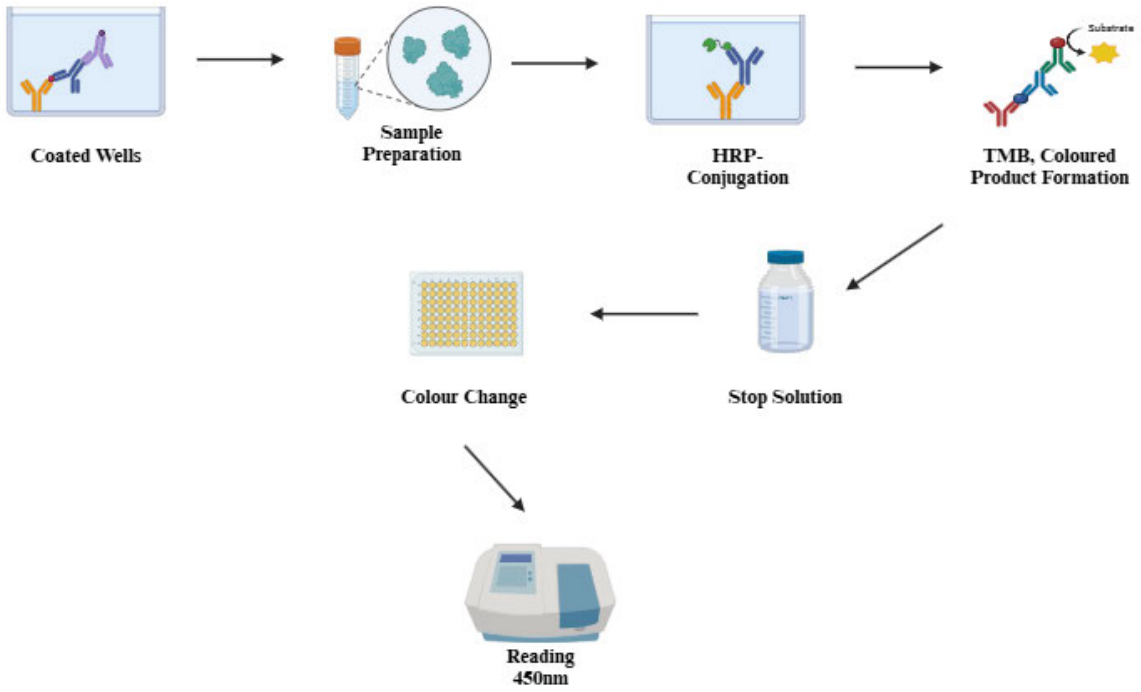

Figure 3.6: An Overview of the Key Steps in the ELISA Assay. The ELISA plates are first coated with the antigen, followed by the addition of samples according to ELISA instructions. Next, an HRP-conjugation solution is added, followed by the substrate TMB, which forms a coloured product. The reaction is allowed to proceed before it is stopped using a stop solution, resulting in a colour change. Finally, the plate is read spectrophotometrically to measure the absorbance of the coloured product at a wavelength of 450 nm. (ELISA: Enzyme-Linked Immunosorbent Assay; HRP: Horseradish Peroxidase; TMB: 3,3',5,5'-Tetramethylbenzidine; PBS: Phosphate-Buffered Saline) Prepared by the Author.

3.7.1 Cytokine ELISA

The levels of proinflammatory cytokines TNF-α (RK00027, Abclonal), IL-6 (RK00008, Abclonal), IL-1β (RK00006, Abclonal), IL-10 (RK00016, Abclonal), and TGF-β1 (RK00057, Abclonal) were quantified using ELISA kits. The biological samples used for these ELISAs were prepared according to the previously mentioned tissue preparation steps, with serum samples specifically used for the assays. Prior to the experiment, all reagents were removed from the refrigerator and allowed to equilibrate to room temperature. Following the manufacturer's instructions, the reagents were prepared as follows: the standard solution was created by adding 1 ml of standard sample diluent (R1) to the lyophilised standard, producing a stock solution of 2000 pg/ml. The stock solution was then diluted with 250 µl of R1 to prepare serial dilutions ranging from 2000 to 0 pg/ml. Next, the working biotin-conjugate antibody was prepared by diluting 20 µl of concentrated biotin conjugate into 1980 µl of R2 to create 2000 µl of working biotin solution. The working streptavidin-HRP solution was prepared by adding

20 µl of concentrated streptavidin-HRP to 1980 µl of streptavidin-HRP diluent (R3), resulting in 2000 µl of working streptavidin-HRP buffer. Finally, the wash buffer was prepared by diluting 20 ml of concentrated wash buffer in 380 ml of deionised water to make 400 ml of solution. Once all reagents were prepared, the ELISA procedure commenced with washing the wells three times with 350 µl of wash buffer solution. After washing, 50 µl of standards, controls, and FB_1 samples were aliquoted into the wells and incubated for 2 hours at 37°C. After incubation, the solutions were aspirated, and the washing steps were repeated. Thereafter, 50 µl of the working biotin-conjugate antibody was added to each well and incubated at 37°C for 1 hour. Following incubation, the wells were aspirated, and three additional washing steps were performed. Then, 50 µl of working streptavidin-HRP conjugate was added and incubated for 30 minutes at 37°C. After this, the wells were aspirated, and the washing steps were repeated. Once washing concluded, 50 µl of TMB substrate was pipetted into each well and incubated away from light for 15–20 minutes at 37°C. After incubation, 25 µl of stop solution was added, and optical density was measured within 5 minutes using the SPECTROstar® Nano microplate reader at 450 nm with a reference wavelength of 630 nm. The data obtained was used to generate a standard curve and the equation from the curve was extrapolated to quantify the concentrations of the relevant cytokines.

3.7.2 Global DNA Methylation ELISA

Prior to the commencement of the DNA methylation ELISA, DNA was isolated from the prepared tissue. The remaining aqueous phase, sitting on the interphase of the Qiazol-prepared tissue, was carefully extracted and transferred to new microcentrifuge tubes. To the supernatant, 30 µl of 100% ethanol was added per 1 ml of Qiazol, and the mixture was gently inverted for 2–3 minutes. This was followed by centrifugation at 2000 ×g at 4°C for 5 minutes to obtain the pelleted DNA. The DNA pellet was then resuspended in 300 µl of 0.1 M sodium citrate and incubated for 30 minutes with occasional inversion. The sample was subsequently centrifuged at 2000 ×g for 5 minutes at 4°C. The pellet was resuspended in 1 ml of 75% ethanol, incubated for 10–20 minutes with gentle inversions, and centrifuged for 5 minutes at 2000 ×g at 4°C. After centrifugation, the supernatant was discarded, and the pellet was left to air dry for 10 minutes. The pellet was then solubilised in 300 µl of 8 mM sodium hydroxide, followed by centrifugation at 2000 ×g for 10 minutes at 4°C. The DNA yield was obtained and was used to standardise the DNA concentration to 15 ng/µl. The standardised DNA was used to quantify global DNA methylation using the Methylated DNA Quantification ELISA Kit (Abcam, ab117128). To the strip wells, 80 µl of binding solution was added, followed by 1 µl each of

the negative control (unmethylated DNA, which contains 0% methylation), diluted positive control (contains methylated DNA with a known percentage of methylation), and 8 µl of control and FB_1-treated samples. The samples were incubated for 90 minutes at 37°C. Following incubation, the wells were aspirated and washed 3 times with 150 µl of wash buffer. After washing, the diluted capture antibody (1:1000 in wash buffer) was dispensed at 50 µl per well and incubated for 60 minutes at room temperature. Following incubation, the wells were aspirated and washed again. Next, the detection antibody (diluted 1:2000 in wash buffer) was added at 50 µl per well and incubated at room temperature for 30 minutes. After incubation, the wells were aspirated, and 4 additional washes were performed. The diluted enhancer solution was prepared at a 1:5000 ratio, and 50 µl was added to each well. The samples were incubated at room temperature for 30 minutes. After incubation, the wells were aspirated and washed 5 times with 150 µl of wash buffer. Developer solution (100 µl) was added to each well and incubated in the dark for 10 minutes. Once a colour change was observed, 50 µl of stop solution was added to end the reaction. The plate was then read using the SPECTROstar® Nano microplate reader at 450 nm. The optical densities obtained were used to generate a standard curve, which was used to determine the levels of 5-methylcytosine (5-mC) present.

3.8 Statistical Analysis

Statistical analyses were performed using GraphPad Prism. A t-test with Welch's correction was conducted for each assay. Assessment of the relative changes in gene expression was determined using the comparative threshold cycle method (ΔΔCq method). The ΔΔCq method involves several steps with the first step being thedetermination of ΔCq value for each sample which is calculated by subtracting the Cq value of the reference gene from the Cq value of the target gene. Next, the ΔΔCq value is determined by subtracting the ΔCq of a calibrator sample (often a control or untreated sample) from the ΔCq of the experimental sample. Finally, the relative fold change in gene expression is calculated using the formula $2-\Delta\Delta Cq 2-\Delta\Delta Cq$. The optical densities were obtained from the corrected absorbance readings. Thereafter, the standard absorbances were used to create a standard curve using the standard concentrations. The equation of the line from this standard curve was then used to determine the concentration of the specific product. A standard curve was prepared using Excel for the NOS assay, BCA assay, and all ELISAs performed to determine the concentrations of relevant cytokines and DNA methylation levels. To ensure reliability, each assay was conducted three times. The laboratory data was deemed significant, with p-values found to be significant at ($*p<0.05$), ($**p<0.005$), and ($***p<0.0001$).

Chapter 4: Results

4.1 FB_1 binds to TNF-α, iNOS, NF-κB (p65), and NF-κB (p50)

Molecular docking is a computational technique that illustrates the interaction between small molecules, such as drugs or toxins, and larger molecules like enzymes or proteins. This approach provides insights into the conformation, binding modes, and orientation of the toxin relative to the protein structure. In this study, the FB_1 docking was explored on four proteins responsible for inflammation: TNF-α, iNOS, NF-kB (p65), and NF-kB (p50), to identify possible interactions. The docking energies for the nine conformations of FB_1 with the TNF-α protein ranged from -5.4 kcal/mol to -4.8 kcal/mol, with the most stable conformation binding in the cleft between subunits A, B and C (Figure 4.1). In contrast, FB_1 exhibited a higher docking affinity for iNOS, with scores ranging from -6.5 kcal/mol to -5.6 kcal/mol, the most stable conformation opting to bind in a heme binding site on the surface of iNOS (Figure 4.2A). Furthermore, an interaction with the cysteine 194 residue is possible (Figure 4.2B). This was different from FB_1's docking energy with NF-κB (p65), which was lower, ranging from -4.8 kcal/mol to -4.6 kcal/mol. The posterior region between the two subunits is where the most stable FB_1 conformation bound between the two subunits of NF-κB (p65), with Asn202 and Ser203 being crucial residue interactions with FB_1 (Figure 4.3A, 4.3B and 4.3C). The docking affinity for NF-κB (p50) was similar to that of iNOS, with values ranging from -6.3 kcal/mol to -5.8 kcal/mol. Interestingly, the stable binding of FB_1 selectively facilitated interactions between the DNA structure and the protein subunit of the NF-κB (p50) (Figure 4.4A). Key residues that FB_1 seems to be interacting with include Gln274, Asn244 and Lys275 (Figure 4.4B).

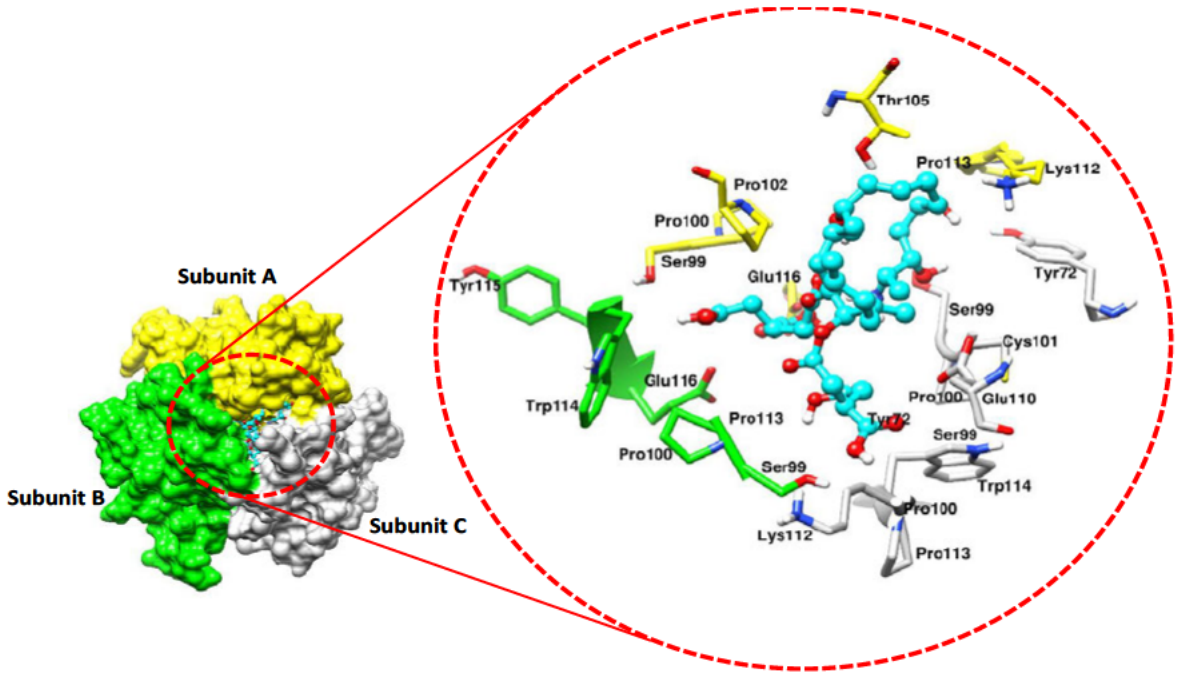

Figure 4.7: The diagram illustrates the docking of FB_1 in-between subunits A, B, and C, potentially leading to the activation of TNF-α. The TNF-α protein is shown in a surface view, with subunits A, B, and C represented in yellow, green, and white, respectively. FB_1 is depicted as a stick cyan blue structure. A topographical view highlights FB_1's most stable binding within the trimeric channel of TNF-α, with Tyr115 and Pro113—crucial residues involved in TNF-α function—highlighted in green. A zoomed-in closer look showcases the potential binding of the TNF-α protein to FB_1, emphasising possible key interactions in the stick figure representation of both the protein and FB_1. UCSF Chimera was used to visualise and prepare the images.

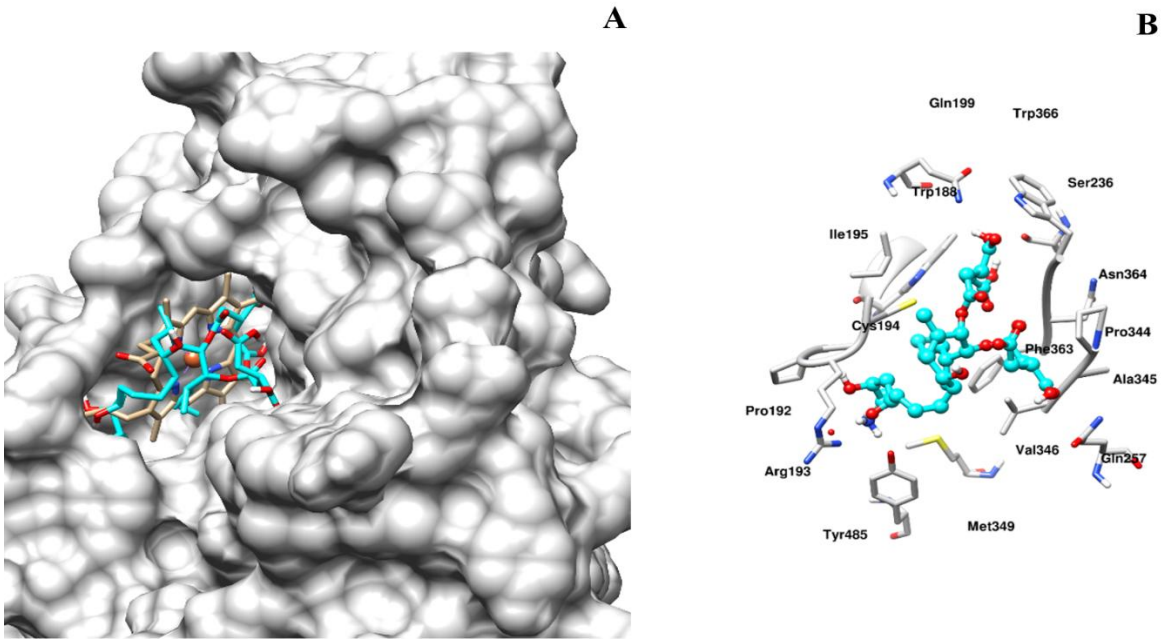

Figure 4.8: Interaction of FB_1 with the Heme Molecule of iNOS. This figure shows the interaction of FB_1 around the heme molecule of iNOS. A pocket around the heme group is characteristic of the iNOS molecule. FB_1 is selectively bound to this pocket and interacts with crucial residues, including Phe363, Cys194, and Tyr485, which are involved in iNOS enzyme function. The picture on the left represents a surface structure of the iNOS molecule in white, with the heme structure depicted as a reddish ball, whereas FB_1 is shown as a cyan blue stick figure. The image on the right shows a stick figure representation of the cyan blue FB_1 and key residues of iNOS, highlighting the potential binding interactions, although the heme molecule is not present in this view. UCSF Chimera was used to visualise and prepare the images.

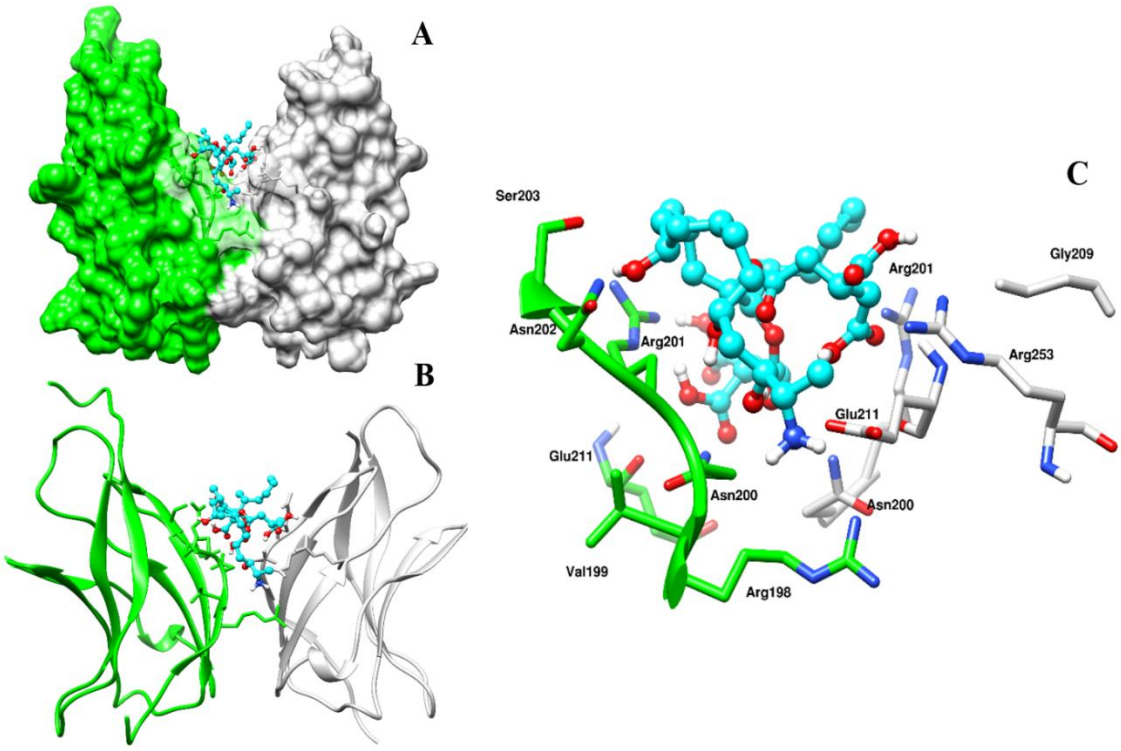

Figure 4.9: Interaction of FB_1 with NF-κB (p65) Subunits. Picture A represents a surface view of NF-κB (p65) with its two subunits shown in white and green, while FB_1 is depicted as a cyan blue stick figure, highlighting possible key interactions between FB_1 and NF-κB (p65). Picture B provides a ribbon rendition of Picture A, offering a different perspective on the structure. Picture C shows a stick figure representation, illustrating the key residues that FB_1 could potentially interact with. This figure suggests that FB_1 may bind in the cleft between subunits, potentially leading to interactional changes between the subunits. It is assumed that the core interactions between FB_1 and NF-κB (p65) occur at residues Asn202 and Ser203, with additional interactions at the Asn200-202 residues cleft, which are thought to be crucial for the complex's function. The diagram was prepared using UCSF Chimera.

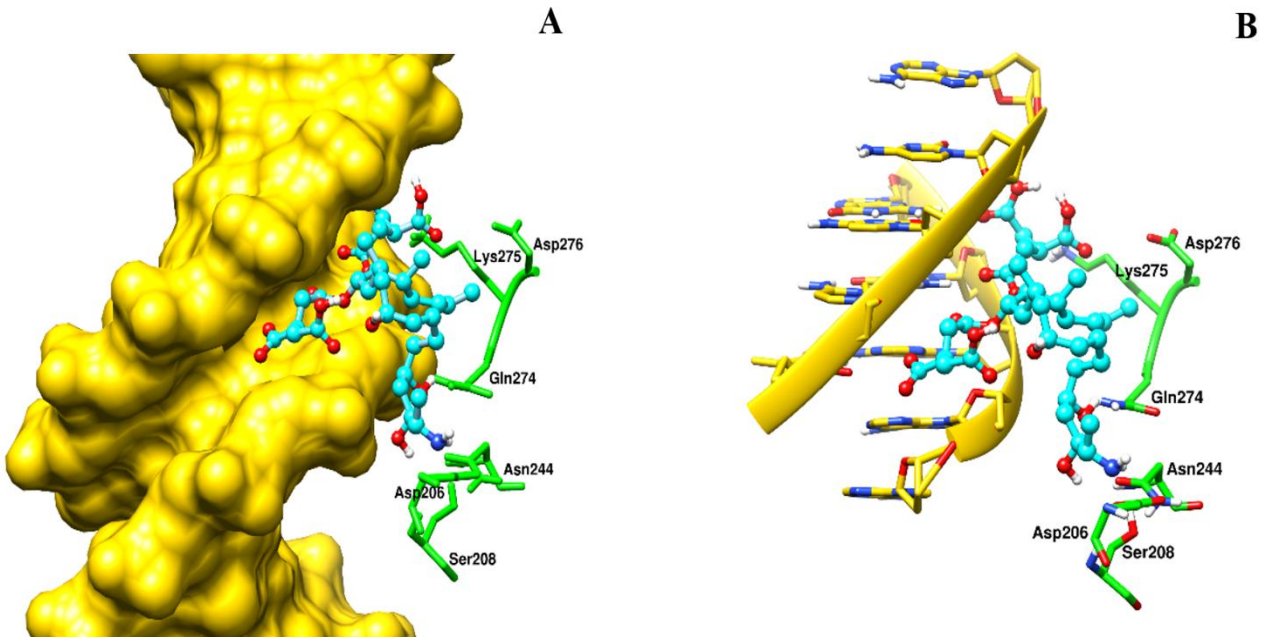

Figure 4.10: Potential Interaction of FB_1 with DNA and NF-κB (p50) Protein Subunit. This figure suggests that the interaction between FB_1, the DNA molecule, and the protein subunit can possibly lead to altered transcriptional activity of NF-κB (p50). Picture A depicts the surface structure of the DNA within the NF-κB (p50) complex, with FB_1 and the protein subunit shown as stick figures in blue and green, respectively. Picture B represents a stick figure depiction of the DNA, FB_1, and NF-κB (p50), being highlighted in yellow, green, and blue. This view further emphasises key residues, such as Gln274, which may be important in affecting the protein function of this complex. UCSF Chimera was used to visualise and prepare the images.

4.2 FB_1 altered the gene expression of key inflammatory cytokines

A key inflammatory cytokine released during the initiation of a pro-inflammatory event is TNF-α. In this study, FB_1 caused *TNF-α* gene expression to be significantly reduced ($p<0.0001$) (Figure 4.5A). The activation of the transcription factor NF-κB is driven by TNF-α induction, this decrease in TNF-α corresponded with a significant reduction in *NF-κB* gene expression ($p= 0.0041$) (Figure 4.5B). NF-κB plays a crucial role in activating downstream cytokines and factors, such as IL-6 and the NLRP3 inflammasome. A marked decline due to FB_1 in the gene expression of *IL-6* ($p<0.0001$) and the *NLRP3* inflammasome ($p<0.0001$) (Figure 4.5C and 4.5D) was observed, coinciding with the decrease in *NF-κB* gene expression. Upon NLRP3 activation, IL-18 is typically activated from its dormant state; however, FB_1 significantly decreased *IL-18* gene expression ($p<0.0001$) (Figure 4.5E), which corresponds to the reduction in *NLRP3* inflammasome gene expression.

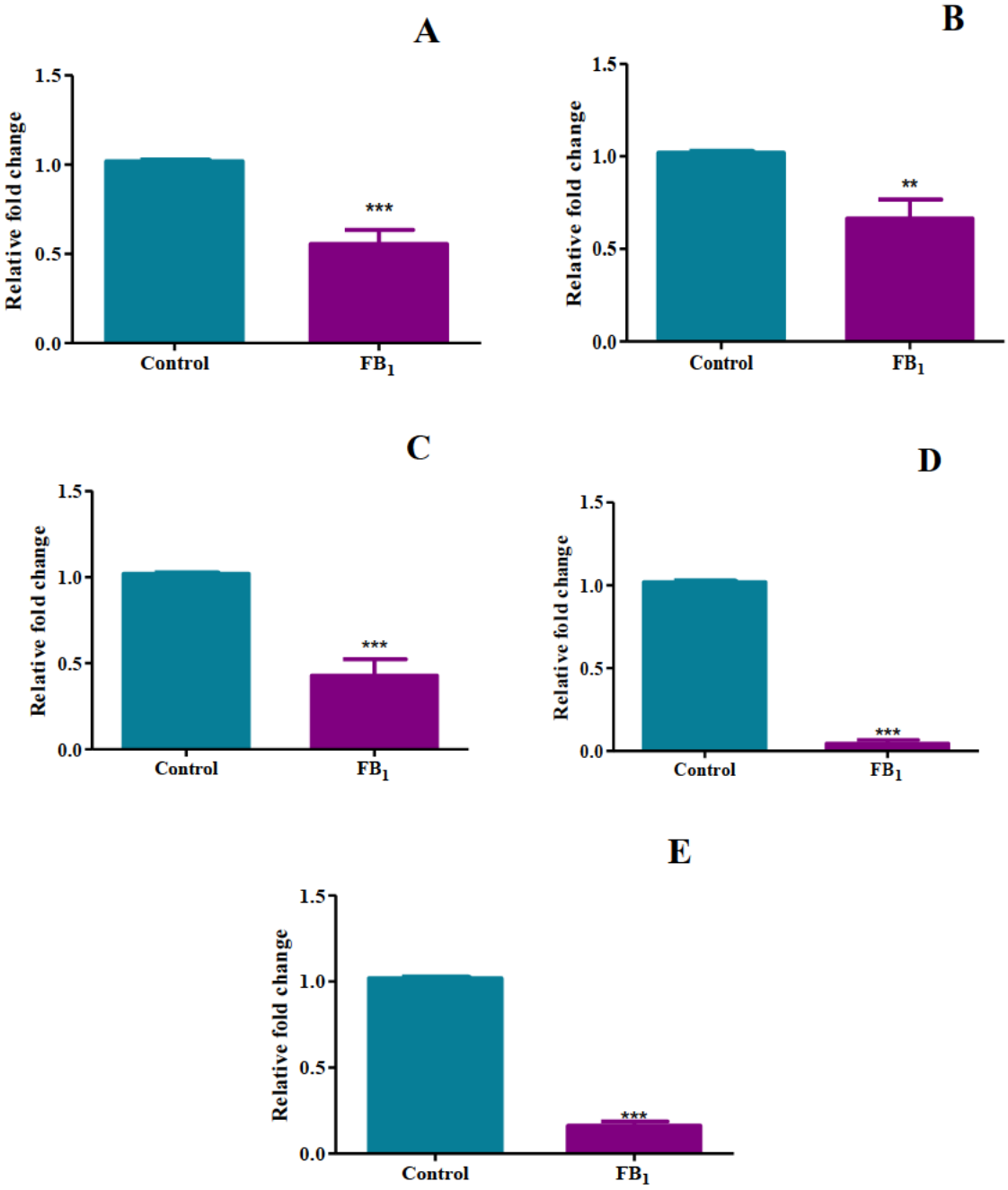

Figure 4.11: Treatment with FB_1 downregulated several inflammatory genes. This figure illustrates the effect of FB_1 on the gene expression of pro-inflammatory genes in C57BL/6 mice hearts. RNA isolated from control and FB_1-treated mice hearts was reverse transcribed into cDNA and analysed by qPCR. Treatment with FB_1 resulted in a significant decline in the expression of several inflammatory genes, including TNF-α (A), NF-κB (B), IL-6 (C), NLRP3 (D), and IL-18 (E). The results are shown as mean ± SEM (n=5/group). An unpaired t-test with Welch's correction was used to determine statistical significance (**p<0.005, ***p<0.0001).

4.3 Expression of inflammatory factors, caspases and associated cell death genes were downregulated by FB_1

The activation of the NLRP3 inflammasome is responsible for the activation of caspase-1, which subsequently cleaves pro-IL-1β into its active form, IL-1β. The FB_1-treated mice showed a significant reduction in the gene expression of both *caspase 1* and *IL-1β* ($p<0.0001$) (Figure 4.6A and Figure 4.6B respectively), which corresponded with the observed changes in the gene expression of upstream inflammatory factors. Caspase 1 activation is not limited to the activation of cytokines but also can activate the executioner of pyroptosis, GSDMD. FB_1 treatment led to a significant decrease in the expression of *GSDMD* ($p<0.0001$) (Figure 4.6C). The pyroptotic pathway is also influenced by another member of the Gasdermin family, GSDME, which is activated by caspase-3. A significant decline in the gene expression of *caspase-3* was observed ($p=0.0283$) by FB_1 (Figure 4.6D), indicating an impediment of the alternative pyroptotic pathway, which is consistent with the findings mentioned above.

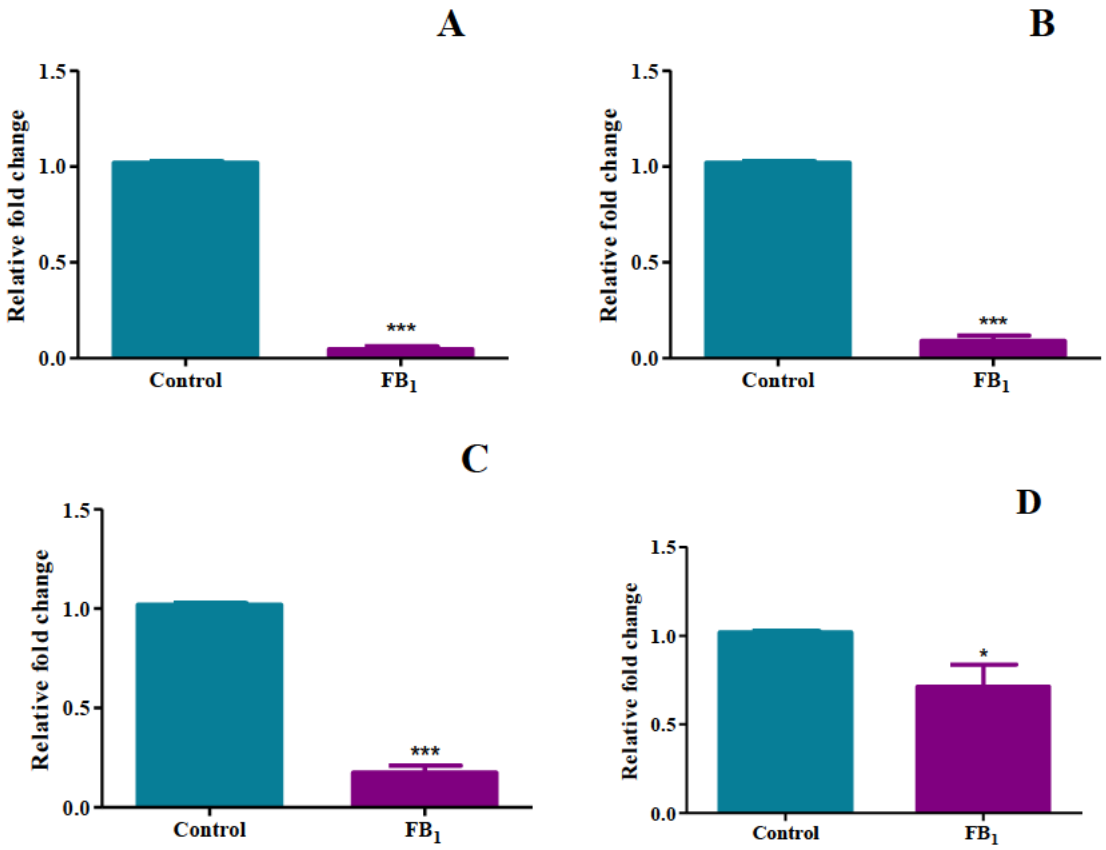

Figure 4.12: A decrease in gene expression of inflammatory factors associated with cell death proteins was induced by FB_1. The effect of FB_1 on the gene expression of pro-inflammatory genes and cell death proteins in C57BL/6 mice hearts. RNA isolated from control and FB_1-treated mice hearts was

reverse transcribed into cDNA and analysed by qPCR. A decrease in gene expression of inflammatory factors associated with cell death proteins was induced by FB_1. A significant decline in caspase 1 (A), IL-1β (B), GSDMD (C), and caspase 3 (D) gene expression was observed in mice treated with FB_1. The results are shown as mean ± SEM (n=5/group). An unpaired t-test with Welch's correction was used to determine statistical significance (*p<0.05, ***p<0.0001).

4.4 Gene expression of key regulatory factors in the inflammation pathway was decreased by FB_1

An emerging chemokine involved in the inflammatory response is CT-1. CT-1 has been shown to activate NF-kB through its interaction with the IκBα molecule. In this study, the gene expression of *CT-1* was found to be downregulated (p=0.0301) by FB_1 (Figure 4.7A), suggesting that its downstream effects, such as NF-kB activation, are inhibited. To counteract the pro-inflammatory response, IL-10 is typically activated to limit inflammation and promote healing. However, this study observed a decrease in *IL-10* gene expression by FB_1 (p=0.0031) (Figure 4.7B), indicating a more complex interplay in FB_1's ability to modulate gene expression.

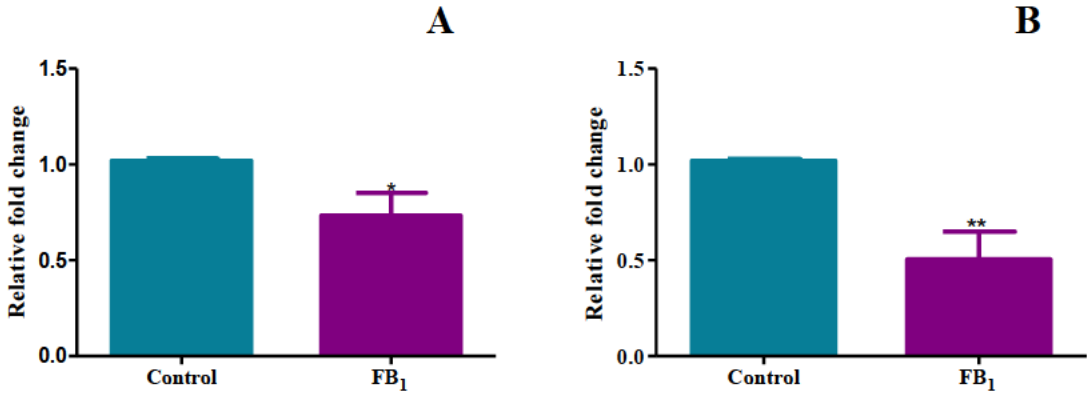

Figure 4.13: A decrease in gene expression of associated inflammatory factors, CT-1 and IL-10 was induced by FB_1. The effect of FB_1 on the gene expression of pro-inflammatory genes in C57BL/6 mice hearts. RNA isolated from control and FB_1-treated mice hearts was reverse transcribed into cDNA and analysed by qPCR. A decrease in gene expression of associated inflammatory factors, CT-1 and IL-10, was induced by FB_1. A significant decrease in chemokine CT-1 (A) and anti-inflammatory cytokine IL-10 (B) was observed after acute 24-hour exposure to FB_1. The results are shown as mean ± SEM (n=5/group). An unpaired t-test with Welch's correction was used to determine statistical significance (*p<0.05, **p<0.005).

4.5 Acute exposure to FB_1 leads to an increase in reactive nitrogen metabolites

A vital modulator of the inflammatory response is NO; however, due to its short half-life, its precursor metabolites, NO_2 and NO_3, can provide insight via the NOS assay. In this study, acute exposure of FB_1 revealed an upregulation in RNS concentration (p=0.0028) (Figure 4.8), which can lead to alterations in the inflammatory response.

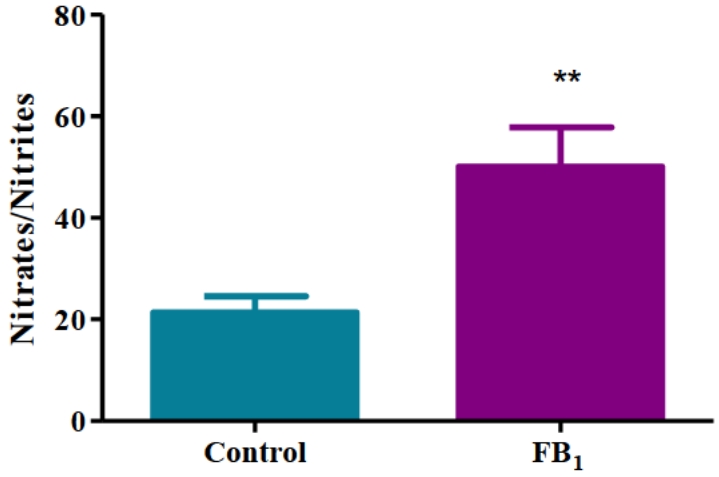

Figure 4.14: FB_1 induced Nitrate/Nitrite concentration during acute exposure. The effect of FB_1 on the gene expression of pro-inflammatory genes in C57BL/6 mice hearts. RNA isolated from control and FB_1-treated mice hearts was reverse transcribed into cDNA and analysed by qPCR. FB_1 treatment resulted in a significant upregulation of RNS, contributing to the inflammatory response. A significant increase in nitrate/nitrite concentration was observed during acute exposure to FB_1 (**p<0.005). The results are shown as mean ± SEM (n=5/group). An unpaired t-test with Welch's correction was used to determine statistical significance (**p<0.005).

4.6 FB_1 treatment increased protein expression of mediators of the inflammatory response

A key transcriptional activator of crucial pro-inflammatory cytokines that heightens the pro-inflammatory response is NF-κB. When NF-κB becomes activated through phosphorylation, it can lead to the transcriptional activation of downstream mediators of the inflammatory process. In this study, phosphorylated NF-κB (P-NF-κB) was significantly upregulated by FB_1, indicating an increase in subsequent pro-inflammatory cytokines (p=0.0051) (Figure 4.9A). The exacerbation of the inflammatory response has been shown to activate cell death pathways.

In this investigation, executioner caspase-3 was significantly increased by FB_1, indicating the onset of programmed cell death (apoptosis) (p=0.0082) (Figure 4.9B).

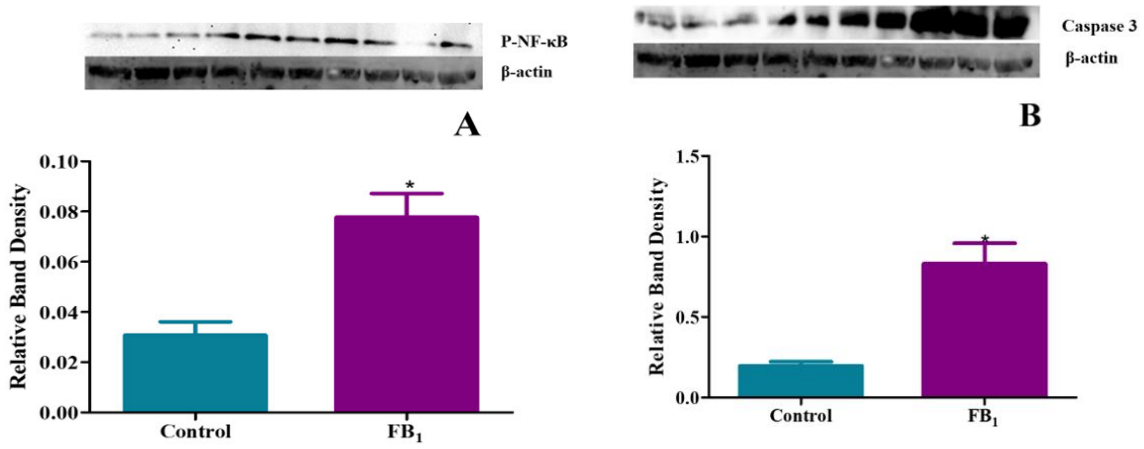

Figure 4.15: The treatment with FB_1 led to upregulation in proinflammatory cytokine expression
The effect of FB_1 on the protein expression of pro-inflammatory proteins in C57BL/6 mice hearts. Protein isolated from control and FB_1-treated mice hearts was standardised and quantified using western blotting. The transcription regulator of cytokine production in its active form showed significantly increased P-NFKB expression (A) and Caspase 3 (B). Bands 1 to 5 represent the control, and bands 6 to 10 represent the FB_1 treatment. These are representative blots which have been independently performed 3 times. The results are shown as mean ± SEM (n=5/group). An unpaired t-test with Welch's correction was used to determine statistical significance (*p<0.05).

4.7 Treatment of FB_1 led to significant upregulation of inflammation

The quantification of inflammatory cytokines in the serum revealed a significant contrast to the expression of inflammatory genes. TNF-α, typically produced by macrophages in response to toxic insults, was significantly increased by FB_1 ($p < 0.0001$) (Figure 4.10A). Both IL-6 and IL-1β were highly expressed (p<0.0001) (Figures 4.10B and 4.10C) due to FB_1, indicating an increase in the pro-inflammatory response. Conversely, the anti-inflammatory cytokine IL-10 showed a concurrent increase in response to FB_1 exposure (p=0.0087) (Figure 4.10D). Furthermore, TGF-β1, a cytokine known for its involvement in inflammation and its association with cardiac pathology such as heart failure and cardiac fibrosis, was significantly upregulated (p<0.0001) (Figure 4.9E). These data highlight the potential of FB_1 to trigger pathways associated with cardiac distress.

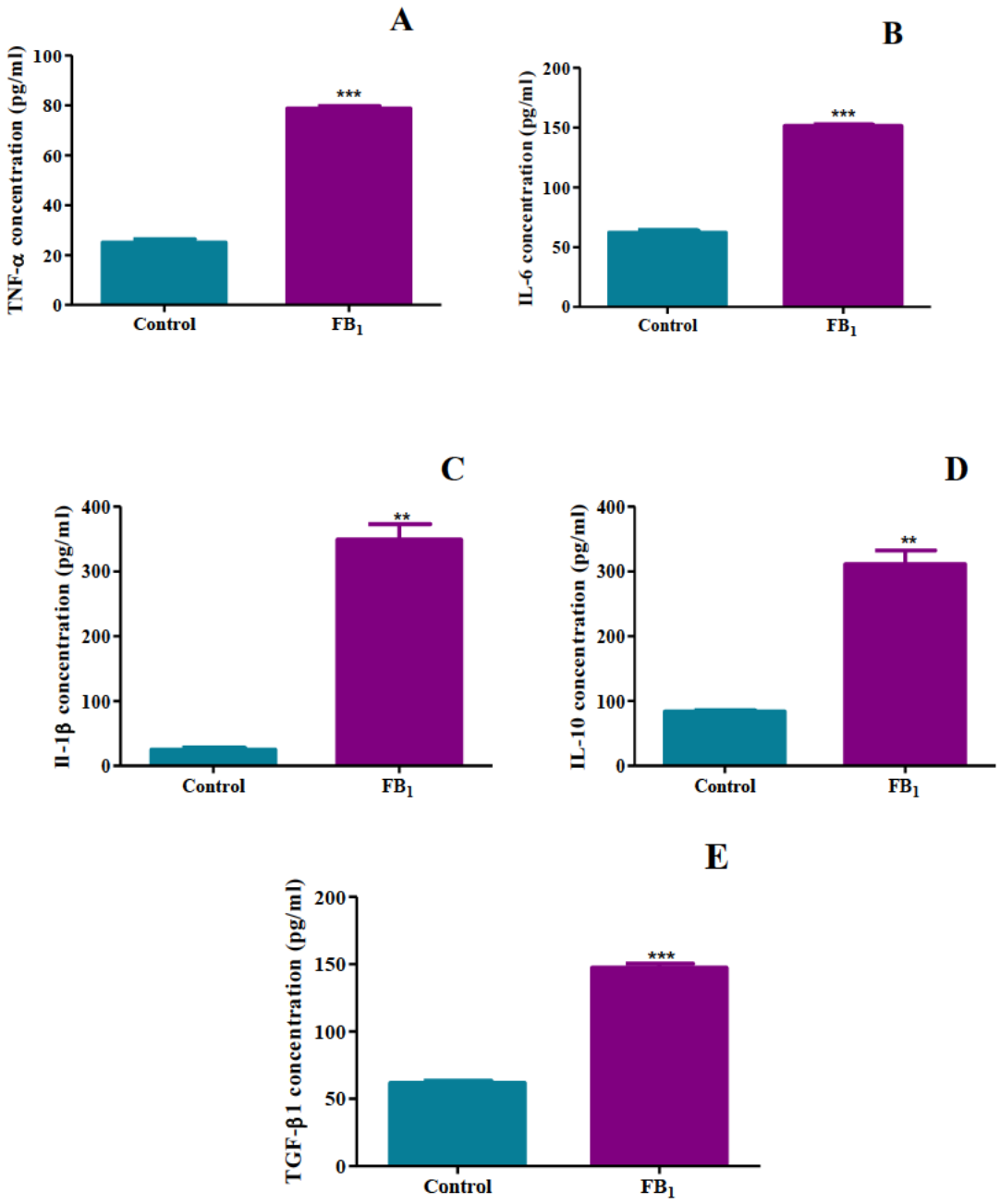

Figure 4.16: The induction of inflammatory factors by FB_1 in mice. The effect of FB_1 on the protein expression of pro-inflammatory proteins in C57BL/6 mice hearts. Mice heart serum was prepared by homogenizing control and FB_1-treated mice hearts and was quantified using ELISA. Serum levels of TNF-α (A), IL-6 (B), IL-1β (C), IL-10 (D), and TGF-β1 (E) were significantly upregulated in mice after FB_1 exposure. The results are shown as mean ± SEM (n=5/group). An unpaired t-test with Welch's correction was used to determine statistical significance (*$p<0.05$, **$p<0.005$, ***$p<0.0001$).

4.8 Global DNA Methylation levels were increased with FB_1 treatment

Global DNA methylation levels were found to be significantly increased in mice exposed to FB_1 (p=0.0196) as compared to the controls (Figure 4.11A). However, this contrasted with the gene expression analysis of DNA methylation-related genes. The protein expression of DNMT1 was significantly upregulated (p= 0,0036) (Figure 4.11B). However, MBD2 a demethylase, depicted a non-significant increase (p=0.0804) (Figure 4.11C) in expression.

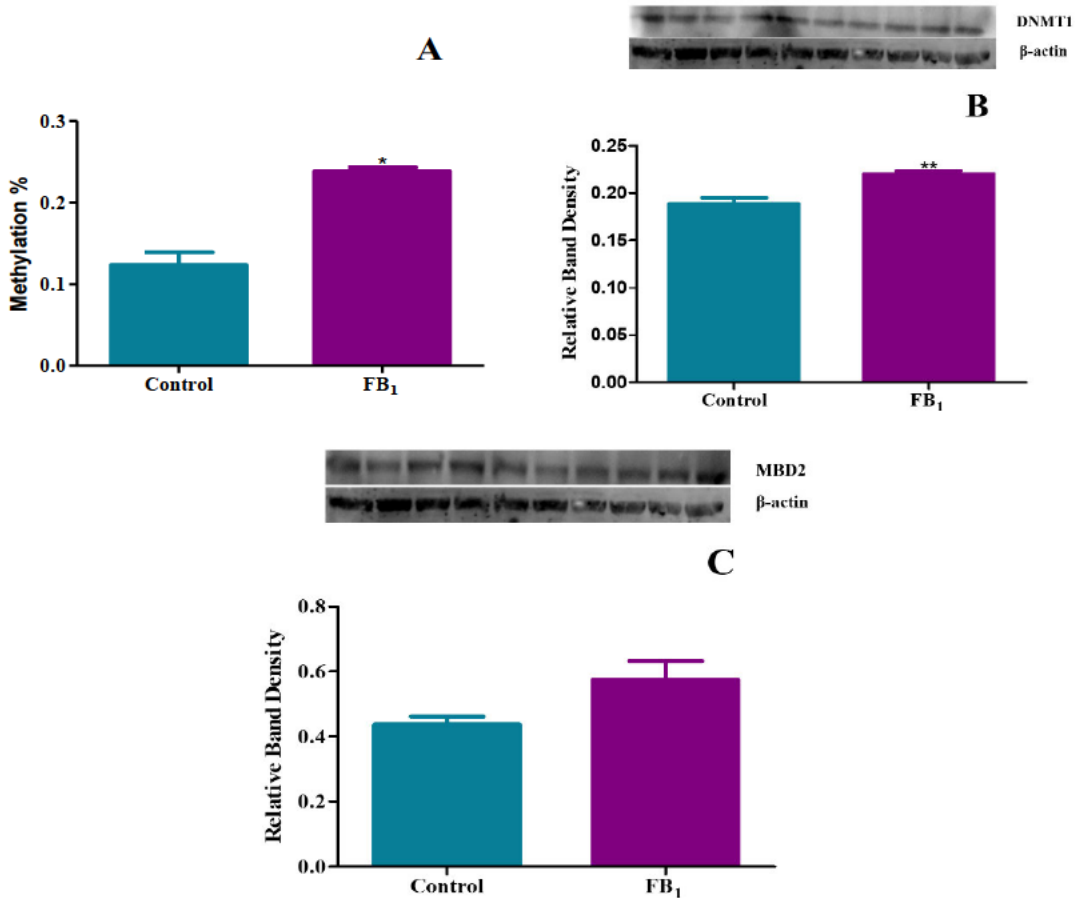

Figure 4.17: FB_1 exposure led to increased DNA methylation. The effect of FB_1 on the protein expression of DNA methylation regulators in C57BL/6 mice hearts. Protein isolated from control and FB_1-treated mice hearts as well as serum was standardised and quantified using ELISA and western blotting. A significant increase in global DNA methylation was observed with FB_1 treatment (A). The protein expression of DNMT1 was significantly upregulated (B), while MBD2 was non-significantly increased (C). Bands 1 to 5 represent the control, and bands 6 to 10 represent the FB_1 treatment. These are representative blots which have been independently performed 3 times. The results are shown as mean ± SEM (n=5/group). An unpaired t-test with Welch's correction was used to determine statistical significance (*p<0.05, **p<0.005).

4.9 Gene expression of DNMTs was decreased with FB_1 treatment

DNA methylation is an important regulator of gene expression. However, this contrasted with the protein expression analysis of DNA methylation-related factors. Specifically, the gene expression of *DNMT1*, *DNMT3A*, and *DNMT3B* were all significantly decreased ($p<0.0001$, $p<0.0001$, and $p=0.0396$, respectively) (Figure 4.12A, Figure 4.12C and Figure 4.12D). For example, *MDB2* (demethylase) showed a non-significant increase ($p=0.0567$) (Figure 4.12D), which corresponded with a dysregulation in *DNA methyltransferase* (DNMT) expression. This suggests that FB_1 exposure has the potential to disrupt gene regulation through altered DNA methylation.

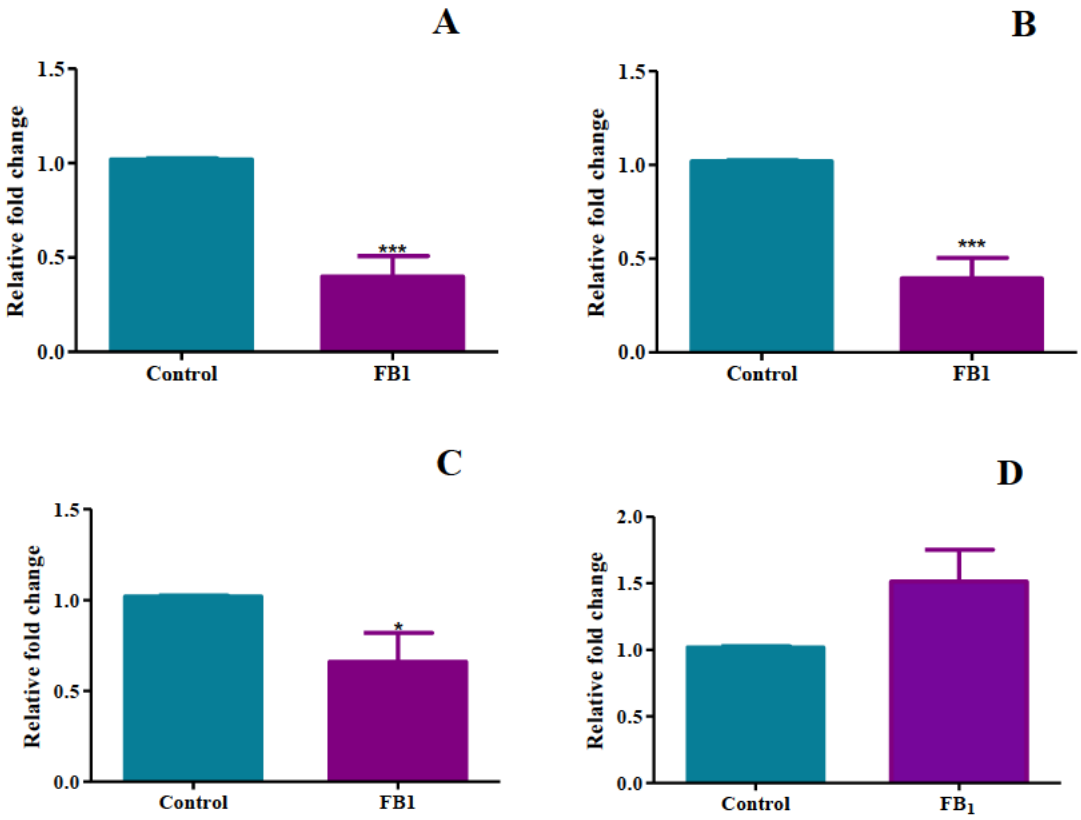

Figure 4.18: FB_1 exposure led to dysregulation of DNA methylation-associated genes. The effect of FB_1 on the gene expression of DNA methylation genes in C57BL/6 mice hearts. RNA isolated from control and FB_1-treated mice hearts was reverse transcribed into cDNA and analysed by qPCR. FB_1 exposure led to dysregulation of DNA methylation-associated genes. Gene expression of DNMT1 (A), DNMT3A (B), and DNMT3B (C) were decreased, while MBD2 was non-significantly increased compared to the controls. The results are shown as mean ± SEM (n=5/group). An unpaired t-test with Welch's correction was used to determine statistical significance (*p<0.05, ***p<0.0001)

Chapter 5: Discussion and Conclusion

5.1 Discussion

The prevalence of mycotoxins has been increasing at an alarming rate globally. Their impact is not limited to economic loss and food insecurity; they also threaten human and animal health. Among these fungal secondary metabolites, FB_1 has been identified as a significant contributor to global mycotoxin contamination, with rates exceeding 80% in countries such as Algeria, Brazil, Nigeria, South Africa, and South Korea (Gao *et al*., 2023). Due to its increasing toxicity, scientists still need to elucidate the cardiotoxic effects of FB_1, as studies remain limited, while other toxic effects in organs such as the liver and kidney have been highlighted. Previous studies showed that FB_1 induced oxidative stress, mitochondrial dysfunction, altered sphingolipid metabolism, triggered apoptosis, and epigenetic modifications (DNA methylation) (Merrill Jr *et al*., 2001, Kim *et al*., 2018, Gao *et al*., 2023). However, studies on FB_1's cardiotoxic effects are limited, and other regulatory pathways, such as inflammation and DNA methylation, need further understanding. This pilot study highlights the complex interplay between acute FB_1 exposure, inflammatory pathways, and DNA methylation, leading to toxic effects in the hearts of mice.

The molecular docking of FB_1 on the TNF-α protein suggests its potential to cause the trimerization of the molecule by facilitating binding in the cleft among three subunits. Preliminary structural bioinformatics findings indicate that FB_1 could potentially bind and interact at Tyrosine115 (Tyr115), Proline113 (Pro113), and Serine99 (Ser99) residues on each subunit (Figure 4.1). These residues have been highlighted in the literature for specific functions as mentioned below. It is assumed that Tyr115 present in subunits A, B, and C interacts with Ser99 in subunits C, A, and B to form hydrogen bonds at a length of 3.0 Å. Pro113 on subunits B, C, and A is thought to interact with Tyr72 in subunits A, B, and C to form conserved hydrogen bonds present in the channel between the two adjacent subunits. The importance of Tyr115 has been suggested as a site crucial for receptor binding in modelling studies to facilitate the activation of the molecule, in agreement with Pro113, which FB_1 may be able to interact with to create hydrogen bonds and interactions that may facilitate inactivation of the molecule (Baeyens *et al*., 1999). In Figure 4.1, FB_1 binding to TNF-α appears to not only lead to the possible trimerization of the molecule but also tries to fit itself into the groove. This trimerization is highlighted as an important process for the biological activation of the TNF receptors, thus indicating that FB_1 could theoretically prompt the activation of TNF-α. However, structural dynamics studies are needed to determine the exact

contacts and interactions between FB_1 and the proteins, and further validation of these suggestions is required.

Following the assumed key interaction between FB_1 and TNF-α in silico, a crucial modulator of the pro-inflammatory response, iNOS, was docked with FB_1. The docking of iNOS and FB_1 suggests the potential affinity of FB_1 to bind to the haeme molecule binding site while prompting a subsequent interaction with cysteine 194 (Cys194) (Figure 4.2). This crucial interaction is assumed to cause dimerization of the molecule to facilitate its activation, whereas a mutation at the Cys194 residue is thought to prevent haeme from functioning. Given this information and the assumed position of FB_1, it is hypothesized that FB_1 could enhance the activation of this enzyme, leading to an alteration in the inflammatory response at an *in silico* level (Cinelli *et al*., 2020). However, structural dynamics studies using LigPlot+ to determine the exact contacts and interactions between FB_1 and the proteins are needed, and further validation of these suggestions is required.

The induction of factors such as TNF-α is assumed to lead to the subsequent activation of NF-κB, which comprises p65 and p50 subunits. The preliminary in-silico findings of FB_1 docking on the NF-κB (p60) subunit suggest the potential affinity of FB_1 to interact with Asn202 and Ser203 residues (Figure 4.3). Studies have shown that mutations or interference at these residues can lead to impaired binding of inhibitor of kappa B alpha (IκBα), resulting in the loss of inhibition of the NF-κB molecule (Huxford *et al*., 2002). These findings, however, contrast with FB_1 docking on the p50 subunit of NF-κB, which showed interaction with the DNA molecule of NF-κB and the residue Gln274 (Figure 4.4). Emerging computational studies have depicted the importance of the p50 homodimer in facilitating specific gene target activation. The dimerization of this subunit is assumed to occur due to interactions with Gln274 (Zhu *et al*., 2023). Given that FB_1 uses this interaction between the DNA molecule and the p50 subunit at the Gln274 residue, it can be assumed that there may be a potential effect on the gene targets of NF-κB due to FB_1. However, these findings are preliminary, and structural dynamics studies using LigPlot+ to determine the exact contacts and interactions between FB_1 and the proteins are needed, and further validation of these suggestions is required.

The in-silico findings prompted an examination of the gene expression of inflammatory and DNA methylation factors in vitro. A significant dysregulation in the gene expression of *TNF-α, NF-κB, IL-6, NLRP3* inflammasom*e, IL-18, Caspase 1, IL-1β, GSDMD, Caspase 3, CT-1,* and *IL-10* (Figures 4.5, 4.6, and 4.7) was observed in the mice treated with FB_1. Given that this

was a preliminary structural bioinformatics study, it led to predictions that could be tested through experimental methods. These gene expression studies partly aligned with the predictions of the FB1-NF-KB *in-silico* docking studies. However, these findings contradicted another study , which showed that FB_1 upregulated the gene expression of *IL-6, IL-1β, TNF-α, IFN-γ,* and *caspase 3* in porcine alveolar macrophages, with a subsequent increase in serum concentrations of these cytokines (Jin *et al*., 2022). This decline in the expression of both pro-inflammatory and anti-inflammatory genes as well as associated apoptosis genes, indicated a complex alteration in the inflammation process. Therefore, the quantification of the crucial modulator of the inflammatory response, NO, was imperative. The indirect measure of NO levels using RNS in this study depicted an increase in its metabolites, nitrates and nitrites (Figure 4.8). This increase suggested a more complex interplay in the inflammatory process as NO upregulation can lead to the activation of iNOS by pro-inflammatory cytokines in immune cells such as macrophages, causing an excessive increase beyond normal physiological quantities. Excess production of NO can mediate a heightened pro-inflammatory response, which can be correlated with tissue damage (Sharma *et al*., 2007). Reactive nitrogen species (RNS) and nitrates/nitrites have a simple metabolites that have similar metabolic pathways in common. RNS, such as nitric oxide (NO) and peroxynitrite (ONOO-), are reactive molecules involved in various physiological and pathological processes. Whereas nitrates (NO3-) and nitrites (NO2-) are part of the nitrogen cycle and can be converted into RNS through enzymatic and non-enzymatic pathways(Tiso and Schechter, 2015). The observed upregulation of RNS, which was 2.5 times higher than the control, is sufficient to elicit an inflammatory response. This is because elevated levels of RNS can activate redox-sensitive transcription factors such as NF-κB, leading to the increased transcription of pro-inflammatory cytokines and chemokines(Korhonen *et al*., 2005).

These findings were consistent with a study conducted in murine macrophages, which found that FB_1 treatment at 24 hours led to an increase in NO and subsequently peroxynitrite. The study further elaborated on a possible link between these metabolites and programmed cell death (Lanubile *et al*., 2022). In light of this evidence, further examination of pro-inflammatory cytokine protein expression was imperative.

The determination of the protein expression of key cytokines and modulators of inflammation revealed a significant upregulation in P-NF-κB, TNF-α, IL-6, IL-1β, IL-10, and TGF-β1 (Figure 4.9 and Figure 4.10). The upregulation of these pro-inflammatory markers indicated a heightened pro-inflammatory response. Specifically, the increase in TNF-α concentration

revealed that the toxic insult of FB_1 triggered the activation of the pro-inflammatory pathway, leading to the subsequent activation of P-NF-κB. This further transcribed the activation of pro-inflammatory mediators IL-6, IL-18, and IL-1β. Concurrently, anti-inflammatory mediators IL-10 and TGF-β1 were also upregulated. These results are consistent with previous studies conducted in porcine kidney cells, which depicted the key role of TNF-α in activating inflammatory responses at a protein level, in addition to upregulated NF-κB and caspase 3 activity, further exemplifying the critical role FB_1 plays in inflammation-associated apoptosis (Chen *et al*., 2020). Additionally, a similar study showed the implication of the cytokine network in FB_1-mediated toxicity, where cytokines such as TNF-α, IL-1β, IL-6, and IL-10 were all concurrently upregulated, which was similar to this study as all of these cytokines were upregulated (Bhandari *et al*., 2001b). The concurrent stimulation of IL-10 could be crucial in understanding the mediated response, as a study conducted in intestinal tissue showed that IL-10 is a positive regulator of NF-κB pathway transcription, similar to findings in this study (Papoutsopoulou *et al*., 2022). Interestingly, a study conducted on mice liver revealed the potential ability of increased TGF-β1 expression to cause apoptosis due to FB_1 treatment on rat liver. These findings correlated with this study, which not only had a marked increase in TGF-β1 expression but also in caspase 3 expression (Figure 4.9 and Figure 4.10) (Lemmer *et al*., 1999).

The disparity observed between the inflammatory cytokines' gene and protein expression could be due to transcriptional or translational modifications of the gene expression of the cytokines. Post-transcriptional modifications play key roles in biological processes and could be the reason for the disparity observed between gene and protein expression. This is because translational regulation relies on the recruitment of various mRNA species to the ribosome to prompt protein synthesis however this leads to decreased correlation between the amount of mRNA and the amount of encoded protein (Halbeisen *et al*., 2007). Other regulatory mechanisms include epigenetic mechanisms such as DNA methylation which are crucial transcriptional processes involved in the modulation of gene expression (Sebastian *et al*., 2018, Poetsch and Plass, 2011). Global DNA methylation levels were significantly upregulated, with a notable increase in DNMT1 and no significant change in MBD2, indicating DNA hypermethylation (Figure 4.11). However, these findings contradicted the expression patterns of the DNA methylation genes. Despite the observed DNA hypermethylation, the expression of all DNMT genes significantly decreased, while MBD2 expression showed a non-significant increase. (Figure 4.12). This suggests a complex interplay such as mRNA stability as

mentioned above could be a factor. Other tests, such as Northern blots and microarray assays, can be used to confirm the findings. This study's findings correlated with a study conducted on HEK293 cells treated with FB_1, which showed upregulation of global DNA methylation and DNMT activity (Sugiyama *et al*., 2021). However, other studies highlight the role of microRNAs in the regulation of gene expression. A notable study conducted in cardiomyocytes demonstrated that miR-29b can decrease the gene expression of DNMTs in these cells (Wu *et al*., 2022). These findings are consistent with this study, further suggesting that complex mechanisms may be involved in gene silencing. Another study conducted on human kidney cells revealed that FB_1 treatment increased DNA methylation in a set of genes, further implicating FB_1 in gene modulation (Bayoglu *et al*., 2024).

Increasing evidence suggests that DNA methylation can further affect cytokine activity. This was shown in a study conducted in bone marrow-derived mast cells, which demonstrated that DNA methylation can suppress the gene activity of NF-κB, further modulating TNF-α, IL-13, and IL-6 expression. The inhibition of DNA methylation with azacytidine (5-AZA) resulted in increased gene expression of these cytokines. It does highlight that further experiments using 5-AZA might be useful to investigate the effects of FB_1 on cytokine gene expression. (Li *et al*., 2024). These inhibitors are furthermore valuable for exploring the epigenetic landscape of cells. By blocking DNA methylation, researchers can examine how alterations in methylation patterns influence gene expression and impact the effects of FB_1 on inflammatory pathways in the mice heart, particularly focusing on cytokine regulation and disease progression. Similar presentations were correlated in this study, as FB_1 treatment resulted in increased DNA methylation, which led to subsequent gene silencing. This contrasted with increased protein expression of crucial cytokines TNF-α, NF-κB, IL-6, IL-1β, IL-18, IL-10, and TGF-β1 in mice.

The amalgamation of these pathways has been shown to contribute to the onset of various cardiac distresses. The pathogenesis of cardiac distresses, such as HF, has been associated with elevated TGF-β1 levels, which are activated upon acute ischemia, norepinephrine, or angiotensin II stimulation. Upon stimulation, increased TGF-β1 in cardiomyocytes leads to exacerbated fibrosis and hypertrophy in the heart. This can be correlated with this study which depicted elevations in TGF-β1 (Figure 4.10E) (Osmancik and Louckova, 2017). Studies have established that increased TNF-α in circulation can lead to the development of cardiac hypertrophy. Furthermore, TNF-α has been shown to exert its potent effects on the heart by inducing apoptosis and decreasing contractility in vitro (Krown *et al*., 1996). The complexity of TNF-α signalling, indicative of NF-κB activation, is associated with the pathologies of HF.

Provided with this evidence, cytokines have been shown to be associated with the onset of cardiac distress (Figure 4.9A and Figure 4.10A) (Hilfiker-Kleiner *et al*., 2006). Other studies indicate that IL-6 has been a crucial diagnostic marker for those presenting with HF, as IL-6 levels are significantly upregulated (Figure 4.10B) (Tsutamoto *et al*., 1998). In light of this evidence, there is a strong link between cardiac stresses and the inflammatory response. Therefore, we can conclude that FB_1 has the ability to affect inflammatory and DNA methylation pathways with the potential to cause cardiac distress.

5.2 Conclusion

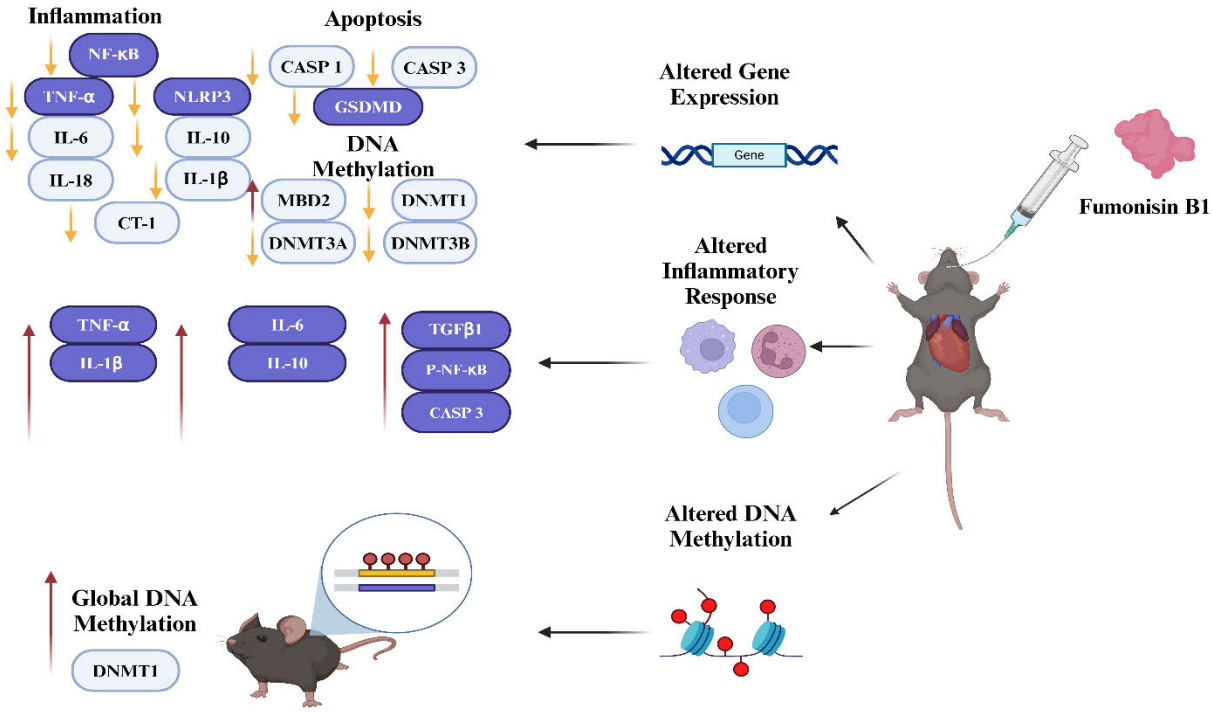

Figure 5.1: A graphical overview of this study which demonstrated the silencing of key genes involved in inflammation and DNA methylation which was contrasted with increased protein expression of mediators and factors which activated inflammation and DNA methylation pathways.

This study investigates the cardiotoxic effects of FB_1 on mice, focusing on inflammatory pathways and cytokine regulation. The research highlights the complex interplay between FB_1 exposure, inflammatory responses, and DNA methylation. Molecular docking studies revealed that FB_1 has the potential to bind to key residues on the TNF-α protein, possibly facilitating its trimerization and activation. Specifically, FB_1 has the potential to interact with Tyrosine115 (Tyr115), Proline113 (Pro113), and Serine99 (Ser99) residues, which are crucial for receptor binding and activation. Additionally, FB_1 was found to potentially interact with the haeme molecule binding site of iNOS, potentially enhancing its activation and altering the inflammatory response. The docking studies also suggested that FB_1 might interact with the NF-κB subunits, affecting their binding and activation.

In vitro gene expression analysis showed significant dysregulation of inflammatory and DNA methylation factors, including TNF-α, NF-κB, IL-6, NLRP3 inflammasome, IL-18, Caspase 1, IL-1β, GSDMD, Caspase 3, CT-1, and IL-10. Protein expression analysis revealed upregulation

of pro-inflammatory cytokines (TNF-α, IL-6, IL-1β) and anti-inflammatory mediators (IL-10, TGF-β1), indicating a heightened inflammatory response. The study also observed increased global DNA methylation, with upregulation of DNMT1 and no significant change in MBD2, suggesting DNA hypermethylation.

These findings suggest that FB_1 can activate inflammatory pathways and potentially cause cardiac distress through epigenetic modifications and cytokine dysregulation. The study underscores the importance of further research to understand the mechanisms underlying FB_1-induced cardiotoxicity and the potential use of DNA methylation inhibitors to explore the epigenetic landscape and its impact on gene expression and disease progression.

5.3 Limitations and Future Plans

Limitations of this study include its pilot nature, which focused solely on acute exposure. Future studies can be aimed at conducting molecular dynamics simulations on the docked ligands to validate the docking for each compound, as well as performing contact analysis using LigPlot+ to determine the nature of the non-covalent interactions and the distance of hydrogen bonds. Consequently, further research is needed to investigate the effects of prolonged exposure to FB_1 on the hearts of mice. Additionally, employing a cardiovascular disease model could help determine the specific cardiac distress induced by FB_1. Future studies should focus on determining the specific DNA methylation patterns at the promoter regions of key cytokine genes, such as TNF-α, IL-6, and IL-1β, to determine if FB_1-induced methylation is responsible for gene silencing. By employing techniques such as methylation-specific PCR, researchers can elucidate the methylation status of these promoter regions and correlate it with gene expression levels. This approach will help determine whether the observed downregulation of cytokine gene expression is directly linked to epigenetic modifications. Furthermore, post-transcriptional and post-translational modifications should be looked at for future work.

References

ABDULKHALEQ, L., ASSI, M., ABDULLAH, R., ZAMRI-SAAD, M., TAUFIQ-YAP, Y. & HEZMEE, M. 2018. The crucial roles of inflammatory mediators in inflammation: A review. *Veterinary world,* 11**,** 627.

ADEBO, O. A., KAYITESI, E. & NJOBEH, P. B. 2019. Reduction of Mycotoxins during Fermentation of Whole Grain Sorghum to Whole Grain Ting (a Southern African Food). *Toxins,* 11**,** 180.

AGARWAL, S. & MEHROTRA, R. 2016. An overview of molecular docking. *JSM chem,* 4**,** 1024-1028.

AHANGARKANI, F., ROUHI, S. & GHOLAMOUR AZIZI, I. 2014. A review on incidence and toxicity of fumonisins. *Toxin Reviews,* 33**,** 95-100.

AHMED, A. U. 2011. An overview of inflammation: mechanism and consequences. *Frontiers in Biology,* 6.

AKINMUSIRE, O. O., EL-YUGUDA, A.-D., MUSA, J. A., OYEDELE, O. A., SULYOK, M., SOMORIN, Y. M., EZEKIEL, C. N. & KRSKA, R. 2019. Mycotoxins in poultry feed and feed ingredients in Nigeria. *Mycotoxin Research,* 35**,** 149-155.

ALHARBI, K. S., ALENEZI, S. K. & GUPTA, G. 2023. Chapter 1 - Pathophysiology and pathogenesis of inflammation. *In:* PRASHER, P., ZACCONI, F. C., WITHEY, J. H., RATHBONE, M. & DUA, K. (eds.) *Recent Developments in Anti-Inflammatory Therapy.* Academic Press.

ANUMUDU, C. K., EKWUEME, C. T., UHEGWU, C. C., EJILEUGHA, C., AUGUSTINE, J., OKOLO, C. A. & ONYEAKA, H. 2024. A Review of the Mycotoxin Family of Fumonisins, Their Biosynthesis, Metabolism, Methods of Detection and Effects on Humans and Animals. *International Journal of Molecular Sciences,* 26**,** 184.

ARMENANTE, F., MEROLA, M., FURIA, A. & PALMIERI, M. 1999. Repression of the IL-6 gene is associated with hypermethylation. *Biochem Biophys Res Commun,* 258**,** 644-7.

ARUMUGAM, T. & CHUTURGOON, A. A. 2021. Toxicoepigenetic consequences of fumonisin B1 exposure: current knowledge and future perspective. *Epigenomics,* 13**,** 1849-1852.

AWUCHI, C. G., ONDARI, E. N., NWOZO, S., ODONGO, G. A., ESEOGHENE, I. J., TWINOMUHWEZI, H., OGBONNA, C. U., UPADHYAY, A. K., ADELEYE, A. O. & OKPALA, C. O. R. 2022. Mycotoxins' Toxicological Mechanisms Involving Humans, Livestock and Their Associated Health Concerns: A Review. *Toxins,* 14**,** 167.

AYDIN, S. 2015. A short history, principles, and types of ELISA, and our laboratory experience with peptide/protein analyses using ELISA. *Peptides,* 72**,** 4-15.

BAEYENS, K. J., DE BONDT, H. L., RAEYMAEKERS, A., FIERS, W. & DE RANTER, C. J. 1999. The structure of mouse tumour-necrosis factor at 1.4 A resolution: towards modulation of its selectivity and trimerization. *Acta Crystallogr D Biol Crystallogr,* 55**,** 772-8.

BAYOGLU, S. O., KARAMAN, E. & OZDEN, S. 2024. Effects of fumonisin B1 on gene-specific DNA methylation related to cancer pathways of p53 signalling and PI3K/Akt signalling in human kidney cells. *World Mycotoxin Journal,* 1**,** 1-13.

BEGUM, H., MURUGESAN, P. & TANGUTUR, A. D. 2022. Western blotting: a powerful staple in scientific and biomedical research. *Biotechniques,* 73**,** 58-69.

BEUKES, I., ROSE, L.J., SHEPHARD, G.S., FLETT, C.F. AND VILJOEN, A. 2017. Mycotoxigenic Fusarium species associated with grain crops in South Africa– A review. . *South African Journal of Science,* 113.

BHANDARI, N., HE, Q. & SHARMA, R. P. 2001. Gender-related differences in subacute fumonisin B1 hepatotoxicity in BALB/c mice. *Toxicology,* 165**,** 195-204.

BIRD, A. 2002. DNA methylation patterns and epigenetic memory. *Genes & Development,* 16**,** 6-21.

CAO, C., XIAN, R., LIN, F., LI, X., LI, X., QIANG, F. & LI, X. 2022. Fumonisin B1 induces hepatotoxicity in mice through the activation of oxidative stress, apoptosis and fibrosis. *Chemosphere,* 296**,** 133910.

CARNEIRO, B. A. & EL-DEIRY, W. S. 2020. Targeting apoptosis in cancer therapy. *Nature reviews Clinical oncology,* 17**,** 395-417.

CHAI, R., XUE, W., SHI, S., ZHOU, Y., DU, Y., LI, Y., SONG, Q., WU, H. & HU, Y. 2022. Cardiac Remodeling in Heart Failure: Role of Pyroptosis and Its Therapeutic Implications. *Frontiers in Cardiovascular Medicine,* 9.

CHEN, J., WEI, Z., WANG, Y., LONG, M., WU, W. & KUCA, K. 2021a. Fumonisin B1: Mechanisms of toxicity and biological detoxification progress in animals. *Food and Chemical Toxicology,* 149**,** 111977.

CHEN, J., WEN, J., TANG, Y., SHI, J., MU, G., YAN, R., CAI, J. & LONG, M. 2021b. Research Progress on Fumonisin B1 Contamination and Toxicity: A Review. *Molecules,* 26**,** 5238.

CHEN, J., WEN, J., TANG, Y., SHI, J., MU, G., YAN, R., CAI, J. & LONG, M. 2021c. Research Progress on Fumonisin B1 Contamination and Toxicity: A Review. *Molecules,* 26.

CHEN, J., YANG, S., HUANG, S., YAN, R., WANG, M., CHEN, S., CAI, J., LONG, M. & LI, P. 2020. Transcriptome study reveals apoptosis of porcine kidney cells induced by fumonisin B1 via TNF signalling pathway. *Food Chem Toxicol,* 139**,** 111274.

CHEN, L., DENG, H., CUI, H., FANG, J., ZUO, Z., DENG, J., LI, Y., WANG, X. & ZHAO, L. 2018. Inflammatory responses and inflammation-associated diseases in organs. *Oncotarget,* 9**,** 7204-7218.

CHEN, X., TIAN, P.-C., WANG, K., WANG, M. & WANG, K. 2022. Pyroptosis: Role and Mechanisms in Cardiovascular Disease. *Frontiers in Cardiovascular Medicine,* 9.

CHRISTOFFELS, V. M., SMITS, G. J., KISPERT, A. & MOORMAN, A. F. M. 2010. Development of the Pacemaker Tissues of the Heart. *Circulation Research,* 106**,** 240-254.

CHRUN, E. S., MODOLO, F. & DANIEL, F. I. 2017. Histone modifications: A review about the presence of this epigenetic phenomenon in carcinogenesis. *Pathology-Research and Practice,* 213**,** 1329-1339.

CHUTURGOON, A., PHULUKDAREE, A. & MOODLEY, D. 2014. Fumonisin B1 induces global DNA hypomethylation in HepG2 cells – An alternative mechanism of action. *Toxicology,* 315**,** 65-69.

CINELLI, M. A., DO, H. T., MILEY, G. P. & SILVERMAN, R. B. 2020. Inducible nitric oxide synthase: Regulation, structure, and inhibition. *Med Res Rev,* 40**,** 158-189.

CONSTABLE, P. D., SMITH, G. W., ROTTINGHAUS, G. E. & HASCHEK, W. M. 2000. Ingestion of fumonisin B1-containing culture material decreases cardiac contractility and mechanical efficiency in swine. *Toxicology and applied pharmacology,* 162**,** 151-160.

DAVEY, D. D., ADLER, M., ARNAIZ, D., EAGEN, K., ERICKSON, S., GUILFORD, W., KENRICK, M., MORRISSEY, M. M., OHLMEYER, M., PAN, G., PARADKAR, V. M., PARKINSON, J., POLOKOFF, M., SAIONZ, K., SANTOS, C., SUBRAMANYAM, B., VERGONA, R., WEI, R. G., WHITLOW, M., YE, B., ZHAO, Z. S., DEVLIN, J. J. & PHILLIPS, G. 2007. Design, synthesis, and activity of 2-imidazol-1-ylpyrimidine derived inducible nitric oxide synthase dimerization inhibitors. *J Med Chem,* 50**,** 1146-57.

DEY, D. K., KANG, J. I., BAJPAI, V. K., KIM, K., LEE, H., SONWAL, S., SIMAL-GANDARA, J., XIAO, J., ALI, S., HUH, Y. S., HAN, Y.-K. & SHUKLA, S. 2023. Mycotoxins in food and feed: toxicity, preventive challenges, and advanced detection techniques for associated diseases. *Critical Reviews in Food Science and Nutrition,* 63**,** 8489-8510.

DICK, S. A. & EPELMAN, S. 2016. Chronic Heart Failure and Inflammation. *Circulation Research,* 119**,** 159-176.

DOMIJAN, A.-M. 2012. Fumonisin B1: A Neurotoxic Mycotoxin / Fumonizin B1: Neurotoksični Mikotoksin. *Archives of Industrial Hygiene and Toxicology,* 63**,** 531-544.

FRANCHI, L., EIGENBROD, T., MUÑOZ-PLANILLO, R. & NUÑEZ, G. 2009. The inflammasome: a caspase-1-activation platform that regulates immune responses and disease pathogenesis. *Nature Immunology,* 10**,** 241-247.

GAO, Z., LUO, K., ZHU, Q., PENG, J., LIU, C., WANG, X., LI, S. & ZHANG, H. 2023. The natural occurrence, toxicity mechanisms and management strategies of Fumonisin B1 : A review. *Environmental Pollution,* 320**,** 121065.

GAZZAR, M. E., YOZA, B. K., CHEN, X., HU, J., HAWKINS, G. A. & MCCALL, C. E. 2008. G9a and HP1 Couple Histone and DNA Methylation to TNFα Transcription Silencing during Endotoxin Tolerance. *Journal of Biological Chemistry,* 283**,** 32198-32208.

GELDERBLOM, W., CAWOOD, M., SNYMAN, S. & MARASAS, W. 1994. Fumonisin B1 dosimetry in relation to cancer initiation in rat liver. *Carcinogenesis,* 15**,** 209-214.

GHAZI, T., NAGIAH, S., DHANI, S. & CHUTURGOON, A. A. 2020. Fusaric acid-induced epigenetic modulation of hepatic H3K9me3 triggers apoptosis in vitro and in vivo. *Epigenomics,* 12**,** 955-972.

GIBNEY, E. R. & NOLAN, C. M. 2010. Epigenetics and gene expression. *Heredity,* 105**,** 4-13.

GUSEV, E. & ZHURAVLEVA, Y. 2022. Inflammation: A New Look at an Old Problem. *International Journal of Molecular Sciences,* 23**,** 4596.

GUZIK, T., KORBUT, R. & ADAMEK-GUZIK, T. 2003. Nitric oxide and superoxide in inflammation. *J physiol pharmacol,* 54**,** 469-487.

GWOZDZ, T. & DOREY, K. 2017. Chapter 6 - Western Blot. *In:* JALALI, M., SALDANHA, F. Y. L. & JALALI, M. (eds.) *Basic Science Methods for Clinical Researchers.* Boston: Academic Press.

HALBEISEN, R. E., GALGANO, A., SCHERRER, T. & GERBER, A. P. 2007. Post-transcriptional gene regulation: From genome-wide studies to principles. *Cellular and Molecular Life Sciences,* 65**,** 798.

HAMILTON, J. P. 2011. Epigenetics: Principles and Practice. *Digestive Diseases,* 29**,** 130-135.

HANSSON, G. K., LIBBY, P. & TABAS, I. 2015. Inflammation and plaque vulnerability. *Journal of Internal Medicine,* 278**,** 483-493.

HANWELL, M. D., CURTIS, D. E., LONIE, D. C., VANDERMEERSCH, T., ZUREK, E. & HUTCHISON, G. R. 2012. Avogadro: an advanced semantic chemical editor, visualization, and analysis platform. *Journal of cheminformatics,* 4**,** 1-17.

HASCHEK, W. M., GUMPRECHT, L. A., SMITH, G., TUMBLESON, M. E. & CONSTABLE, P. D. 2001. Fumonisin toxicosis in swine: an overview of porcine pulmonary edema and current perspectives. *Environ Health Perspect,* 109 Suppl 2**,** 251-7.

HAYES, J. D., DINKOVA-KOSTOVA, A. T. & TEW, K. D. 2020. Oxidative Stress in Cancer. *Cancer Cell,* 38**,** 167-197.

HE, Q., GOSHI, E. & ZHOU, G. 2019. Nitric oxide detection methods in vitro and in vivo. *Medical Gas Research,* 9**,** 192.

HEDAYAT, M., MAHMOUDI, M. J., ROSE, N. R. & REZAEI, N. 2010. Proinflammatory cytokines in heart failure: double-edged swords. *Heart Failure Reviews,* 15**,** 543-562.

HENDRICKS, K. 1999. Fumonisins and neural tube defects in South Texas. *Epidemiology,* 10**,** 198-200.

HILFIKER-KLEINER, D., LANDMESSER, U. & DREXLER, H. 2006. Molecular Mechanisms in Heart Failure. *Journal of the American College of Cardiology,* 48**,** A56-A66.

HUXFORD, T., MISHLER, D., PHELPS, C. B., HUANG, D. B., SENGCHANTHALANGSY, L. L., REEVES, R., HUGHES, C. A., KOMIVES, E. A. & GHOSH, G. 2002. Solvent exposed non-contacting amino acids play a critical role in NF-kappaB/IkappaBalpha complex formation. *J Mol Biol,* 324**,** 587-97.

JALALI, M., ZABOROWSKA, J. & JALALI, M. 2017. The polymerase chain reaction: PCR, qPCR, and RT-PCR. *Basic science methods for clinical researchers.* Elsevier.

JAMJOUM, R., MAJUMDER, S., ISSLENY, B. & STIBAN, J. 2024. Mysterious sphingolipids: metabolic interrelationships at the center of pathophysiology. *Frontiers in Physiology,* 14**,** 1229108.

JIANG, M., QI, L., LI, L. & LI, Y. 2020. The caspase-3/GSDME signal pathway as a switch between apoptosis and pyroptosis in cancer. *Cell Death Discovery,* 6.

JIN, J., SHAN, Y., ZHANG, L., WU, Z., WU, S., SUN, M. & BAO, W. 2022. Pterostilbene Ameliorates Fumonisin B1-Induced Cytotoxic Effect by Interfering in the Activation of JAK/STAT Pathway. *Antioxidants,* 11**,** 2360.

JOSHI, M. & DESHPANDE, J. 2010. Polymerase chain reaction: methods, principles and application. *International Journal of Biomedical Research,* 2**,** 81-97.

JOUGASAKI, M. 2010. Cardiotrophin-1 in cardiovascular regulation. *Adv Clin Chem,* 52**,** 41-76.

KANWAL, R. & GUPTA, S. 2012. Epigenetic modifications in cancer. *Clinical Genetics,* 81**,** 303-311.

KAPIL, V., KHAMBATA, R. S., JONES, D. A., RATHOD, K., PRIMUS, C., MASSIMO, G., FUKUTO, J. M. & AHLUWALIA, A. 2020. The Noncanonical Pathway for In Vivo Nitric Oxide Generation: The Nitrate-Nitrite-Nitric Oxide Pathway. *Pharmacological Reviews,* 72**,** 692-766.

KELLERMAN, T. S., MARASAS, W. F. O., THIEL, P., GELDERBLOM, W., CAWOOD, M. & COETZER, J. A. 1990. Leukoencephalomalacia in two horses induced by oral dosing of fumonisin B_1.

KHAZAN, M. & HDAYATI, M. 2015. The role of nitric oxide in health and diseases. *Heart failure,* 4**,** 38-43.

KIM, D.-H., LEE, I.-H., DO, W.-H., NAM, W.-S., LI, H., JANG, H.-S. & LEE, C. 2013. Incidence and levels of deoxynivalenol, fumonisins and zearalenone contaminants in animal feeds used in Korea in 2012. *Toxins,* 6**,** 20-32.

KIM, S. H., SINGH, M. P., SHARMA, C. & KANG, S. C. 2018. Fumonisin B1 actuates oxidative stress-associated colonic damage via apoptosis and autophagy activation in murine model. *Journal of Biochemical and Molecular Toxicology,* 32**,** e22161.

KIM, T. J., PYUN, D. H., PARK, S. Y., LEE, H. J., ABD EL-ATY, A. M., SONG, J.-H., SHIN, Y. K., JEONG, J. H. & JUNG, T. W. 2021. Patchouli alcohol improves wound healing in high fat diet-fed mice through AMPK-mediated suppression of inflammation and TGFb1 signaling. *Biochemical and Biophysical Research Communications,* 561**,** 136-142.

KORHONEN, R., LAHTI, A., KANKAANRANTA, H. & MOILANEN, E. 2005. Nitric oxide production and signaling in inflammation. *Curr Drug Targets Inflamm Allergy,* 4**,** 471-9.

KRISHNAMOORTHY, S. & HONN, K. V. 2006. Inflammation and disease progression. *Cancer and Metastasis Reviews,* 25**,** 481-491.

KROUT-GREENBERG, N., PUSCHNER, B., DAVIDSON, M. & DEPETERS, E. 2013. Preliminary study to assess mycotoxin concentrations in whole corn in the California feed supply. *Journal of Dairy Science,* 96**,** 2705-2712.

KROWN, K. A., PAGE, M. T., NGUYEN, C., ZECHNER, D., GUTIERREZ, V., COMSTOCK, K. L., GLEMBOTSKI, C. C., QUINTANA, P. J. & SABBADINI, R. A. 1996. Tumor necrosis factor alpha-induced apoptosis in cardiac myocytes. Involvement of the sphingolipid signaling cascade in cardiac cell death. *Journal of Clinical Investigation,* 98**,** 2854-2865.

KRYSTON, T. B., GEORGIEV, A. B., PISSIS, P. & GEORGAKILAS, A. G. 2011. Role of oxidative stress and DNA damage in human carcinogenesis. *Mutation Research/Fundamental and Molecular Mechanisms of Mutagenesis,* 711**,** 193-201.

LAFUSE, W. P., WOZNIAK, D. J. & RAJARAM, M. V. S. 2020. Role of Cardiac Macrophages on Cardiac Inflammation, Fibrosis and Tissue Repair. *Cells,* 10**,** 51.

LANUBILE, A., DE MICHELE, R., LOI, M., FAKHARI, S., MAROCCO, A. & PACIOLLA, C. 2022. Cell death induced by mycotoxin fumonisin B1 is accompanied by oxidative stress and transcriptional modulation in Arabidopsis cell culture. *Plant Cell Reports,* 41**,** 1733-1750.

LAROUX, F., PAVLICK, K., HINES, I., KAWACHI, S., HARADA, H., BHARWANI, S., HOFFMAN, J. & GRISHAM, M. 2001. Role of nitric oxide in inflammation. *Acta Physiologica Scandinavica,* 173**,** 113-118.

LEI, H., HU, J., SUN, K. & XU, D. 2021. The role and molecular mechanism of epigenetics in cardiac hypertrophy. *Heart Failure Reviews,* 26**,** 1505-1514.

LEMMER, E. R., DE LA MOTTE HALL, P., OMORI, N., OMORI, M., SHEPHARD, E. G., GELDERBLOM, W. C., CRUSE, J. P., BARNARD, R. A., MARASAS, W. F., KIRSCH, R. E. & THORGEIRSSON, S. S. 1999. Histopathology and gene expression changes in rat liver during feeding of fumonisin B1, a carcinogenic mycotoxin produced by Fusarium moniliforme. *Carcinogenesis,* 20**,** 817-24.

LI, M., NING, P., BAI, R., TIAN, Z., LIU, S. & LI, L. 2024. DNA Methylation Negatively Regulates Gene Expression of Key Cytokines Secreted by BMMCs Recognizing FMDV-VLPs. *International Journal of Molecular Sciences,* 25**,** 10849.

LI, X., CAO, C., ZHU, X., LI, X. & WANG, K. 2020. Fumonisins B1 exposure triggers intestinal tract injury via activating nuclear xenobiotic receptors and attracting inflammation response. *Environmental Pollution,* 267**,** 115461.

LI, Y. 2021. Modern epigenetics methods in biological research. *Methods,* 187**,** 104-113.

LIU, A., SUN, Y., WANG, X., IHSAN, A., TAO, Y., CHEN, D., PENG, D., WU, Q., WANG, X. & YUAN, Z. 2019. DNA methylation is involved in pro-inflammatory cytokines expression in T-2 toxin-induced liver injury. *Food and Chemical Toxicology,* 132**,** 110661.

LOTHER, A., BERGEMANN, S., DENG, L., MOSER, M., BODE, C. & HEIN, L. 2018. Cardiac Endothelial Cell Transcriptome. *Arteriosclerosis, Thrombosis, and Vascular Biology,* 38**,** 566-574.

LUHESHI, N. M., GILES, J. A., LOPEZ-CASTEJON, G. & BROUGH, D. 2012. Sphingosine regulates the NLRP3-inflammasome and IL-1β release from macrophages. *European Journal of Immunology,* 42**,** 716-725.

LUMSANGKUL, C., TSO, K.-H., FAN, Y.-K., CHIANG, H.-I. & JU, J.-C. 2021. Mycotoxin Fumonisin B1 Interferes Sphingolipid Metabolisms and Neural Tube Closure during Early Embryogenesis in Brown Tsaiya Ducks. *Toxins,* 13**,** 743.

MAHDINIA, E., SHOKRI, N., TAHERI, A. T., ASGHARZADEH, S., ELAHIMANESH, M. & NAJAFI, M. 2023. Cellular crosstalk in atherosclerotic plaque microenvironment. *Cell Communication and Signaling,* 21**,** 125.

MAHDJOUBI, C. K., ARROYO-MANZANARES, N., HAMINI-KADAR, N., GARCÍA-CAMPAÑA, A. M., MEBROUK, K. & GÁMIZ-GRACIA, L. 2020. Multi-mycotoxin occurrence and exposure assessment approach in foodstuffs from Algeria. *Toxins,* 12**,** 194.

MARASAS, W. F. 1996. Fumonisins: history, world-wide occurrence and impact. *Adv Exp Med Biol,* 392**,** 1-17.

MARASAS, W. F., KELLERMAN, T. S., GELDERBLOM, W. C., COETZER, J. A., THIEL, P. G. & VAN DER LUGT, J. J. 1988. Leukoencephalomalacia in a horse induced by fumonisin B1 isolated from Fusarium moniliforme. *Onderstepoort J Vet Res,* 55**,** 197-203.

MARCELLONI, A. M., PIGINI, D., CHIOMINTO, A., GIOFFRÈ, A. & PABA, E. 2023. Exposure to airborne mycotoxins: the riskiest working environments and tasks. *Annals of Work Exposures and Health,* 68**,** 19-35.

MERRILL JR, A. H. 2011. Sphingolipid and glycosphingolipid metabolic pathways in the era of sphingolipidomics. *Chemical reviews,* 111**,** 6387-6422.

MERRILL JR, A. H., SULLARDS, M. C., WANG, E., VOSS, K. A. & RILEY, R. T. 2001. Sphingolipid metabolism: roles in signal transduction and disruption by fumonisins. *Environmental health perspectives,* 109**,** 283-289.

MINIC, R. & ZIVKOVIC, I. 2020. Optimization, validation and standardization of ELISA. *Norovirus.* IntechOpen London, UK.

MOBIO, T. A., ANANE, R., BAUDRIMONT, I., CARRATÚ, M.-R., SHIER, T. W., DANO, S. D., UENO, Y. & CREPPY, E. E. 2000. Epigenetic Properties of Fumonisin B1: Cell Cycle Arrest and DNA Base Modification in C6 Glioma Cells. *Toxicology and Applied Pharmacology,* 164**,** 91-96.

NURAL-GUVENER, H. F., ZAKHAROVA, L., NIMLOS, J., POPOVIC, S., MASTROENI, D. & GABALLA, M. A. 2014. HDAC class I inhibitor, Mocetinostat, reverses cardiac fibrosis in heart failure and diminishes CD90+ cardiac myofibroblast activation. *Fibrogenesis & tissue repair,* 7**,** 1-14.

OSMANCIK, P. & LOUCKOVA, A. 2017. Biomarkers of apoptosis, inflammation, and cardiac extracellular matrix remodelling in the prognosis of heart failure. *Kardiologia Polska,* 75**,** 295-305.

PAGADALA, N. S., SYED, K. & TUSZYNSKI, J. 2017. Software for molecular docking: a review. *Biophysical Reviews,* 9**,** 91-102.

PAHWA, R., GOYAL, A. & JIALAL, I. 2024. Chronic Inflammation. *StatPearls.* Treasure Island (FL).

PAPOUTSOPOULOU, S., POLLOCK, L., WILLIAMS, J. M., ABDUL-MAHDI, M. M. L. F., DOBBASH, R., DUCKWORTH, C. A. & CAMPBELL, B. J. 2022. Interleukin-10 Deficiency Impacts on TNF-Induced NFκB Regulated Responses In Vivo. *Biology,* 11**,** 1377.

PETERSON, C. L. & LANIEL, M.-A. 2004. Histones and histone modifications. *Current Biology,* 14**,** R546-R551.

PETTERSEN, E. F., GODDARD, T. D., HUANG, C. C., COUCH, G. S., GREENBLATT, D. M., MENG, E. C. & FERRIN, T. E. 2004. UCSF Chimera—a visualization system for exploratory research and analysis. *Journal of computational chemistry,* 25**,** 1605-1612.

POETSCH, A. R. & PLASS, C. 2011. Transcriptional regulation by DNA methylation. *Cancer Treatment Reviews,* 37**,** S8-S12.

PRALHADA RAO, R., VAIDYANATHAN, N., RENGASAMY, M., MAMMEN OOMMEN, A., SOMAIYA, N. & JAGANNATH, M. 2013. Sphingolipid metabolic pathway: an overview of major roles played in human diseases. *Journal of lipids,* 2013**,** 178910.

QUINVILLE, B. M., DESCHENES, N. M., RYCKMAN, A. E. & WALIA, J. S. 2021. A Comprehensive Review: Sphingolipid Metabolism and Implications of Disruption in Sphingolipid Homeostasis. *International Journal of Molecular Sciences,* 22**,** 5793.

R SKEEN, V., PATERSON, I., PARASKEVA, C. & C WILLIAMS, A. 2012. TGF-β1 signalling, connecting aberrant inflammation and colorectal tumorigenesis. *Current pharmaceutical design,* 18**,** 3874-3888.

RHEEDER, J. P., MARASAS, W. F. & VISMER, H. F. 2002. Production of fumonisin analogs by Fusarium species. *Appl Environ Microbiol,* 68**,** 2101-5.

RILEY, R. T. & MERRILL, A. H. 2019. Ceramide synthase inhibition by fumonisins: a perfect storm of perturbed sphingolipid metabolism, signaling, and disease. *Journal of Lipid Research,* 60**,** 1183-1189.

SCHMID-SCHÖNBEIN, G. W. 2006. Analysis of inflammation. *Annual Review of Biomedical Engineering,* 8**,** 93-151.

SEBASTIAN, ALVARO, CLARISSA, KOK, JARED, MARTINEZ, M., SEREDA, R., MEHTA, S. & JUAN 2018. Global landscape of mouse and human cytokine transcriptional regulation. *Nucleic Acids Research,* 46**,** 9321-9337.

SHAFFER, F., MCCRATY, R. & ZERR, C. L. 2014. A healthy heart is not a metronome: an integrative review of the heart's anatomy and heart rate variability. *Frontiers in Psychology,* 5.

SHAIKH, P. Z. 2011. Cytokines & their physiologic and pharmacologic functions in inflammation: A review. *International Journal of Pharmacy & Life Sciences,* 2.

SHARMA, J. N., AL-OMRAN, A. & PARVATHY, S. S. 2007. Role of nitric oxide in inflammatory diseases. *Inflammopharmacology,* 15**,** 252-259.

SHARMA, R. P., HE, Q. & JOHNSON, V. J. 2003. Deletion of IFN-gamma reduces fumonisin-induced hepatotoxicity in mice via alterations in inflammatory cytokines and apoptotic factors. *J Interferon Cytokine Res,* 23**,** 13-23.

SHI, C. & PAMER, E. G. 2011. Monocyte recruitment during infection and inflammation. *Nature Reviews Immunology,* 11**,** 762-774.

SIBIYA, T. 2018. *Fumonisin B1 induced antioxidant response in C57BL/6 male mice brain.*

SINGAL, R. & GINDER, G. D. 1999. DNA methylation. *Blood, The Journal of the American Society of Hematology,* 93**,** 4059-4070.

SORIANO, J., GONZALEZ, L. & CATALA, A. 2005. Mechanism of action of sphingolipids and their metabolites in the toxicity of fumonisin B1. *Progress in lipid research,* 44**,** 345-356.

STEEN, E. H., WANG, X., BALAJI, S., BUTTE, M. J., BOLLYKY, P. L. & KESWANI, S. G. 2020. The role of the anti-inflammatory cytokine interleukin-10 in tissue fibrosis. *Advances in wound care,* 9**,** 184-198.

SUGIYAMA, K.-I., KINOSHITA, M., FURUSAWA, H., SATO, K. & HONMA, M. 2021. Epigenetic effect of the mycotoxin fumonisin B1 on DNA methylation. *Mutagenesis,* 36**,** 295-301.

TEBELE, S. M., GBASHI, S., ADEBO, O., CHANGWA, R., NAIDU, K. & NJOBEH, P. B. 2020. Quantification of multi-mycotoxin in cereals (maize, maize porridge, sorghum and wheat) from Limpopo province of South Africa. *Food Addit Contam Part A Chem Anal Control Expo Risk Assess,* 37**,** 1922-1938.

THOMAS, T. P. & GRISANTI, L. A. 2020. The dynamic interplay between cardiac inflammation and fibrosis. *Frontiers in physiology,* 11**,** 529075.

TISO, M. & SCHECHTER, A. N. 2015. Nitrate reduction to nitrite, nitric oxide and ammonia by gut bacteria under physiological conditions. *PLoS One,* 10**,** e0119712.

TRIPATHI, P. & AGGARWAL, A. 2006. NF-kB transcription factor: a key player in the generation of immune response. *Current Science,* 90**,** 519-531.

TROTT, O. & OLSON, A. J. 2010. AutoDock Vina: improving the speed and accuracy of docking with a new scoring function, efficient optimization, and multithreading. *Journal of computational chemistry,* 31**,** 455-461.

TSUCHIYA, K., NAKAJIMA, S., HOSOJIMA, S., THI NGUYEN, D., HATTORI, T., MANH LE, T., HORI, O., MAHIB, M. R., YAMAGUCHI, Y., MIURA, M., KINOSHITA, T., KUSHIYAMA, H., SAKURAI, M., SHIROISHI, T. & SUDA, T. 2019. Caspase-1 initiates apoptosis in the absence of gasdermin D. *Nature Communications,* 10**,** 2091.

TSUTAMOTO, T., HISANAGA, T., WADA, A., MAEDA, K., OHNISHI, M., FUKAI, D., MABUCHI, N., SAWAKI, M. & KINOSHITA, M. 1998. Interleukin-6 Spillover in the Peripheral Circulation Increases With the Severity of Heart Failure, and the High Plasma Level of Interleukin-6 Is an Important Prognostic Predictor in Patients With Congestive Heart Failure. *Journal of the American College of Cardiology,* 31**,** 391-398.

VARELA, M. L., MOGILDEA, M., MORENO, I. & LOPES, A. 2018. Acute Inflammation and Metabolism. *Inflammation,* 41**,** 1115-1127.

VUJIC, A., ROBINSON, E., ITO, M., HAIDER, S., ACKERS-JOHNSON, M., SEE, K., METHNER, C., FIGG, N., BRIEN, P. & RODERICK, H. L. 2015. Experimental heart failure modelled by the cardiomyocyte-specific loss of an epigenome modifier, DNMT3B. *Journal of molecular and cellular cardiology,* 82**,** 174-183.

WAN, L.-Y. M., WOO, C.-S. J., TURNER, P. C., WAN, J. M.-F. & EL-NEZAMI, H. 2013. Individual and combined effects of Fusarium toxins on the mRNA expression of pro-inflammatory cytokines in swine jejunal epithelial cells. *Toxicology Letters,* 220**,** 238-246.

WANG, X., WU, Q., WAN, D., LIU, Q., CHEN, D., LIU, Z., MARTÍNEZ-LARRAÑAGA, M. R., MARTÍNEZ, M. A., ANADÓN, A. & YUAN, Z. 2016. Fumonisins: oxidative stress-mediated toxicity and metabolism in vivo and in vitro. *Archives of Toxicology,* 90**,** 81-101.

WASSMANN, S., STUMPF, M., STREHLOW, K., SCHMID, A., SCHIEFFER, B., BOHM, M. & NICKENIG, G. 2004. Interleukin-6 induces oxidative stress and endothelial dysfunction by overexpression of the angiotensin II type 1 receptor. *Circ Res,* 94**,** 534-41.

WEI, M., WANG, L., WU, T., XI, J., HAN, Y., YANG, X., ZHANG, D., FANG, Q. & TANG, B. 2016. NLRP3 Activation Was Regulated by DNA Methylation Modification duringMycobacterium tuberculosisInfection. *BioMed Research International,* 2016**,** 1-10.

WOODCOCK, E. A. & MATKOVICH, S. J. 2005. Cardiomyocytes structure, function and associated pathologies. *The International Journal of Biochemistry & Cell Biology,* 37**,** 1746-1751.

WRIGLEY, C. W. 2019. 18 - Cereals. *In:* SWAINSON, M. (ed.) *Swainson's Handbook of Technical and Quality Management for the Food Manufacturing Sector.* Woodhead Publishing.

WU, F., YANG, Q., MI, Y., WANG, F., CAI, K., ZHANG, Y., WANG, Y., WANG, X., GUI, Y. & LI, Q. 2022. miR-29b-3p Inhibitor Alleviates Hypomethylation-Related Aberrations Through a Feedback Loop Between miR-29b-3p and DNA Methylation in Cardiomyocytes. *Frontiers in Cell and Developmental Biology,* 10.

YLI-MATTILA, T. & SUNDHEIM, L. 2022. Fumonisins in african countries. *Toxins,* 14**,** 419.

YOO, H.-S., NORRED, W. P., SHOWKER, J. & RILEY, R. T. 1996. Elevated sphingoid bases and complex sphingolipid depletion as contributing factors in fumonisin-induced cytotoxicity. *Toxicology and applied pharmacology,* 138**,** 211-218.

YU, P., ZHANG, X., LIU, N., TANG, L., PENG, C. & CHEN, X. 2021. Pyroptosis: mechanisms and diseases. *Signal transduction and targeted therapy,* 6**,** 128.

ZAHRA, N., SAEED, M. K., SHEIKH, A., KALIM, I., AHMAD, S. R. & JAMIL, N. 2019. A Review of Mycotoxin Types, Occurrence, Toxicity, Detection Methods and Control. *Biological Sciences - PJSIR,* 62**,** 206-218.

ZENG, H. Y., LI, C. Y. & YAO, N. 2020. Fumonisin B1: A Tool for Exploring the Multiple Functions of Sphingolipids in Plants. *Front Plant Sci,* 11**,** 600458.

ZHANG, Q., WANG, J., DENG, F., YAN, Z., XIA, Y., WANG, Z., YE, J., DENG, Y., ZHANG, Z., QIAO, M., LI, R., DENDULURI, S. K., WEI, Q., ZHAO, L., LU, S., WANG, X., TANG, S., LIU, H., LUU, H. H., HAYDON, R. C., HE, T.-C. & JIANG, L. 2015. TqPCR: A Touchdown qPCR Assay with Significantly Improved Detection Sensitivity and Amplification Efficiency of SYBR Green qPCR. *PLOS ONE,* 10**,** e0132666.

ZHANG, Y., SUN, Z., JIA, J., DU, T., ZHANG, N., TANG, Y., FANG, Y. & FANG, D. 2021. Overview of histone modification. *Histone Mutations and Cancer***,** 1-16.

ZHU, N., MEALKA, M., MITCHEL, S., MILANI, C., ACUNA, L. M., ROGERS, E., LAHANA, A. N. & HUXFORD, T. 2023. X-ray Crystallographic Study of Preferred Spacing by the NF-kappaB p50 Homodimer on kappaB DNA. *Biomolecules,* 13.

ZMORA, N., LEVY, M., PEVSNER-FISHCER, M. & ELINAV, E. 2017. Inflammasomes and intestinal inflammation. *Mucosal Immunology,* 10**,** 865-883.

Appendix A: Review Article

Unveiling the Potential Cardiotoxicity of Fumonisin B1: A Focus on Inflammatory Pathways and Epigenetic Modifications

Authors: Selwyn Kyle Gounder, Anil Amichund Chuturgoon and Terisha Ghazi

Affiliations: Discipline of Medical Biochemistry, School of Laboratory Medicine and Medical Sciences, University of KwaZulu-Natal, Durban, South Africa

Corresponding author: Terisha Ghazi

Abstract

This review is centered around the cardiotoxic effects of Fumonisin B1 (FB_1), particularly its impact on sphingolipid metabolism, inflammation, and epigenetics. FB_1 is a mycotoxin produced by *Fusarium* fungi, which mainly contaminates cereal grains and poses an adverse health risk, which includes cancer and cardiovascular diseases. It disrupts sphingolipid metabolism by inhibiting ceramide synthase, leading to cellular dysfunction and contributes to conditions such as hypertension and eventual heart failure. FB_1 is responsible for an altered inflammatory response, whereby it increases pro-inflammatory cytokines such as IL-6 and IL-1β, which contribute to cardiovascular diseases. Moreover, FB_1 induces significant epigenetic changes, including DNA hypermethylation, histone modifications such as increased H3K9me2 and H3K9me3, inhibition of histone acetyltransferase activity and changes in microRNA expression. These epigenetic alterations can silence or activate inflammatory genes, exacerbating disease progression. The review thus highlights the need for further research to elucidate the connections between FB_1, inflammation, epigenetic modifications, and cardiotoxicity, which could lead to better strategies for managing FB_1-related adverse health risks.

Keywords: Fumonisin B1 (FB_1), inflammation, cardiotoxicity, epigenetics, DNA methylation, microRNAs, and toxicology.

Abbreviations

CAM - Cell Adhesion Molecule

Cer - Ceramide

Cers - Ceramide Synthase

C1P - Ceramide-1-phosphate

CLRs - C-type Lectin Receptors

DNMTs - DNA Methyltransferases

FB_1 - Fumonisin B1

HATs - Histone Acetyltransferases

HDACs - Histone Deacetylases

ICAM - Intracellular Adhesion Molecule

IFN-γ - Interferon-gamma

IL-1β - Interleukin-1 beta

IL-2 - Interleukin-2

IL-4 - Interleukin-4

IL-6 - Interleukin-6

IL-10 - Interleukin-10

IL-12 - Interleukin-12

m6A - N6-methyladenosine

miRNA - MicroRNA

NF-κB - Nuclear factor kappa B

NLRs - NOD-like Receptors

NOS2A - Gene encoding inducible nitric oxide synthase

PRRs - Pathogen Recognition Receptors

RLRs - RIG-1-like Receptors

ROS - Reactive Oxygen Species

Sa/So ratio - Sphinganine/Sphingosine ratio

S1P - Sphingosine-1-phosphate

S1PR1 - Sphingosine-1-phosphate receptor 1

SPT - Serine Palmitoyltransferase

STAT - Signal Transducer and Activator of Transcription

TNF-α - Tumor Necrosis Factor-alpha

TLRs - Toll-like Receptors

Contents

1. Introduction

Mycotoxins are potent secondary metabolites produced by fungi such as *Aspergillus*, *Fusarium*, and *Penicillium* that contaminate a plethora of food and feed. These mycotoxins have been shown to be vastly associated with a variety of health-related complications for both humans and animals due to their carcinogenic, immunosuppressive, teratogenic, and mutagenic properties. More than 500 mycotoxins have been identified, including zearalenone, aflatoxins, ochratoxins, patulin, fusaric acid, and fumonisins. Fumonisins are a group of polyketide mycotoxins that are produced by *Fusarium verticillioides* (previously known as *F. moniliforme*) and *F. proliferatum*, these isolates were discovered in South Africa (Gelderblom *et al*., 1988). Subsequent research detailed the discovery of 28 analogues of fumonisins, with fumonisin B1 (FB_1) being of most interest due to its abundant prevalence in worldwide contamination cases and its implications in various associated adverse health risks. Global food contamination rates of FB_1 are currently at a pestiferous rate of 70%, thus implying the severity of FB_1 contamination in grain which not only contributes to economic losses but is accompanied by adverse health complications (Haque *et al*., 2020, Chen *et al*., 2021a). These health-related risks have been identified in both animals and humans. A multitude of research has depicted the ability of FB_1 to cause disease in animal models such as hepatitis in broilers, turkeys, and ducks, leukoencephalomalacia in horses, porcine pulmonary oedema, and is a potent liver and kidney carcinogen in rats and mice (Sheik Abdul and Marnewick, 2020, He *et al*., 2002, Tardieu *et al*., 2004). This is contrasted with limited research in humans. Data from Transkei, South Africa, provided a possible correlation between oesophageal cancer and the consumption of FB_1 contaminated corn (Marasas, 1996). Other studies revealed that there could be a possible link between FB_1 and human neural tube defects, which was precedent at the same time as an outbreak of leukoencephalomalacia ravaged the Texas-Mexico border (Hendricks, 1999). These studies provided vague associations between human health risks and FB_1 and necessitated further research to elucidate the adverse health risks of FB_1 consumption to human health. However, FB_1 has been shown to induce a variety of complex pathways such as sphingolipid biosynthesis alteration, oxidative stress, apoptosis, mitochondrial dysfunction, and inflammation which are involved in the pathogenesis of human diseases. This review focuses on the current research on the mechanisms of action of FB1-induced cardiotoxicity, an often-neglected organ of study in toxicology.

2. FB_1 and Sphingolipid Metabolism

The structure of FB_1 is characterised as a diester of propane-1,2,3-tricarboxylic acid and 2S-amino-12S,16R-dimethyl-3S,5R,10R,14S,15R-pentahydroxyeicosane, which is esterified at the terminal carboxy group of propane-1,2,3-tricarboxylic acid at C-14 and C-15. This structural capability of FB_1 is crucial as the diester structural component, which is identified as the tricarballylic acid with a polyhydric alcohol backbone, bares an analogous structure to sphingosine and sphinganine (Figure 1). Therefore, FB_1 is an effective competitive inhibitor of ceramide synthase (Cers), an enzyme in the sphingolipid biosynthesis pathway that is responsible for the acetylation of sphingosine. Sphingosine belongs to the sphingolipid family, which is a collection of lipids that structurally contain sphingosine and a sphingoid base backbone and can be found in the cell membranes of cardiomyocytes and neurons. When fatty acids interact with sphingosine, they form a core molecule known as ceramide (Cer), which is crucial in sphingolipid metabolism as Cer can further interact with other moieties and form complex sphingolipids. A prime example is the attachment of Cer and phosphorylcholine which forms sphingomyelin. Due to their complexity, sphingolipids are important in various metabolic processes and act as signalling molecules. Amongst the different sphingolipids, there are major molecules which can be derived from them such as sphingosine-1-phosphate (S1P), Cer, and ceramide 1-phosphate (C1P). These molecules execute a diversity of roles such as cell signalling, cell migration, and cell death (Pralhada Rao *et al*., 2013b, Jamjoum *et al*., 2024). The initial step in sphingolipid metabolism is initiated when palmitoyl CoA undergoes condensation by utilising the rate-limiting enzyme, serine palmitoyltransferase (SPT). This leads to the formation of 3-keto-dihydrosphingosine which utilises a reductase to form dihydrosphingosine (sphinganine). Sphinganine is acetylated by Cers to form dihydroceramide which is then catalysed by dihydroceramide synthase to form Cer. Cer is the central molecule in sphingolipid metabolism as it can act as a substrate to form ceramide-1-phosphate (C1P) via ceramide kinase. In addition, Cer can form sphingosine that can be converted to S1P (Merrill, 2002, Gault *et al*., 2010). Alterations in these reactions by FB_1 trigger an increase in intracellular sphinganine and sphingosine and their related 1-phosphate substrates while subsequently preventing the formation of dihydroceramides, complex sphingolipids, and ceramides (Figure 2). Due to this sphingolipid alteration, scientists were able to use the sphingosine levels as a biomarker for FB_1 toxicity in the form of the sphinganine/sphingosine

ratio (Sa/So ratio), an elevation of the Sa/So ratio was, therefore, an indicator of FB_1 mediated toxicity (Riley and Merrill, 2019b, Soriano *et al*., 2005b, Yoo *et al*., 1996b).

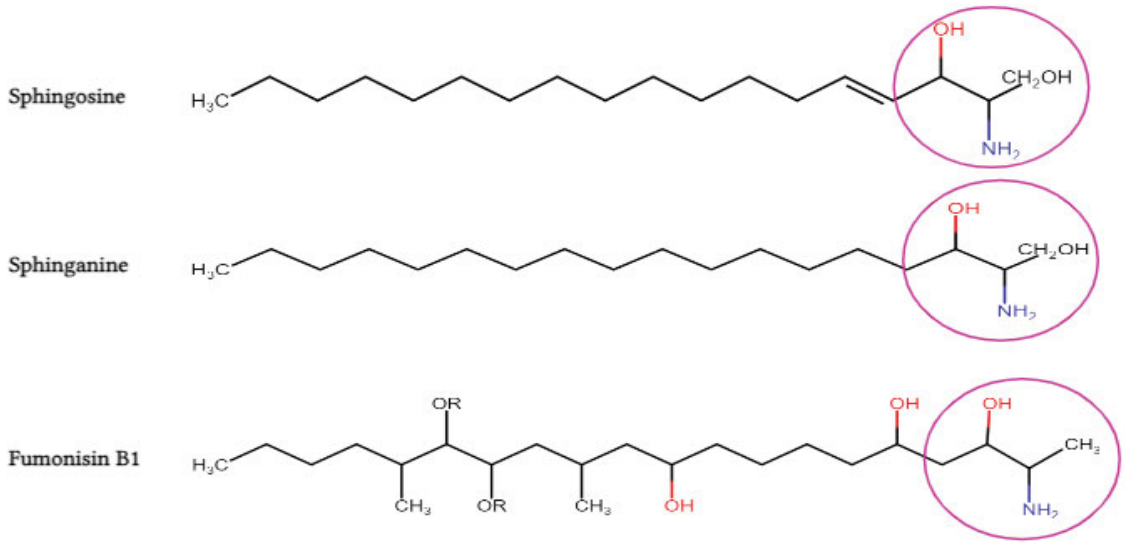

Figure 1: Structural similarities observed between FB_1 and sphingolipid metabolites, sphinganine and sphingosine.

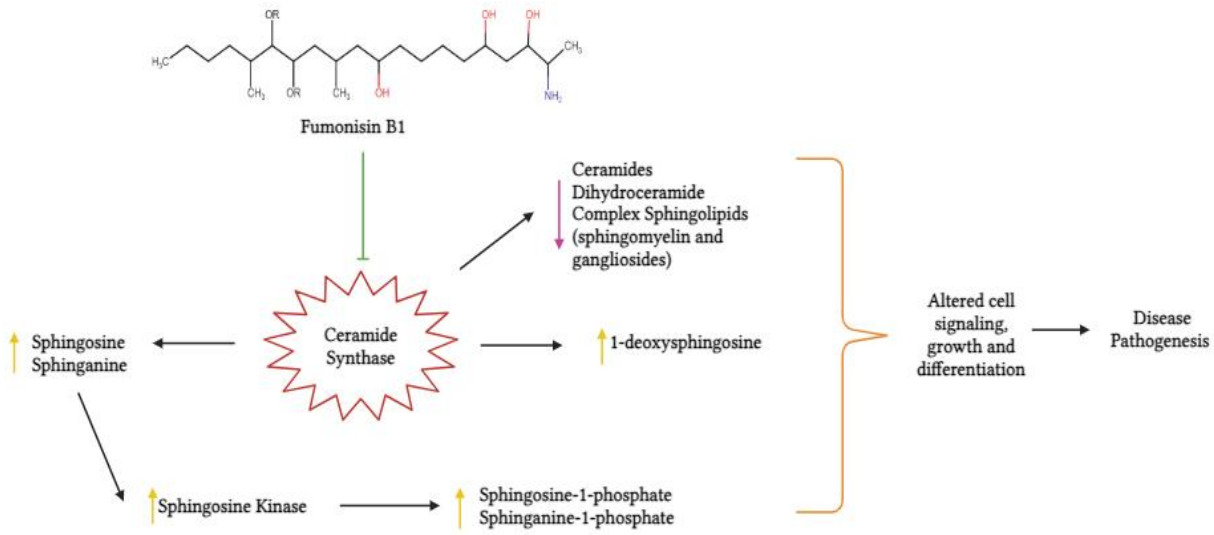

Figure 2: Alterations in sphingolipid biosynthesis which leads to altered cell signalling and disease.

The disruption of sphingolipids mediated by FB_1 leads to aberrant cell growth, differentiation, and eventually cell death. Specific alterations have been linked with the onset of cardiac distress such as hypertension, atherosclerosis, and heart failure. A study revealed an increase

in plasma S1P was associated with hypertension induced by angiotensin II; this was also found in another study where patients with a systolic blood pressure of ≥140 mmHg had increased S1P plasma levels when compared to patients with systolic blood pressure below 120 mmHg (Siedlinski *et al*., 2017, Jujic *et al*., 2021). Other studies showed that both acute and chronic heart failure are linked to increased S1P levels and an increase in expression of the *S1PR1* gene acted as a pro-atherosclerotic factor as it leads to the induction of pro-inflammatory endothelial factors such as vascular cell adhesion molecule 1 (Gowda *et al*., 2021, Galvani *et al*., 2015). Studies have not elucidated the effects of altered sphingolipid synthesis in the heart. Accordingly, limited research has been done on FB_1 in terms of sphingolipid and cardiac toxicity. Studies providing insight on these alterations, specifically the inhibition of Cers, could explain the following pathogenesis observed by FB_1 such as liver lesions, heart failure, inhibition of cell growth, apoptosis, pulmonary oedema, and carcinogenetic effects. The elevation in sphingosine was readily seen in mice kidney tissue and further correlated with fumonisin-induced apoptosis of kidney cells due to sphingolipids' ability to act as signalling molecules (Soriano *et al*., 2005b, Tsunoda *et al*., 1998). A study on pigs fed a FB_1-contaminated diet, depicted a blockage in sphingosine-mediated l-type Ca^{2+} which is attributed to an increase in heart failure events caused by FB_1. Another study on pigs depicted the causal relationship between elevated Sa/So ratio and systemic hypotension and pulmonary hypertension (Constable *et al*., 2003, Hsiao *et al*., 2005). The evidence surrounding sphingolipid metabolism alterations induced by FB_1 and cardiotoxic effects remain limited, therefore further research is needed in animal and human models to elucidate the exact causal relationship between FB_1, increase in Sa/So ratio, and inhibition of Cers in various cardiac distresses.

3. FB_1 and Inflammation

Inflammation is an essential process elicited by an immune response when various insults are present in the system such as tissue injury and infection. This process allows the host to cope and mitigate the negative effects induced by harmful stimuli by prompting its removal as well as healing of the damaged tissue. The first host response is to induce inflammation which can lead to cellular homeostasis in response to harmful stimuli. The inflammatory response can be acute and is referred to as the first-line defence mechanism employed by the innate immune system. Inflammation is readily seen by the prevalence of core symptoms, namely, redness, pain, swelling, and heat. A normal inflammatory response is present temporarily to mitigate the damage, in this time the relevant inflammatory factors are upregulated, however, when the threat has passed, homeostasis is restored. When inflammation persists for longer periods, it transcends from an acute response to a chronic response. Chronic inflammation is persistent inflammation that continuously triggers the immune system to recruit inflammatory cells after the threat has been mitigated, the constant stimulation of this process can lead to damage and subsequent disease onset. The inflammatory pathway relies on the recruitment of white blood cells such as monocytes, basophils, eosinophils, and neutrophils to the site of injury or inflammation (Figure 3). The inflammatory response, whether chronic or acute, is mediated via a complex combination of factors (Ahmed, 2011, Abdulkhaleq *et al*., 2018b, Furman *et al*., 2019).

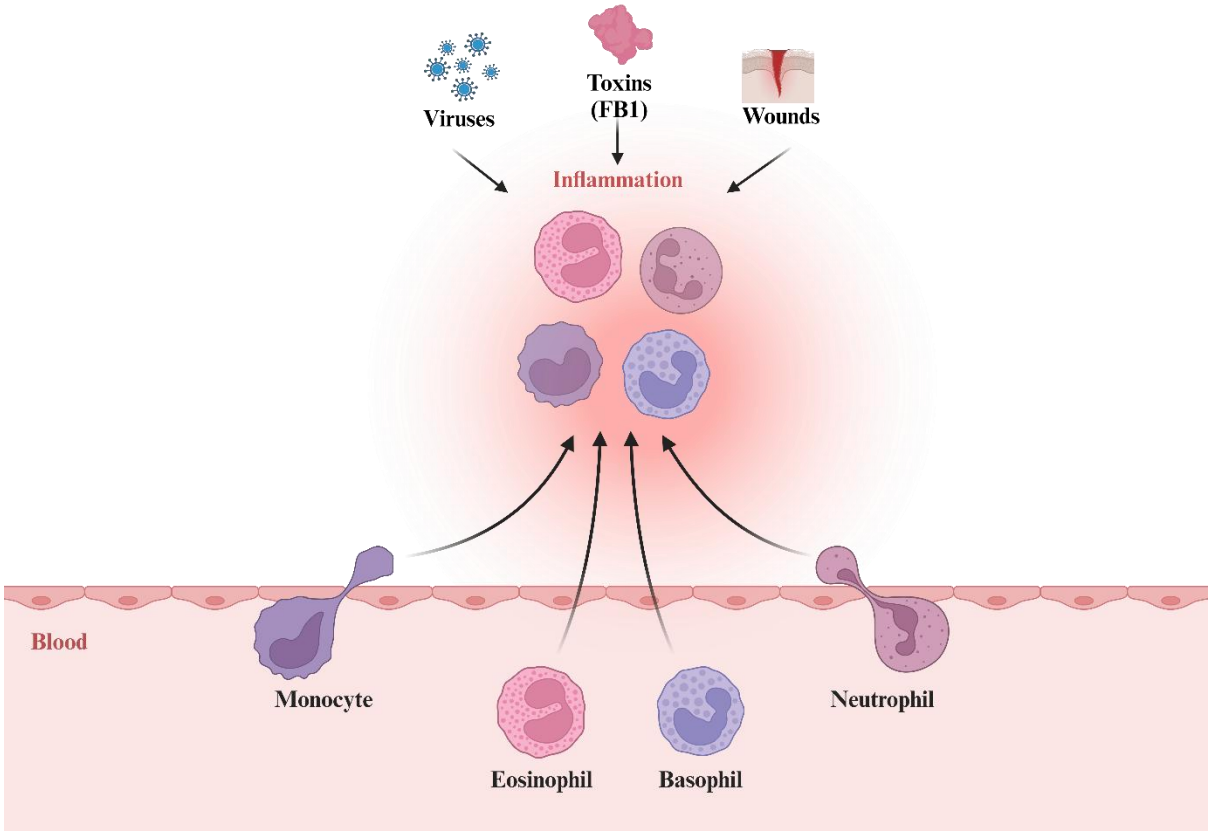

Figure 3: A representation of a triggered inflammatory response when the host is exposed to different stressors namely wounds, toxins such as FB_1, and viruses.

The principal mechanism of inflammation involves immune cells that release a group of secretory mediators and signalling molecules that include cytokines, histamine, prostaglandins, leukotrienes, reactive oxygen species (ROS), and serotonin. The mobilisation pathway is governed by cell adhesion molecules (CAM), which comprises of selectin, integrins, and intracellular adhesion molecules (ICAM)-1 and ICAM-2. The adhesion process occurs due to the interactions between integrins CDII/CDI8, CAM-l, and CAM-2 that are present on white blood cells. The other mediators, histamine and serotonin are present in the inflammation pathway due to secretion from basophils and decarboxylation of tryptophan, respectively. The increase in histamine and serotonin results in the increased release of prostaglandins which elicits pain responses (Abdulkhaleq *et al*., 2018b). Other crucial mediators which exacerbate the inflammatory response include inflammatory cytokines and chemokines, achieving their goal of inducing the inflammatory response by prompting the recruitment of neutrophils and modification of vascular endothelial permeability. The extent of the inflammatory response depends on the duration and damage caused by the original insult. The molecular mechanism that forms the basis of the inflammatory response begins when the initial inflammatory stimuli

are present. When the host detects the inflammatory stimulus, a structure present in microbes known as pathogen recognition receptors (PRRs) recognise specific patterns called pathogen-associated molecular patterns and damage-associated molecular patterns. The PRRs identified include NOD-like receptors (NLRs), Toll-like receptors (TLRs), C-type lectin receptors (CLRs), and RIG-1-like receptors (RLRs). The associations between the receptors and relevant stimuli result in the increased transcription of specific genes that coordinate the inflammatory response. The specific genes code for proteins also known as proinflammatory cytokines namely, Tumor Necrosis Factor-alpha (TNF-α), Interleukin-1 beta (IL-1β), and interleukin-6 (IL-6). Interleukins (IL-1β and IL-6) are synthesised via a two-step process, whereby IL-1β is expressed as pro-IL-1β until it is cleaved by caspase-1 which is initially activated by the presence of inflammasomes (Figure 4). When inflammasomes are assembled they lead to the proteolytic cleavage of procaspase-1 into active caspase-1. Active caspase-1 can convert dormant pro-IL-1β and pro-IL-18 into their active IL-1β and IL-18 which can act as potent pro-inflammatory mediators as they can subsequently transcribe interferon-gamma (IFN-γ), further heightening the inflammatory response. It is important to note that the activation of caspase-1 is not limited to cytokine transcription but it can also invoke cell death pathways such as pyroptosis (Ahmed, 2011, He *et al*., 2016). Data published has revealed that inflammation plays a significant role in hypertension as it could increase ROS production, specifically superoxide in addition to proinflammatory factors IL-6 due to angiotensin II. Cardiovascular distresses such as atherosclerosis have also been affected by inflammatory pathways as angiotensin II was shown to increase the expression of Nuclear factor kappa B (NF-κB), which in turn increases atherosclerotic plaque formation (Krishnamoorthy and Honn, 2006, Ahmed, 2011). Therefore, inflammation has been shown to play an important role in the onset of various diseases, especially cardiac-associated diseases. The link between inflammation and FB_1 has been studied moderately with inflammation being expressed differently due to the difference in tissues. A study published in 2024 on mice kidney tissue revealed an increase in pro-inflammatory cytokines, Il-6 and Il-1β following FB_1 treatment (Ping *et al*., 2024). Another study on intestinal epithelial cells showed abnormalities in the expression of IL-1β, Interleukin-2, Interleukin-4, Intelukin-10 (IL-10), and TNF-α, which are associated with the prevalence of inflammation (Ping *et al*., 2024, Li *et al*., 2020). A past study elaborated on the effects of inflammation on FB_1-treated mice liver which depicted an increase in expression of TNF-α, IFNγ and IL-12 (Bhandari *et al*., 2002). Multiple studies conducted by Sharma *et al*. revealed that TNF-α combined with IFNγ act as key mediators in FB_1-induced hepatotoxicity. Another study conducted by Sharma *et al*. depicted the implications of the cytokine network in

FB_1-mediated hepatotoxicity whereby cytokines TNF-α, IL-1β, IL-6, IL-10, Interleukin-12, and IFNγ were all elevated thus showcasing the exacerbation of the cytokine network (Sharma *et al*., 2003b, Bhandari *et al*., 2001a). The exposure of FB_1 on heart function remains limited, given the link between inflammation and cardiac diseases it remains imperative to study possible future links between inflammatory pathways, FB_1, and the heart.

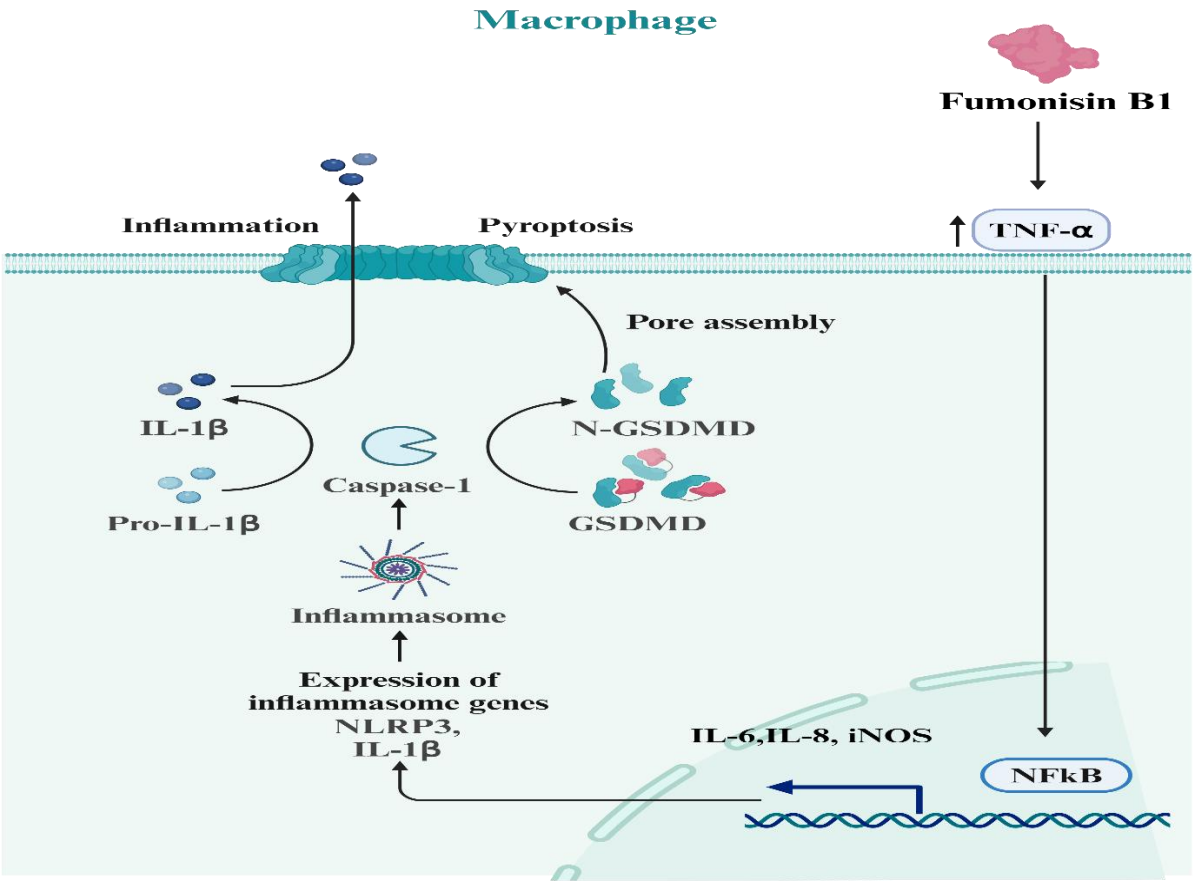

Figure 4: A representation of the pro-inflammatory impacts of FB_1 in organs such as the liver and lung.

4. FB_1 and Epigenetic Alterations

Epigenetics refers to the biochemical alterations that occur on chromatin without initiating modifications on DNA sequences. Epigenetic mechanisms regulate gene expression via the manipulation of various physiological processes. The epigenetic alterations that have been widely studied include DNA methylation, histone modifications, and microRNAs (miRNA). DNA methylation is the reversible addition of a methyl group on the 5^{th} carbon position of cytosine residues; DNA methylation has been generally associated with gene repression. The DNA methyltransferases (DNMTs; DNMT1, DNMT3a, and DNMT3b) catalyse this methylation reaction. The role of DNMT1 is governed by the maintenance of DNA methylation by copying methylation patterns from parent to newly synthesised strands whereas DNMT3a and DNMT3b are used for *de novo* methylation that targets unmethylated CpG dinucleotides. DNA methylation is also regulated by a family of demethylases known as ten-eleven translocation (TET) proteins; their enzyme function is to remove methyl groups which leads to demethylation further modulating the methylation process. Modifications are however not limited to DNA; the associated histone proteins are subjected to these modifications that are influenced by histone deacetylases (HDACs) and histone acetyltransferases (HATs) which maintain the balance between histone acetylation and deacetylation (Figure 5) (Li, 2021, Gibney and Nolan, 2010, Chrun *et al*., 2017b). The influence of FB_1 on these epigenetic factors have been limited. FB_1 was found to induce DNA hypermethylation in C6 glioma cells after 24 h exposure (Demirel *et al*., 2015). Other studies included the increase in DNA hypomethylation initiated by FB1 in human liver cancer cells (Chuturgoon *et al*., 2014a). The effects of FB_1 on epigenetics were further studied and depicted an effect on histone modifications. These effects were seen as an increase in di- and tri-methylation of lysine 9 on histone 3 (H3K9me2 and H3K9me3) in NRK-52E cells, decreased methylation of lysine 20 of histone 4 (H4K20me), and inhibition of histone acetyltransferase activity following FB_1 exposure (Sancak and Ozden, 2015). Other crucial post translational changes that regulate gene expression are microRNAs (miRNAs). miRNAs have been demonstrated to regulate the expression of various mRNAs, with multiple miRNAs often targeting a single mRNA and a single miRNA targeting multiple mRNAs. There are limited studies reporting the effects of FB_1 on miRNAs (Figure 6), one of these studies reported reduced miR-27b coupled with N6-methyladenosine (m6A) variations specifically an increase in m6A-*Keap1* and m6A-*Nrf2* in

FB_1-induced liver toxicity (Arumugam *et al*., 2021). This is comparable to another study that reported the downregulation of miR-135b, miR-181d, miR-27a, miR-27b, and miR-30c, with miR-27b being the only significantly decreased miRNA. The study established a correlation between miR-27b and human cytochrome P450, further suggesting that the reduction in miR-27b could lead to an increase in cytochrome P450, which plays a critical role in the activation of procarcinogens (Chuturgoon *et al*., 2014b).

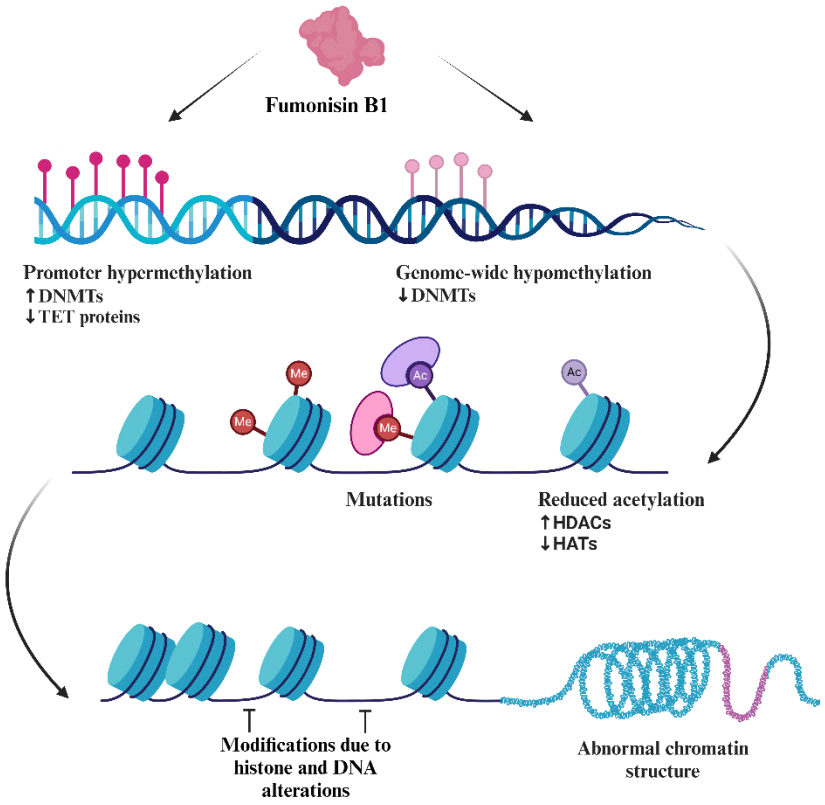

Figure 5: FB_1 has been shown to affect DNA methylation and histone modifications by leading to the reduction and stimulation of specific enzymes characterised by these processes .

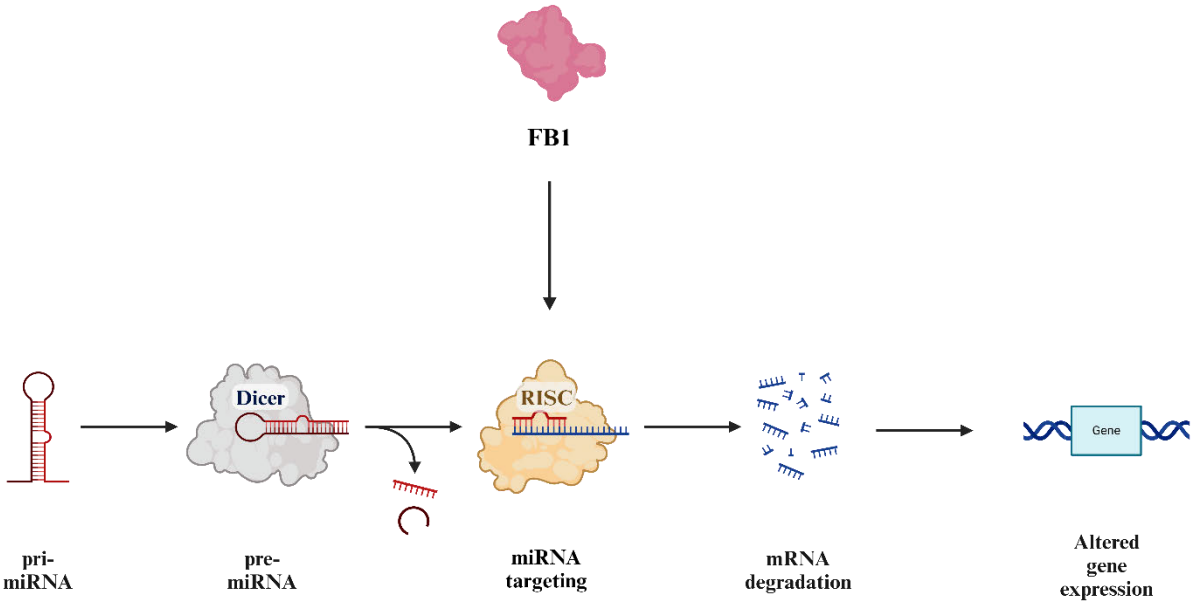

Figure 6: FB_1 can affect the transcriptional activity of specific miRNA's leading to altered gene function.

5. Epigenetics and Inflammation

An overlap between these two pathways is prevalent as transcription of a variety of inflammatory genes is regulated by epigenetic processes such as DNA methylation and histone modifications (Figure 7). A study revealed that transcription factors NF-κB, forkhead box P3, and signal transducer and activator of transcription (STAT) can be affected by epigenetic regulation through DNA methylation and histone modifications (Medzhitov and Horng, 2009). Some of these studies include a study conducted by Mohamed El Gazzar, who reported that during endotoxin tolerance, TNF-alpha expression is silenced via a connection between DNA and histone methylation, specifically via H3K9me2 which leads to downstream repression of the gene (Gazzar *et al*., 2008). Another study conducted on the effects of epigenetics and inflammation revealed that histone acetyltransferase (HATs) can increase acetylation and trigger inflammatory gene transcription which is contrasted when HDAC activation increases histone deacetylation leading to inhibition of inflammatory gene transcription. This is specifically seen in the case of corticosteroids which recruit HDAC2 to active inflammatory genes thus causing an anti-inflammatory response (Barnes, 2009). Inflammatory cytokines have been linked to increased iNOS expression; iNOS produced in response to cytokine induction can affect chromatin structure at the promoter region which was further elaborated in subsequent studies that showed the gene encoding for iNOS (NOS2A) was correlated with high levels of DNA methylation (Wierda *et al*., 2010, Mellott *et al*., 2001). Continual research led to the identification of histone acetylation as a regulatory mechanism of IL-12 transcription by p300; however, this transcription can be repressed via HDAC1 activation (Villagra *et al*., 2010). A previous study found that hypomethylation of the IL-6 gene is linked to reduced DNA methylation and an elevated expression level (Armenante *et al*., 1999). In an epigenetic study, the activation of TNF-α was associated with the trimethylation of histone H3 at lysine 4. Additionally, DNA demethylation was observed in cells expressing TNF-α (Sullivan *et al*., 2007). A study by Villagra *et al*. demonstrated that HDAC11 suppresses IL-10 transcription, resulting in a modified inflammatory response. (Villagra *et al*., 2010). A methylation analysis of inflammation-related genes found that 77 out of 94 genes in the control group exhibited elevated methylation levels, highlighting the significant influence of epigenetic mechanisms in regulating inflammation (Ali *et al*., 2022). A study on miRNAs identified the TNFAIP3 gene as a target of miR-23a-3p, with miR-23a-3p concurrently playing a role in endothelial cells. This finding suggests that miR-23a-3p may regulate inflammatory pathways involved in atherogenesis (Guo *et al*., 2020). A crucial miRNA also implicated in inflammatory response

modulation is miR-155, which has been shown to play a role in the induction of NFKB translocation (Tili *et al*., 2007). Other identified miRNAs that have been associated with altered inflammatory responses include the excessive induction of miR-9, miR-98 or miR-146 and reduced TNF-α and IL-1βfunction (Jones *et al*., 2009). The amalgamation of the above-mentioned studies provides a strong case depicting epigenetics as a key role player in the transcription of inflammatory genes and could thus provide insight into the inflammatory effects seen in various diseases due to the presence of epigenetic alterations.

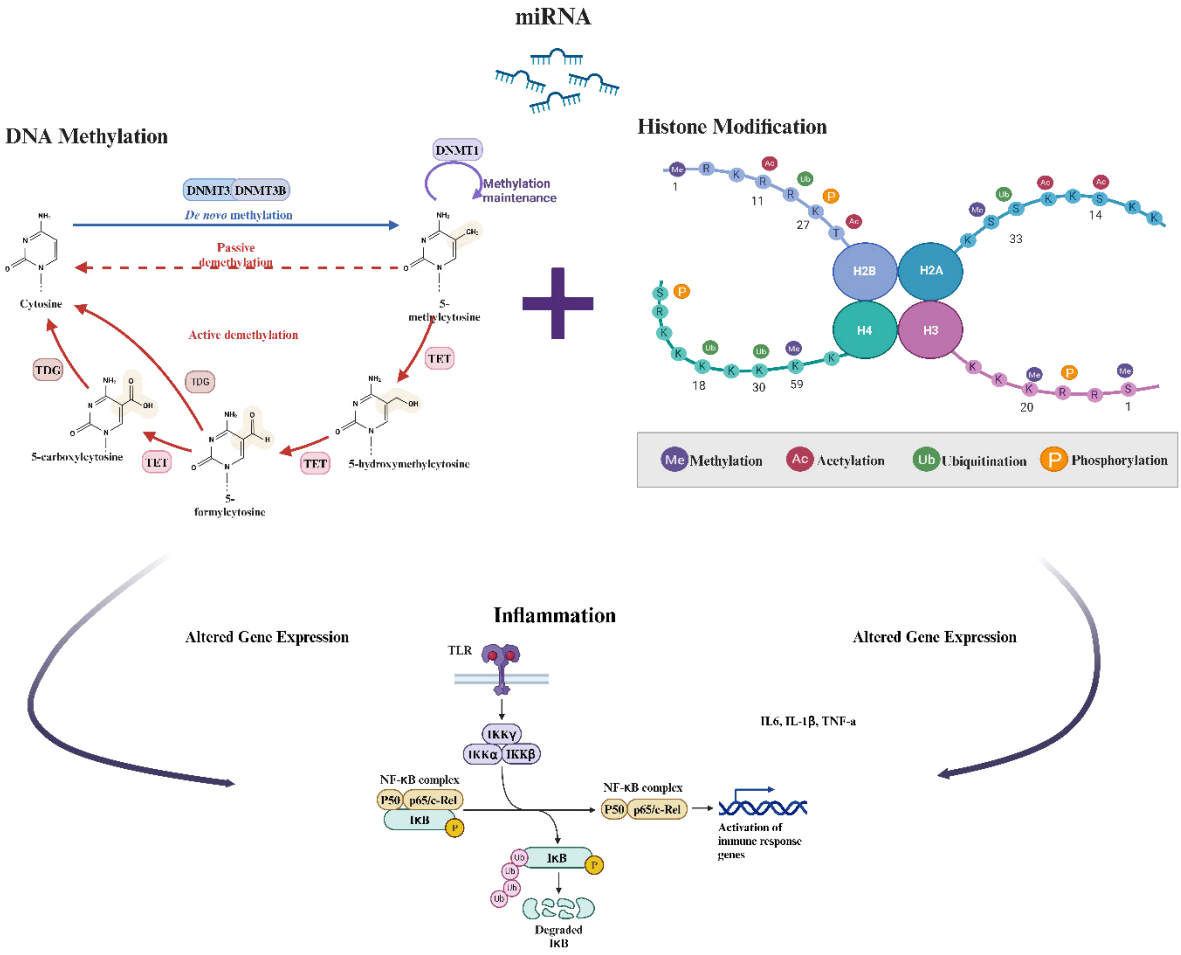

Figure 7: DNA methylation, histone modifications, and miRNAs have been implicated in the alteration of a variety of pro-inflammatory genes such as NFKB.

6. Conclusion

This review highlights the significant cardiotoxic potential of FB_1, a mycotoxin prevalent in widespread contamination of food supplies, particularly corn. Additionally, FB_1 has been shown to alter inflammatory responses by elevating pro-inflammatory cytokines, such as IL-6 and IL-1β. Cytokines play a pivotal role in the onset of various cardiovascular diseases, hence suggesting a role of driving inflammation mediated by FB_1-induced cardiotoxicity. The inflammatory response to FB_1 exposure further underscores the toxin's capacity to initiate and exacerbate cardiovascular conditions.

The epigenetic alterations induced by FB_1, such as DNA hyper- and or hypo-methylation specific histone modifications, including increased H3K9me2 and H3K9me3 methylation and inhibition of histone acetyltransferase activity in addition to miRNA activity have been studied. These epigenetic changes have profound implications for gene expression, particularly in regulating inflammatory pathways, which can further exacerbate cardiovascular diseases. Despite the insights provided by existing studies, the review emphasizes the need for more comprehensive research to fully elucidate the molecular mechanisms underlying FB_1-induced cardiotoxicity. Future research should focus on clarifying the links between FB_1's inflammatory effects, and the resulting epigenetic alterations. Understanding these connections is crucial for developing effective strategies to mitigate the health risks associated with FB_1 exposure, particularly in regions where food contamination by this mycotoxin is prevalent.

Declaration of interest

The authors state that they have no conflicts of interest. The review was independently conceptualized by the authors and provides an impartial evaluation of the available literature. The conclusions reached are solely those of the authors. Furthermore, none of the authors have been involved in any regulatory or legal proceedings concerning the content of this paper within the past 10 years.

Word Count: 4988

References

ABDULKHALEQ, L. A., ASSI, M. A., ABDULLAH, R., ZAMRI-SAAD, M., TAUFIQ-YAP, Y. H. & HEZMEE, M. N. M. 2018. The crucial roles of inflammatory mediators in inflammation: A review. *Vet World,* 11**,** 627-635.

AHMED, A. U. 2011. An overview of inflammation: mechanism and consequences. *Frontiers in Biology,* 6.

ALI, M. M., NAQUIALLAH, D., QURESHI, M., MIRZA, M. I., HASSAN, C., MASRUR, M., BIANCO, F. M., FREDERICK, P., CRISTOFORO, G. P., GANGEMI, A., PHILLIPS, S. A. & MAHMOUD, A. M. 2022. DNA methylation profile of genes involved in inflammation and autoimmunity correlates with vascular function in morbidly obese adults. *Epigenetics,* 17**,** 93-109.

ARMENANTE, F., MEROLA, M., FURIA, A. & PALMIERI, M. 1999. Repression of the IL-6 gene is associated with hypermethylation. *Biochem Biophys Res Commun,* 258**,** 644-7.

ARUMUGAM, T., GHAZI, T. & CHUTURGOON, A. A. 2021. Fumonisin B1 alters global m6A RNA methylation and epigenetically regulates Keap1-Nrf2 signaling in human hepatoma (HepG2) cells. *Archives of Toxicology,* 95**,** 1367-1378.

BARNES, P. J. 2009. Targeting the epigenome in the treatment of asthma and chronic obstructive pulmonary disease. *Proc Am Thorac Soc,* 6**,** 693-6.

BHANDARI, N., BROWN, C. C. & SHARMA, R. P. 2002. Fumonisin B1-induced localized activation of cytokine network in mouse liver. *Food and Chemical Toxicology,* 40**,** 1483-1491.

BHANDARI, N., HE, Q. & SHARMA, R. P. 2001. Gender-related differences in subacute fumonisin B1 hepatotoxicity in BALB/c mice. *Toxicology,* 165**,** 195-204.

CHEN, J., WEI, Z., WANG, Y., LONG, M., WU, W. & KUCA, K. 2021. Fumonisin B1: Mechanisms of toxicity and biological detoxification progress in animals. *Food and Chemical Toxicology,* 149**,** 111977.

CHRUN, E. S., MODOLO, F. & DANIEL, F. I. 2017. Histone modifications: A review about the presence of this epigenetic phenomenon in carcinogenesis. *Pathology - Research and Practice,* 213**,** 1329-1339.

CHUTURGOON, A., PHULUKDAREE, A. & MOODLEY, D. 2014a. Fumonisin B1 induces global DNA hypomethylation in HepG2 cells – An alternative mechanism of action. *Toxicology,* 315**,** 65-69.

CHUTURGOON, A. A., PHULUKDAREE, A. & MOODLEY, D. 2014b. Fumonisin B1 modulates expression of human cytochrome P450 1b1 in human hepatoma (Hepg2) cells by repressing Mir-27b. *Toxicology Letters,* 227**,** 50-55.

CONSTABLE, P. D., SMITH, G. W., ROTTINGHAUS, G. E., TUMBLESON, M. E. & HASCHEK, W. M. 2003. Fumonisin-induced blockade of ceramide synthase in sphingolipid biosynthetic pathway alters aortic input impedance spectrum of pigs. *American Journal of Physiology-Heart and Circulatory Physiology,* 284**,** H2034-H2044.

DEMIREL, G., ALPERTUNGA, B. & OZDEN, S. 2015. Role of fumonisin B1 on DNA methylation changes in rat kidney and liver cells. *Pharmaceutical Biology,* 53**,** 1302-1310.

FURMAN, D., CAMPISI, J., VERDIN, E., CARRERA-BASTOS, P., TARG, S., FRANCESCHI, C., FERRUCCI, L., GILROY, D. W., FASANO, A., MILLER, G. W., MILLER, A. H., MANTOVANI, A., WEYAND, C. M., BARZILAI, N., GORONZY, J. J., RANDO, T. A., EFFROS, R. B., LUCIA, A., KLEINSTREUER, N. &

SLAVICH, G. M. 2019. Chronic inflammation in the etiology of disease across the life span. *Nature Medicine,* 25**,** 1822-1832.
GALVANI, S., SANSON, M., BLAHO, V. A., SWENDEMAN, S. L., OBINATA, H., CONGER, H., DAHLBÄCK, B., KONO, M., PROIA, R. L. & SMITH, J. D. 2015. HDL-bound sphingosine 1-phosphate acts as a biased agonist for the endothelial cell receptor S1P1 to limit vascular inflammation. *Science signaling,* 8**,** ra79-ra79.
GAULT, C. R., OBEID, L. M. & HANNUN, Y. A. 2010. An Overview of Sphingolipid Metabolism: From Synthesis to Breakdown. Springer New York.
GAZZAR, M. E., YOZA, B. K., CHEN, X., HU, J., HAWKINS, G. A. & MCCALL, C. E. 2008. G9a and HP1 Couple Histone and DNA Methylation to TNFα Transcription Silencing during Endotoxin Tolerance. *Journal of Biological Chemistry,* 283**,** 32198-32208.
GELDERBLOM, W., JASKIEWICZ, K., MARASAS, W., THIEL, P., HORAK, R., VLEGGAAR, R. & KRIEK, N. 1988. Fumonisins--novel mycotoxins with cancer-promoting activity produced by Fusarium moniliforme. *Applied and environmental microbiology,* 54**,** 1806-1811.
GIBNEY, E. R. & NOLAN, C. M. 2010. Epigenetics and gene expression. *Heredity,* 105**,** 4-13.
GOWDA, S. B., GOWDA, D., KAIN, V., CHIBA, H., HUI, S.-P., CHALFANT, C. E., PARCHA, V., ARORA, P. & HALADE, G. V. 2021. Inter-Organ Communication in Homeostasis and Disease: Sphingosine-1-phosphate interactions in the spleen and heart reflect extent of cardiac repair in mice and failing human hearts. *American Journal of Physiology-Heart and Circulatory Physiology,* 321**,** H599.
GUO, J., MEI, H., SHENG, Z., MENG, Q., VÉNIANT, M. M. & YIN, H. 2020. Hsa-miRNA-23a-3p promotes atherogenesis in a novel mouse model of atherosclerosis. *Journal of Lipid Research,* 61**,** 1764-1775.
HAQUE, M. A., WANG, Y., SHEN, Z., LI, X., SALEEMI, M. K. & HE, C. 2020. Mycotoxin contamination and control strategy in human, domestic animal and poultry: A review. *Microbial pathogenesis,* 142**,** 104095.
HE, Q., BHANDARI, N. & SHARMA, R. P. 2002. Fumonisin B(1) alters sphingolipid metabolism and tumor necrosis factor alpha expression in heart and lung of mice. *Life Sci,* 71**,** 2015-23.
HE, Y., HARA, H. & NÚÑEZ, G. 2016. Mechanism and Regulation of NLRP3 Inflammasome Activation. *Trends in Biochemical Sciences,* 41**,** 1012-1021.
HENDRICKS, K. 1999. Fumonisins and neural tube defects in South Texas. *Epidemiology,* 10**,** 198-200.
HSIAO, S.-H., CONSTABLE, P. D., SMITH, G. W. & HASCHEK, W. M. 2005. Effects of Exogenous Sphinganine, Sphingosine, and Sphingosine-1-Phosphate on Relaxation and Contraction of Porcine Thoracic Aortic and Pulmonary Arterial Rings. *Toxicological Sciences,* 86**,** 194-199.
JAMJOUM, R., MAJUMDER, S., ISSLENY, B. & STIBAN, J. 2024. Mysterious sphingolipids: metabolic interrelationships at the center of pathophysiology. *Frontiers in Physiology,* 14**,** 1229108.
JONES, S. W., WATKINS, G., LE GOOD, N., ROBERTS, S., MURPHY, C. L., BROCKBANK, S. M., NEEDHAM, M. R., READ, S. J. & NEWHAM, P. 2009. The identification of differentially expressed microRNA in osteoarthritic tissue that modulate the production of TNF-alpha and MMP13. *Osteoarthritis Cartilage,* 17**,** 464-72.
JUJIC, A., MATTHES, F., VANHERLE, L., PETZKA, H., ORHO-MELANDER, M., NILSSON, P. M., MAGNUSSON, M. & MEISSNER, A. 2021. Plasma S1P

(Sphingosine-1-Phosphate) Links to Hypertension and Biomarkers of Inflammation and Cardiovascular Disease: Findings From a Translational Investigation. *Hypertension,* 78**,** 195-209.
KRISHNAMOORTHY, S. & HONN, K. V. 2006. Inflammation and disease progression. *Cancer and Metastasis Reviews,* 25**,** 481-491.
LI, X., CAO, C., ZHU, X., LI, X. & WANG, K. 2020. Fumonisins B1 exposure triggers intestinal tract injury via activating nuclear xenobiotic receptors and attracting inflammation response. *Environmental Pollution,* 267**,** 115461.
LI, Y. 2021. Modern epigenetics methods in biological research. *Methods,* 187**,** 104-113.
MARASAS, W. F. 1996. Fumonisins: history, world-wide occurrence and impact. *Adv Exp Med Biol,* 392**,** 1-17.
MEDZHITOV, R. & HORNG, T. 2009. Transcriptional control of the inflammatory response. *Nature Reviews Immunology,* 9**,** 692-703.
MELLOTT, J. K., NICK, H. S., WATERS, M. F., BILLIAR, T. R., GELLER, D. A. & CHESROWN, S. E. 2001. Cytokine-induced changes in chromatin structure and in vivo footprints in the inducible NOS promoter. *Am J Physiol Lung Cell Mol Physiol,* 280**,** L390-9.
MERRILL, A. H. 2002. De novo sphingolipid biosynthesis: a necessary, but dangerous, pathway. *Journal of Biological Chemistry,* 277**,** 25843-25846.
PING, Z., SHUXIA, Z., XINYU, D., KEHE, H., XINGXIANG, C. & CHUNFENG, W. 2024. Mitophagy-regulated Necroptosis plays a vital role in the nephrotoxicity of Fumonisin B1 in vivo and in vitro. *Food and Chemical Toxicology,* 189**,** 114714.
PRALHADA RAO, R., VAIDYANATHAN, N., RENGASAMY, M., MAMMEN OOMMEN, A., SOMAIYA, N. & JAGANNATH, M. 2013. Sphingolipid metabolic pathway: an overview of major roles played in human diseases. *Journal of lipids,* 2013.
RILEY, R. T. & MERRILL, A. H., JR. 2019. Ceramide synthase inhibition by fumonisins: a perfect storm of perturbed sphingolipid metabolism, signaling, and disease. *J Lipid Res,* 60**,** 1183-1189.
SANCAK, D. & OZDEN, S. 2015. Global histone modifications in Fumonisin B1 exposure in rat kidney epithelial cells. *Toxicology in Vitro,* 29**,** 1809-1815.
SHARMA, R. P., HE, Q. & JOHNSON, V. J. 2003. Deletion of IFN-γ Reduces Fumonisin-Induced Hepatotoxicity in Mice via Alterations in Inflammatory Cytokines and Apoptotic Factors. *Journal of Interferon & Cytokine Research,* 23**,** 13-23.
SHEIK ABDUL, N. & MARNEWICK, J. L. 2020. Fumonisin B₁-induced mitochondrial toxicity and hepatoprotective potential of rooibos: An update. *Journal of Applied Toxicology,* 40**,** 1602-1613.
SIEDLINSKI, M., NOSALSKI, R., SZCZEPANIAK, P., LUDWIG-GAŁĘZOWSKA, A. H., MIKOŁAJCZYK, T., FILIP, M., OSMENDA, G., WILK, G., NOWAK, M., WOŁKOW, P. & GUZIK, T. J. 2017. Vascular transcriptome profiling identifies Sphingosine kinase 1 as a modulator of angiotensin II-induced vascular dysfunction. *Scientific Reports,* 7**,** 44131.
SORIANO, J. M., GONZÁLEZ, L. & CATALÁ, A. I. 2005. Mechanism of action of sphingolipids and their metabolites in the toxicity of fumonisin B1. *Progress in Lipid Research,* 44**,** 345-356.
SULLIVAN, K. E., REDDY, A. B. M., DIETZMANN, K., SURIANO, A. R., KOCIEDA, V. P., STEWART, M. & BHATIA, M. 2007. Epigenetic Regulation of Tumor Necrosis Factor Alpha. *Molecular and Cellular Biology,* 27**,** 5147-5160.
TARDIEU, D., BAILLY, J. D., BENARD, G., TRAN, T. S. & GUERRE, P. 2004. Toxicity of maize containing known levels of fumonisin B1 during force-feeding of ducks. *Poult Sci,* 83**,** 1287-93.

TILI, E., MICHAILLE, J.-J., CIMINO, A., COSTINEAN, S., DUMITRU, C. D., ADAIR, B., FABBRI, M., ALDER, H., LIU, C. G., CALIN, G. A. & CROCE, C. M. 2007. Modulation of miR-155 and miR-125b Levels following Lipopolysaccharide/TNF-α Stimulation and Their Possible Roles in Regulating the Response to Endotoxin Shock. *The Journal of Immunology,* 179**,** 5082-5089.

TSUNODA, M., SHARMA, R. P. & RILEY, R. T. 1998. Early fumonisin B1 toxicity in relation to disrupted sphingolipid metabolism in male BALB/c mice. *Journal of Biochemical and Molecular Toxicology,* 12**,** 281-289.

VILLAGRA, A., SOTOMAYOR, E. M. & SETO, E. 2010. Histone deacetylases and the immunological network: implications in cancer and inflammation. *Oncogene,* 29**,** 157-173.

WIERDA, R. J., GEUTSKENS, S. B., JUKEMA, J. W., QUAX, P. H. A. & VAN DEN ELSEN, P. J. 2010. Epigenetics in atherosclerosis and inflammation. *Journal of Cellular and Molecular Medicine,* 14**,** 1225-1240.

YOO, H. S., NORRED, W. P., SHOWKER, J. & RILEY, R. T. 1996. Elevated sphingoid bases and complex sphingolipid depletion as contributing factors in fumonisin-induced cytotoxicity. *Toxicol Appl Pharmacol,* 138**,** 211-8.

Appendix B

Docking Energy Tables for TNF-α, iNOS, NF-kB (p65) and NF-kB (p50)

Table B1: TNF-α docking energies. The docking of FB_1 on TNF-α revealed a range of -5.4 to -4.8, these energies indicated the conformation which could facilitate and interact with the protein for a longer time period due to the narrow range it indicated that most conformations of FB_1 with TNF-α are mostly stable.

Mode	Affinity (kcal/mol)	Dist. from rmsd l.b.	Best mode rmsd u.b.
1	-5.4	0.000	0.000
2	-5.2	1.697	2.467
3	-5.2	2.575	7.101
4	-5.0	25.407	29.708
5	-5.0	34.029	38.222
6	-5.0	1.823	2.828
7	-4.9	21.056	26.404
8	-4.8	2.841	7.167
9	-4.8	9.511	14.543

Table B2: iNOS docking energies. In contrast with the TNF-α docking energies, FB_1 bound at a higher binding energy with iNOS indicating a stable reaction with this complex indicating a longer interaction between FB_1 and the protein.

Mode	Affinity (kcal/mol)	Dist. from rmsd l.b.	Best mode rmsd u.b.
1	-6.5	0.000	0.000
2	-6.1	3.436	6.840
3	-6.1	3.375	7.584
4	-6.0	3.125	8.098
5	-5.9	3.143	6.702
6	-5.7	2.308	6.512
7	-5.7	2.700	7.265
8	-5.6	2.509	6.218
9	-5.6	2.339	6.263

Table B3: NF-kB (p65) docking energies. The binding of FB_1 to the p65 subunit of NF-kB revealed the lowest binding energy in comparison to the other four docked proteins which entailed a less stable interaction between the complex and FB_1 compared with the other factors; however, the deviation from the other energies is not large.

Mode	Affinity (kcal/mol)	Dist. from rmsd l.b.	Best mode rmsd u.b.
1	-4.8	0.000	0.000
2	-4.8	19.242	23.800
3	-4.8	20.104	24.606
4	-4.8	2.304	5.539
5	-4.7	18.150	22.069
6	-4.7	3.740	8.404
7	-4.6	6.345	12.102
8	-4.6	3.455	7.216
9	-4.6	3.720	9.162

Table B4: NF-kB (p50) docking energies. The binding affinity of FB_1 to the p50 subunit revealed a more stable interaction and similar docking score to iNOS indicating a stronger binding affinity to this subunit of NF-kB.

Mode	Affinity (kcal/mol)	Dist. from rmsd l.b.	Best mode rmsd u.b.
1	-6.3	0.000	0.000
2	-6.1	9.683	15.867
3	-6.1	9.904	16.823
4	-6.1	24.806	27.631
5	-6.0	24.946	27.221
6	-6.0	24.978	27.791
7	-5.9	9.261	15.493
8	-5.9	9.010	15.303
9	-5.8	24.965	27.756

Appendix C

Ethical Approval Letter – In Vivo Study

UNIVERSITY OF KWAZULU-NATAL
INYUVESI YAKWAZULU-NATALI

18 September 2018

Professor Anil Chuturgoon (34866)
School of Laboratory Medicine & Medical Sciences
Howard College Campus

Dear Professor Chuturgoon,

Protocol reference number: AREC/079/016
Project title: The molecular and epigenetic effects of selected mycotoxins on C57B/6 black mice

Full Approval – Renewal Application

With regards to your renewal application received on 24 August 2018. The documents submitted have been accepted by the Animal Research Ethics Committee and **FULL APPROVAL** for the protocol has been granted.

Please note: Any Veterinary and Para-Veterinary procedures must be conducted by a SAVC registered VET or SAVC authorized person.

Any alteration/s to the approved research protocol, i.e Title of Project, Location of the Study, Research Approach and Methods must be reviewed and approved through the amendment/modification prior to its implementation. In case you have further queries, please quote the above reference number.

Please note: Research data should be securely stored in the discipline/department for a period of 5 years.

The ethical clearance certificate is only valid for a period of one year from the date of issue. Renewal for the study must be applied for before 18 September 2019.

Attached to the Approval letter is a template of the Progress Report that is required at the end of the study, or when applying for Renewal (whichever comes first). An Adverse Event Reporting form has also been attached in the event of any unanticipated event involving the animals' health / wellbeing.

I take this opportunity of wishing you everything of the best with your study.

Yours faithfully

[redacted]

Professor S Islam, PhD
Chair: Animal Research Ethics Committee

/ms

Cc Acting Academic Leader Research: Dr Brenda de Gama
Cc Registrar: Mr Simon Mokoena
Cc NSPCA: Ms Anita Engelbrecht
Cc BRU – Dr Linda Bester

Animal Research Ethics Committee (AREC)
Ms Mariette Snyman (Administrator)
Westville Campus, Govan Mbeki Building
Postal Address: Private Bag X54001, Durban 4000
Telephone: +27 (0) 31 260 8350 **Facsimile:** +27 (0) 31 260 4609 **Email:** animalethics@ukzn.ac.za
Website: http://research.ukzn.ac.za/Research-Ethics/Animal-Ethics.aspx

1910 - 2010
100 YEARS OF ACADEMIC EXCELLENCE

Appendix D

Quantification of NOS Levels

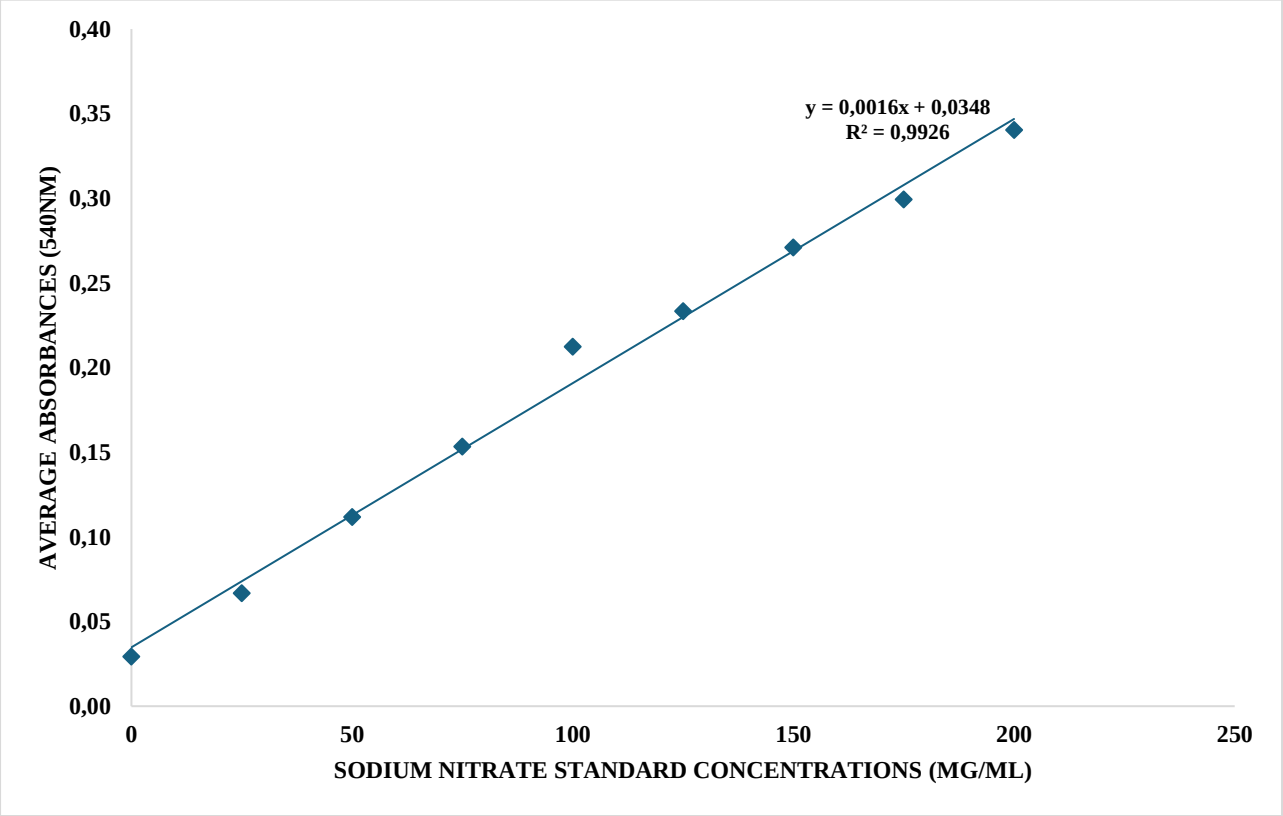

Figure A: NOS standards were utilised to prepare the above standard curve to obtain the equation of the line which was subsequently used to calculate the concentration of RNS metabolites.

Appendix E

Protein Quantification (BCA Assay)

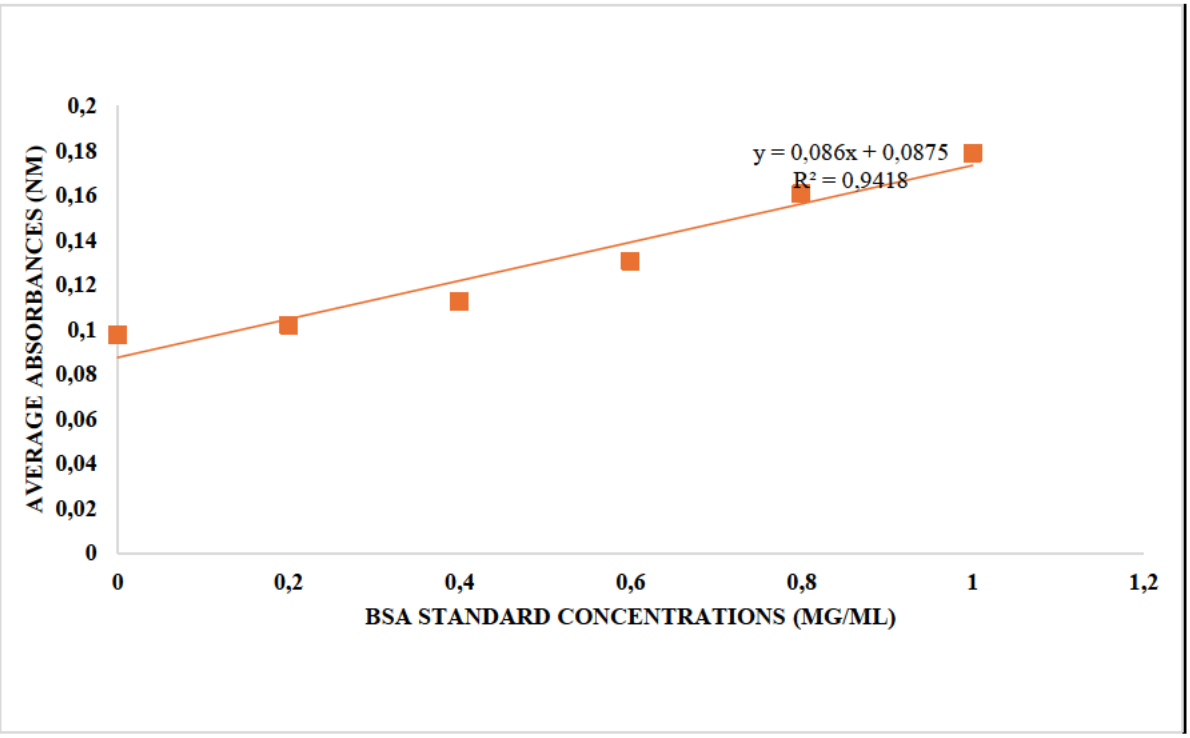

Figure B: The BCA assay was utilised to determine protein concentration. The BSA standards were prepared, and the resulting data were used to extrapolate the equation of the line. This equation was then applied to calculate the protein concentration in all samples. Proteins were subsequently standardised.

Appendix F

Quantification of TNF-α Levels

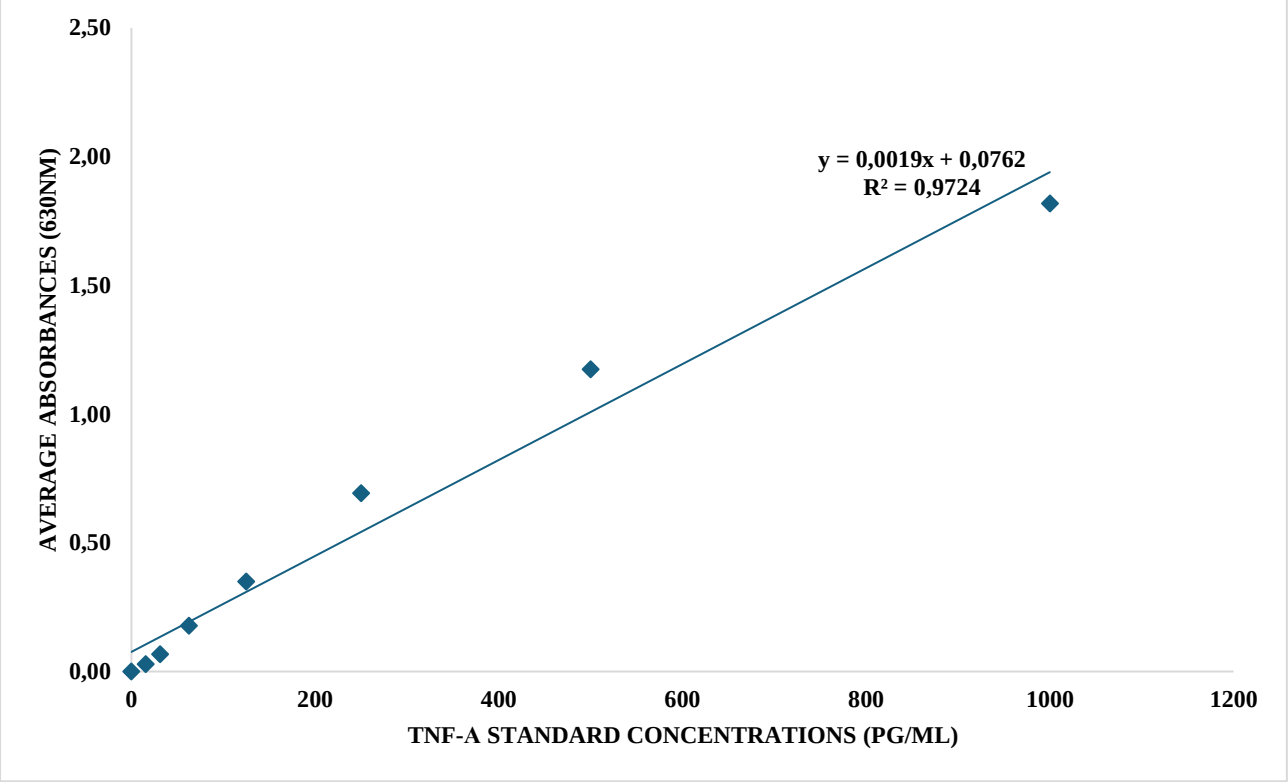

Figure C: TNF-α standards were prepared and used to obtain a standard curve which was used to obtain the equation of the line. This equation was further used to determine the concentration of TNF-α in control and FB_1 samples.

Appendix G

Quantification of IL-6 Levels

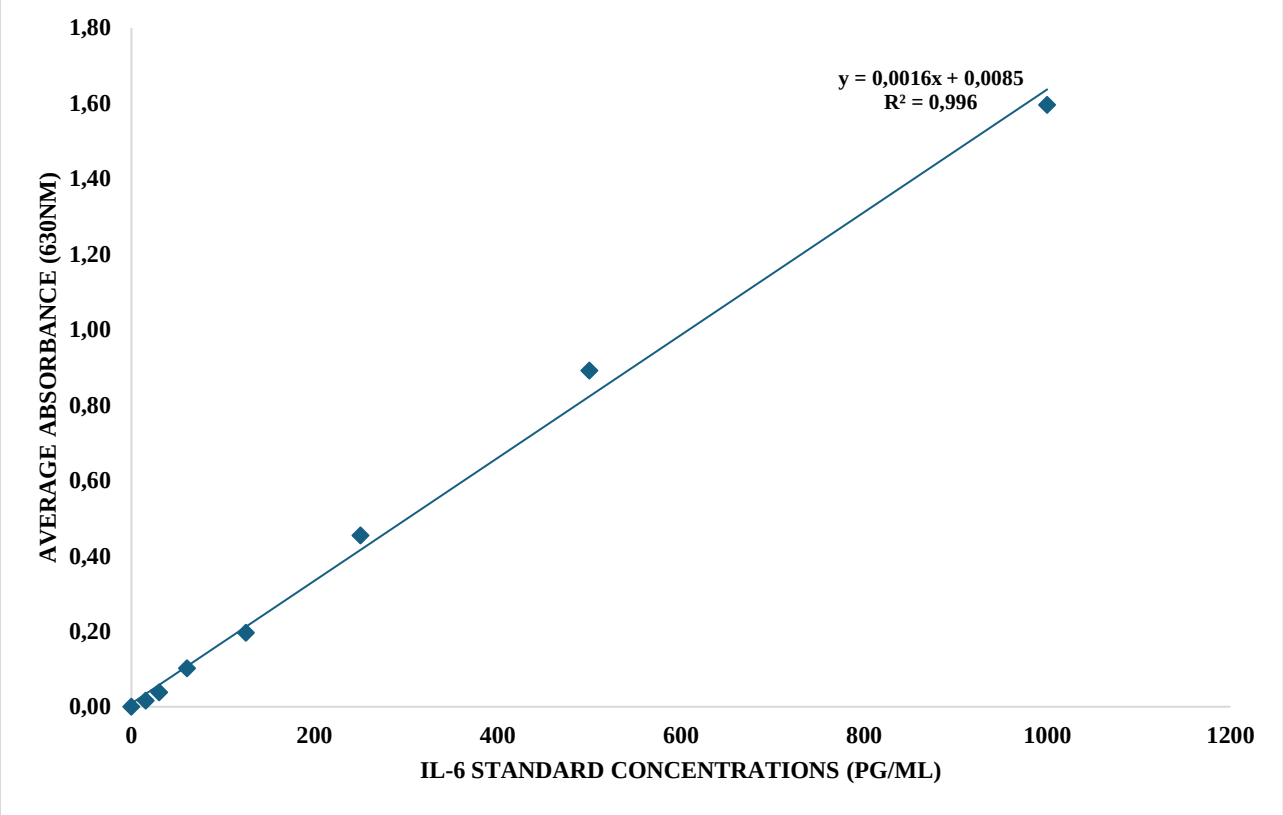

Figure D: IL-6 standards were prepared and used to create a standard curve to obtain the equation of the line which was subsequently used to calculate the concentration of IL-6 levels of control and FB_1 groups.

Appendix H

Quantification of IL-1β Levels

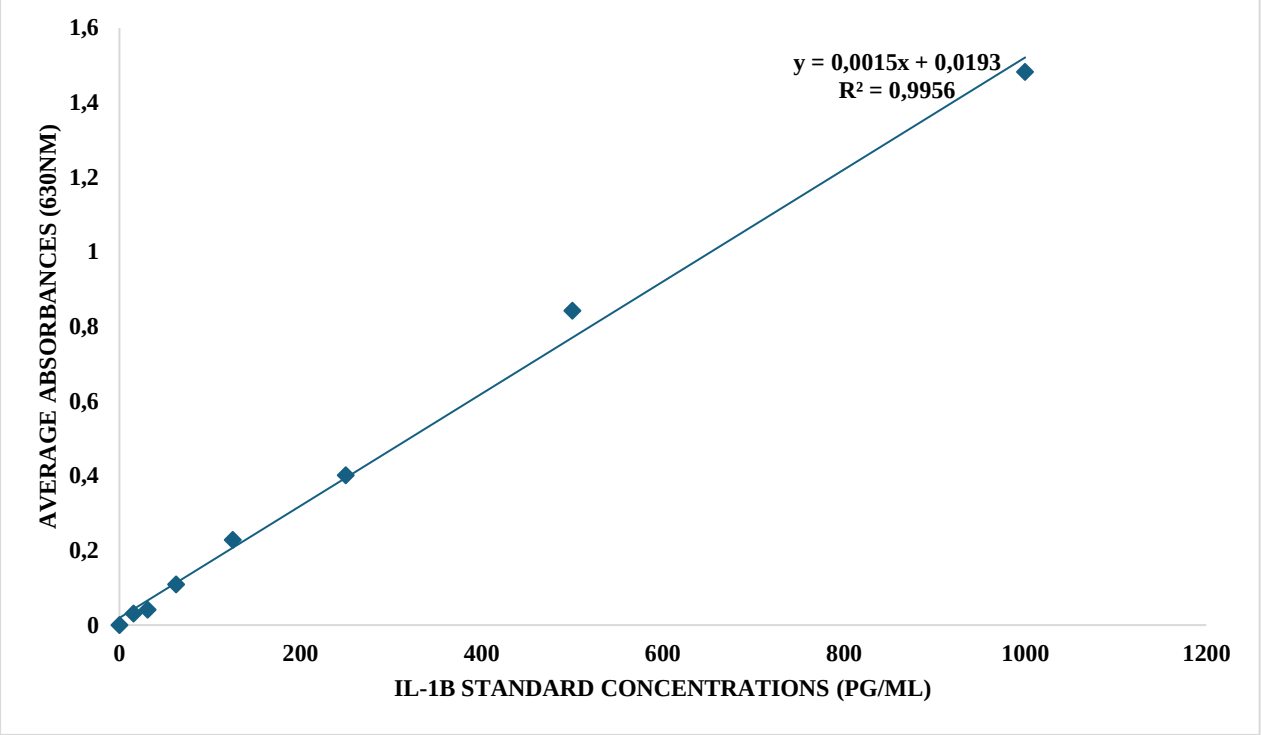

Figure E: The determination of IL-1β standard concentrations was analysed to determine the equation of the line which was used to quantify the concentration of IL-1β levels in control and FB_1 treated groups.

Appendix I

Quantification of IL-10 Levels

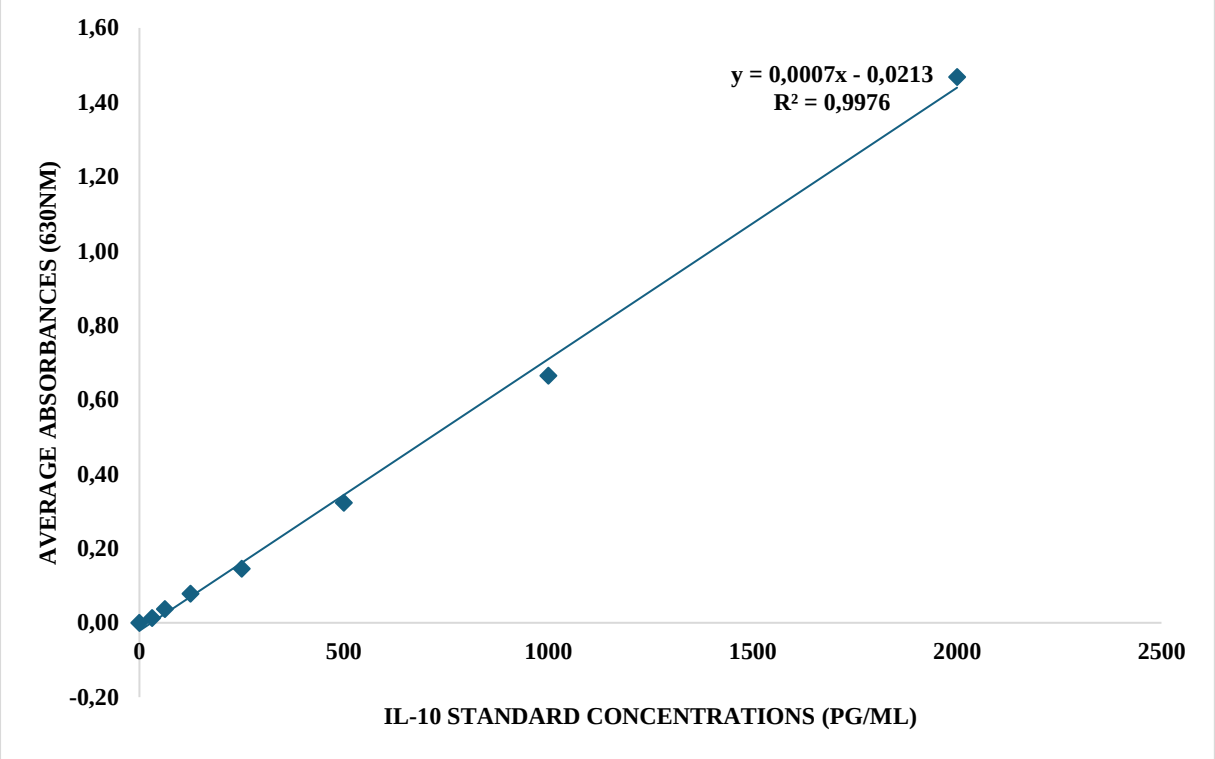

Figure F: The anti-inflammatory cytokine, IL-10 standard concentrations were used to prepare a standard curve. The above curve was used to find the equation of the line which was subsequently used to calculate the expression of IL-10 concentrations in control and FB_1 groups.

Appendix J
Quantification of TGF-β1 Levels

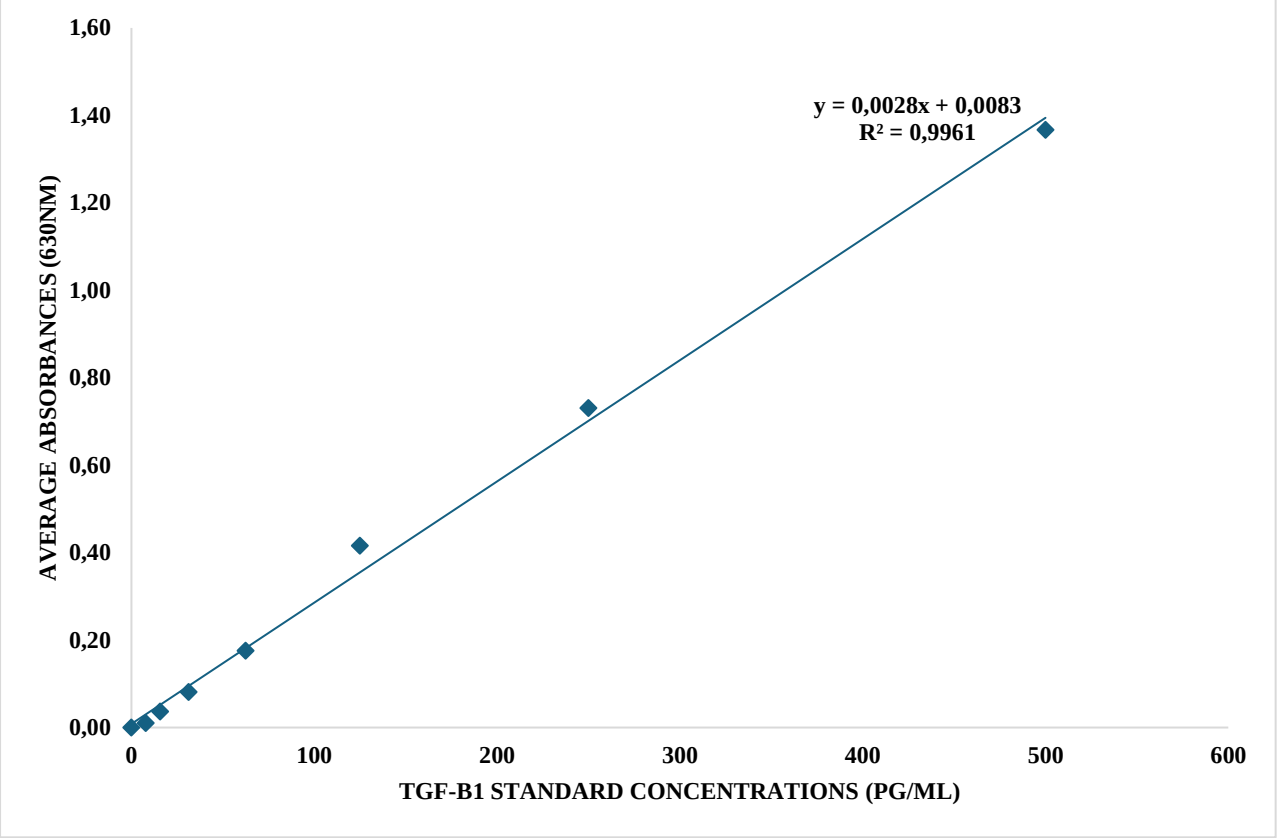

Figure G: A standard curve of TGF-β1 standards was prepared to acquire the equation of the line. This equation was utilised to quantify the concentrations of TGF-β1 present in the serum of mice hearts.

Appendix K

Quantification of Global DNA Methylation Levels

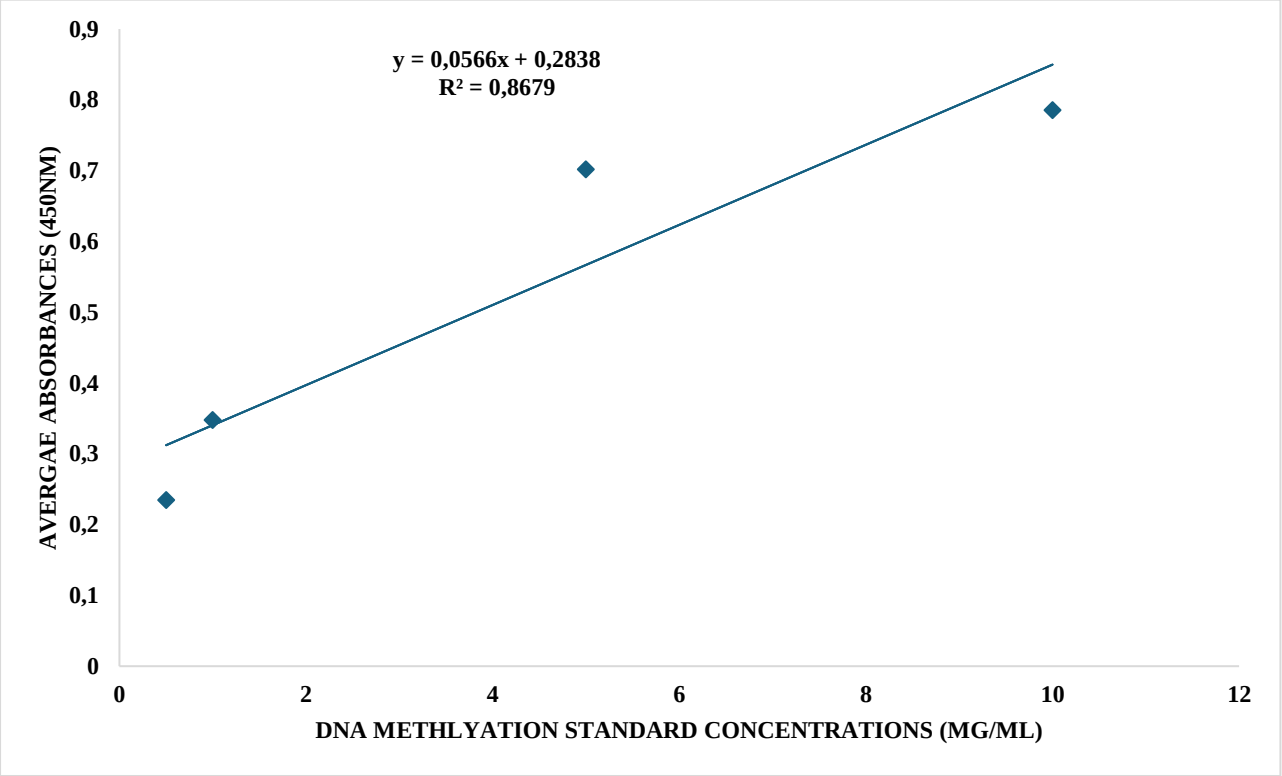

Figure H: Global DNA methylation standards were prepared and their absorbances were used to obtain the above standard curve. This standard curve was further employed to obtain the equation of the line to determine the levels of 5mc present in all samples.